2012

Transport and Fate of Sediment on the Waipaoa River Continental Shelf: Implications for the Formation and Reworking of Flood Deposits

Julia M. Moriarty
College of William and Mary - Virginia Institute of Marine Science

Transport and Fate of Sediment on the Waipaoa River Continental Shelf: Implications for the Formation and Reworking of Flood Deposits

---

A Thesis

Presented to

The Faculty of the School of Marine Science

The College of William and Mary in Virginia

In Partial Fulfillment

of the Requirements for the Degree of

Master of Science

---

by

Julia M. Moriarty

APPROVAL SHEET

This thesis is submitted in partial fulfillment of

the requirements for the degree of

Master of Science

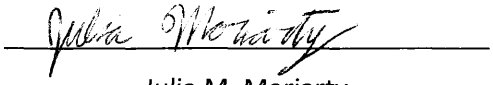

Julia M. Moriarty

Approved, by the Committee, December 2012

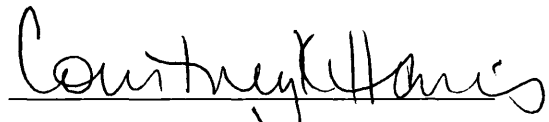

Courtney K. Harris, Ph.D.

Committee Chairman/ Advisor

Carl T. Friedrichs, Ph.D.

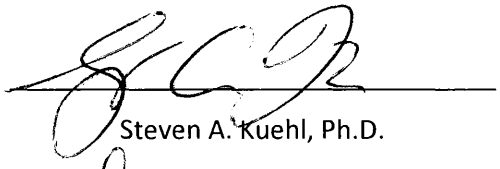

Steven A. Kuehl, Ph.D.

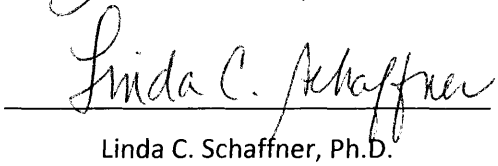

Linda C. Schaffner, Ph.D.

Mark G. Hadfield, Ph.D.

National Institute of Water and Atmosphere

Wellington, New Zealand

Table of Contents

ACKNOWLEDGEMENTS

Many people have guided my path at VIMS. I especially want to thank my advisor Dr. Courtney Harris who provided scientific guidance and acted as a mentor. I also gratefully acknowledge Dr. Mark Hadfield, whose feedback greatly improved the model's development. Thank you to Drs. Carl Friedrichs, Steve Kuehl, and Linda Schaffner for many interesting discussions, advice, and for broadening my perspective. I am also grateful for the many faculty, staff, and students at VIMS whose questions and comments shaped this project and my research interests.

This thesis benefitted from data and technical support provided by many individuals. Members of the Waipaoa Shelf Initiative, including Dr. J.P. Walsh, Dr. Andrea Ogston, Dr. Reide Corbett, Dr. Alan Orpin, Dr. Tara Kniskern, Rip Hale, and Joey Kiker provided data from the 2010 field season, along with many enthusiastic discussions. Dr. Mark Hadfield, Dr. Mike Uddstrom, Dr. Steve Kuehl, Dr. Jesse McNinch, Dr. Scott Stephens, Greg Hall, and Dave Peacock contributed observations and model estimates. Dr. Aaron Bever, Adam Miller, Mary Ann Bynum, Dave Weiss, Tom Crockett, and Albert Kettner dispensed technical assistance for using the computational facilities at VIMS, the SciClone cluster at the College of William & Mary, and the CSDMS computing cluster at University of Colorado. Computational facilities were supported by the NSF, VA Port Authority, Sun Microsystems, and Virginia's Commonwealth Technology Research Fund. Funding for this thesis was provided by NSF MARGINS grant 0841092 and the VIMS fellowship program.

Last, but certainly not least, I am thankful for the love, support, and good humor of my family and friends.

LIST OF TABLES

LIST OF FIGURES

ABSTRACT

As part of a large interdisciplinary study, particulate fluxes in the Waipaoa River sedimentary system in New Zealand have been studied from the terrestrial headlands of the catchment to the oceanic basin over timescales spanning storm events, seasons, and the Holocene. Here, we complement prior efforts by evaluating the formation and reworking of riverine deposits during episodic flood and wave events, and considering their role in accumulation patterns created over longer timescales on the Waipaoa shelf. Using a numerical hydrodynamic and sediment transport model, sediment fluxes and deposition were analyzed from January 2010 through February 2011.

A version of the three dimensional ROMS-CSTMS (Regional Ocean Modeling System – Community Sediment Transport Modeling System) was used to investigate the spatial and temporal variability of sediment fluxes on the Waipaoa shelf. The model could account for river input, waves, winds, larger-scale currents, tides, multiple sediment classes and a multi-layered seabed. Sediment sources to the water column included both the river plume and resuspension from the seabed. For model stability and to prevent the reflection of the river plume at the open boundary, the Waipaoa shelf model was nested within a larger-scale New Zealand ocean model. Model inputs were based on observations and model estimates, depending on availability.

Event sedimentation on the Waipaoa shelf differed from net accumulation patterns, especially over relatively short timescales. During floods, sediment generally deposited near the river mouth and along the coast in water shallower than 30 m. In the days to months following initial emplacement, waves reworked this deposit, preferentially resuspending sediment from shallow depths and redistributing it toward deeper areas where bed stresses were relatively low, including shelf depocenters and offshore. Overall, shelf deposition depended on characteristics of oceanographic transport (wave energy, current velocities) as well as on source (flood size, sediment size distribution).

Transport and Fate of Waipaoa Shelf Sediment

CHAPTER 1: Introduction

Sediment transport and deposition in the coastal ocean impact navigation and shoreline change, habitat suitability, and the geologic record and the natural resources contained there. Yet sediment fluxes remain difficult to predict because they are affected by hydrodynamic and seabed processes (e.g. seabed reworking, flocculation, and seabed consolidation) that depend on sediment type and environmental characteristics (e.g. Wheatcroft et al., 2007; Hill et al., 2000; Parchure and Mehta, 1985). Even at a single field site, sediment fluxes vary in time on scales from minutes to in excess of thousands of years, and on spatial scales from ripples to ocean basins (Sadler, 1981; Wright et al., 1977). This study analyzed sediment fluxes on the Waipaoa Shelf, New Zealand over timescales that ranged from single storms to months as part of a larger effort to understand the transport of material from terrestrial source to oceanic sink.

NSF's MARGINS Source-to-Sink (S2S) program was initiated to study sediment transport and deposition over a variety of temporal and spatial scales that bridged terrestrial and marine environments. The Waipaoa Sedimentary System (see Figure 1-1), the focus of this thesis and an S2S study site, has been well-studied, from sediment production in the terrestrial headlands to sediment accumulation in the ocean, and over time scales of floods to the entire Holocene (see Carter et al., 2010). Three scientific questions guided the S2S program (NSF MARGINS Program, 2004):

1. How do tectonics, climate, sea level fluctuations, and other forcing parameters regulate the production, transfer, and storage of sediments and solutes from their sources to their sinks?

2. What processes initiate erosion and sediment transfer, and how are these processes linked through feedbacks?
3. How do variations in sediment processes and fluxes and longer-term variations such as tectonics and sea level build the stratigraphic record to create a history of global change?

This thesis addressed the second and third questions using a coupled hydrodynamic and sediment transport model for the continental shelf offshore of the Waipaoa River, New Zealand.

Previous studies on this continental margin identified two long-term mid-shelf (40-70 m water depth) depocenters separated by a zone of low accumulation called Poverty Gap (Miller and Kuehl, 2010; Gerber et al., 2010). Analyses of these seabed observations alone, however, were unable to identify the mechanisms responsible for delivering sediment to the depocenters, or to evaluate the extent of modification of the sedimentary signal between the river mouth and preservation in the geologic record. In response, the Waipaoa Shelf Initiative (described in Chapter 3) proposed to obtain seabed and hydrodynamic observations to characterize sediment transport and deposition on event- to seasonal-time scales. As part of this, three instrumented tripods were deployed on the Waipaoa continental shelf from January, 2010 – February, 2011, and hundreds of sediment bed samples were obtained during the five associated research cruises. Complementing these observations, we used a numerical model to estimate and analyze sediment fluxes on the continental shelf.

Numerical models complement observations in the investigation of sediment transport and depositional processes. Field experiments carry a high cost and are hampered by difficulties of observing water column sediment fluxes during energetic conditions such as floods and storms, except at discrete points

served by deployed instruments. Numerical models can interpolate point observations to continuous spatial scales, however, and extrapolate beyond the spatial and temporal coverage of field experiments.

Numerical sediment transport models range from one to three dimensions. For example, one-dimensional bottom boundary layer models have been useful for providing high vertical resolution (Grant and Madsen, 1979; Madsen, 1994; Wiberg et al. 1994). Two-dimensional models, e.g. the plan-view gravity flow model by Scully et al., 2003 or the depth-resolving suspended transport model by Harris and Wiberg, 2001, resolve horizontal gradients in processes but avoid the computational requirements of three dimensional models. Three-dimensional circulation and sediment transport models, such as the Community Sediment Transport Modeling System (CSTMS; Warner et al., 2008) which has been recently implemented within the numerical circulation model Regional Ocean Modeling System (ROMS; Haidvogel et al., 2000; Haidvogel et al., 2008; Shchepetkin and McWilliams, 2005, 2009), fully resolve horizontal and vertical gradients, all of which can be important in the coastal ocean. Although increased model complexity and resolution carries a heavier computational load, a three dimensional model is necessary to represent the Waipaoa shelf's complex bathymetry, bottom boundary layer, and river plume dynamics.

Many three-dimensional coastal sediment transport models have either neglected larger-scale currents or simplified them by using temporal and/or spatial averages to specify currents at the model's boundary (e.g. Bever and Harris, submitted; Ralston et al., in press; Xu et al., 2011; Ganju and Schoelhamer, 2010; Chen et al., 2009). For example, Bever and Harris (submitted) developed a numerical model for Poverty Bay, the coastal portion of the Waipaoa Sedimentary System, that accounted for wind, wave, tidal, and river plume processes that act to disperse sediment there. At the

open boundaries, Bever and Harris (submitted) accounted for tides and allowed waves to propagate through the boundary by using Chapman (1985), Flather and Procter (1983), Marchesiello et al. (2001), and a no-gradient boundary condition for the free surface, two and three dimensional currents, and tracers, respectively. More recently, however, numerical models of continental shelf sediment transport have specified conditions along open boundaries based on estimates of coastal currents, temperature, and salinity from larger scale, lower resolution models (Blaas et al. 2006, Xue et al., 2012). Like Blaas et al. (2006) and Xue et al. (2012), we build on previous efforts by nesting a finer-scale grid within a larger scale hydrodynamic model, thereby accounting for larger scale circulation patterns. For the event-driven Waipaoa shelf model, nesting not only allowed us to account for larger scale currents, but was necessary to prevent the reflection of freshwater and sediment from the river plume at the model boundary, and to increase the stability of the model.

This thesis used the CSTMS – ROMS numerical model implemented for the Waipaoa continental shelf for a thirteen month period. Chapter Two describes the model in detail, with model input files provided in the Appendix. Chapter Three provides an analysis of model estimates. As described in that section, sediment fluxes and the resulting depositional patterns differed between floods, wave events, and fairweather periods. In the months following floods, energetic waves and currents resuspended sediment and redistributed riverine deposits. Preferential resuspension of shallow deposits encouraged sediment accumulation in deeper areas, including mid-shelf depocenters.

References

Bever, A.J. and Harris, C.K., 2012. Storm and fair-weather driven sediment-transport within Poverty Bay, New Zealand, evaluated using coupled numerical models. Continental Shelf Research. *Submitted.*

Blaas, M., Dong, C., Marchesiello, P, McWilliams, J.C., and Stolzenbach, K.D., 2006. Sediment-transport modeling on Southern California shelves: A ROMS case study. Continental Shelf Research, 27: 832-853.

Carter, L., Orpin, A. R., and Kuehl, S. A., 2010. From mountain source to ocean sink – the passage of sediment across an active margin, Waipaoa sedimentary system, New Zealand. Marine Geology, 270(1-4): 1-10.

Chapman, D. C., 1985. Numerical treatment of cross-shelf open boundaries in a barotropic coastal ocean model. Journal of Physical Oceanography, 15: 1060-1075.

Chen, S-N., Sanford, L.P, and Ralston, D.K., 2009. Lateral circulation and sediment transport driven by axial winds in an idealized, partially mixed estuary. Journal of Geophysical Research,114: C12006. doi:10.1029/2008JC005014.

Flather, R.A. and Proctor, R., 1988. Prediction of North Sea storm surges using numerical models: Recent developments in the U.K. In: J. Sundermann and W. Lenz (Editors). North Sea Dynamics. Springer-Verlag, New York.

Ganju, N.K. and Schoelhamer, D.H., 2010. Decadal-Timescale Estuarine Geomorphic Change Under Future Scenarios of Climate and Sediment Supply. Estuaries and Coasts,33 (1): 15-29.

Gerber, T. P., Pratson, L. F., Kuehl, S., Walsh, J. P., Alexander, C., and Palmer, A., 2010. The influence of sea level and tectonics on late Pleistocene through Holocene sediment storage along the high-sediment supply Waipaoa continental shelf. Marine Geology, 270(1-4): 139-159.

Grant, W.D. and O Madesen. , 1979. Combined wave and current interaction with a rough bottom. Journal of Geophysical Research, 84: 1797-1808.

Harris, C. K., and Wiberg, P. L., 2001. A two-dimensional, time-dependent model of suspended sediment transport and bed reworking for continental shelves. Computers & Geosciences, 27(6): 675-690.

Haidvogel, D. B., Arango, H. G., Hedstrom, K., Beckmann, A., Malanotte-Rizzoli, P., and Shchepetkin, A. F., 2000. Model evaluation experiments in the North Atlantic basin: Simulations in nonlinear terrain-following coordinates. Dynamics of Atmospheres and Oceans, 32(3-4): 239-281.

Haidvogel, D. B., Arango, H., Budgell, W. P., Cornuelle, B. D., Curchitser, E., Di Lorenzo, E., et al., 2008. Ocean forecasting in terrain-following coordinates: Formulation and skill assessment of the regional ocean modeling system. Journal of Computational Physics, 227(7): 3595-3624.

Hill, P.S., Milligan, T.G., and Geyer, W.R., 2000. Controls on effective settling velocity of suspended sediment in the Eel River flood plume. Continental Shelf Research, 20 (16): 2095-2111.

Madsen, O.S., 1994. Spectral wave-current bottom boundary layer flows. Proceedings of the 24th International Conference on Coastal Engineering, ASCE, Kobe, 1: 384-398.

Marchesiello, P., McWilliams, J. C., and Shchepetkin, A., 2001. Open boundary conditions for long-term integration of regional oceanic models. Ocean Modelling, 3(1-2): 1-20.

Miller, A. J., and Kuehl, S. A., 2010. Shelf sedimentation on a tectonically active margin: A modern sediment budget for Poverty continental shelf, New Zealand. Marine Geology, 270(1-4): 175-187.

NSF MARGINS Program, 2004. MARGINS Sciences Plans 2004. http://www.nsf-margins.org/Publications/SciencePlans/MARGINS_SciencePlans2004.pdf. Accessed on 30 July 2012.

Parchure, T. M., and Mehta, A. J., 1985. Erosion of soft cohesive sediment deposits. Journal of Hydraulic Engineering, 111(10): 1308-1326.

Ralston, D.K., Geyer, W.R., Traycovski, P.A., and Nidzieko, N.J., 2012. Effects of estuarine and fluvial processes on sediment transport over deltaic tidal flats. Continental Shelf Research. *In press.*

Sadler, P.M., 1981. Sediment Accumulation Rates and the Completeness of Stratigraphic Sections. Journal of Geology, 89 (5): 569-584.

Shchepetkin, A. F., and McWilliams, J. C., 2005. The regional oceanic modeling system (ROMS): A split-explicit, free-surface, topography-following-coordinate oceanic model. Ocean Modelling, 9 (4): 347-404.

Shchepetkin, A. F., and McWilliams, J. C., 2009. Correction and commentary for "Ocean forecasting in terrain-following coordinates: Formulation and skill assessment of the regional ocean modeling system" by Haidvogel et al., J. comp. phys. 227, pp. 3595–3624. Journal of Computational Physics, 228(24): 8985-9000.

Scully, M.E., Friedrichs, C.T., and Wright, L.D, 2003. Numerical modeling of gravity-driven sediment transport and deposition on an energetic continental shelf: Eel River, northern California. Journal of Geophysical Research, 108 (C4): 3120. doi: 1029/2002JC001467.

Warner, J. C., Sherwood, C. R., Signell, R. P., Harris, C. K., and Arango, H. G., 2008. Development of a three-dimensional, regional, coupled wave, current, and sediment-transport model. Computers & Geosciences, 34(10): 1284-1306.

Wiberg, P. L., Drake, D. E., and Cacchione, D. A., 1994. Sediment resuspension and bed armoring during high bottom stress events on the northern California inner continental shelf: Measurements and predictions. Continental Shelf Research, 14(10-11): 1191-1219.

Wheatcroft, R. A., Wiberg, P. L., Alexander, C. R., Bentley, S. J., Drake, D. E., Harris, C. K., et al., 2007. Post-depositional alteration and preservation of sedimentary strata. In C. A. Nittrouer, et al. (Eds.), Continental margin sedimentation: From sediment transport to sequence stratigraphy. International Association of Sedimentologists, pp. 101-155.

Wright, L.D., 1977. Sediment transport and deposition at river mouths: A synthesis. Geological Society of America Bulletin, 88 (6): 857-868.

Xu, K, Harris, C.K., Hetland, R.D. , and Kaihatu, J.P., 2011. Dispersal of Mississippi and Atchafalaya sediment on the Texas-Louisiana shelf: Model estimates for the year 1993. Continental Shelf Research, 31: 1558-1575.

Xue, Z., He, R., Liu, J.P., and Warner, J.C., 2012. Modeling transport and deposition of the Mekong River sediment. Continental Shelf Research, 37: 66 – 78.

Figures

Figure 1-1: Map of Waipaoa Sedimentary System (WSS)

After Carter et al., 2010. Oceanic crust of the Pacific Plate (PP) is subducted under the Australian Plate, uplifting the North Island axial ranges (NIAR), including the Raukumara Ranges (RR). Also labeled are the Taupo Volcanic Zone (TVZ), Lake Tutira (LT), and Pakarae River (PR).

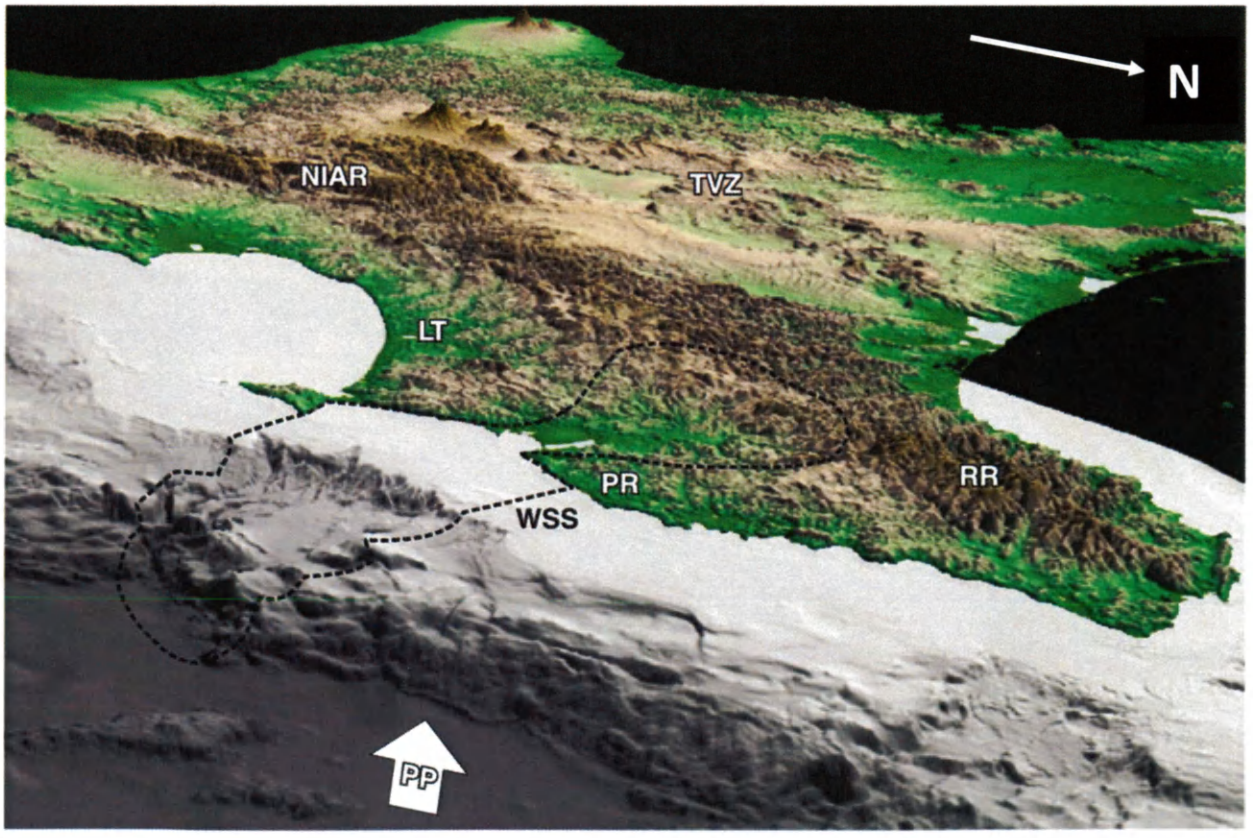

CHAPTER 2 : Implementation of a hydrodynamic and sediment transport model for the Waipaoa Shelf, New Zealand

2.1 Abstract

This chapter details the numerical hydrodynamic and sediment transport model implemented for the Waipaoa Shelf, New Zealand, describing the formulations used to estimate sediment fluxes and deposition from January 15, 2010 to February 15, 2011. The model was based on Release 3.6 of ROMS-CSTMS (Regional Ocean Modeling System – Community Sediment Transport Modeling System; see Warner et al, 2008; Haidvogel et al., 2000; Haidvogel et al., 2008; Shchepetkin and McWilliams, 2005, 2009). This primitive equation model used a finite difference solution to the equations for conservation of momentum, water mass, and concentrations of sediment, temperature, and salinity. To represent the complex shelf bathymetry offshore of the Waipaoa River mouth, the model grid had a horizontal resolution of about 450 m. Sediment sources to the water column included riverine discharge and resuspension of material from the seabed. In addition to fluvial input, fluxes of water and particulates were forced by spatially-and temporally- variable winds, waves, and tides. Model nesting, a relatively new capability for sediment transport models, allowed larger-scale currents to affect local processes.

2.2 Model development

This section describes the equations and numerical schemes used to specify hydrodynamic and sediment transport processes within the model and at the boundaries of the grid. Table 2-1 lists symbols for all equations.

2.2.1 Hydrodynamic model and numerical schemes

ROMS-CSTMS, a community-developed numerical circulation and sediment transport model, solves the equations for Reynolds-averaged Navier-Stokes (1-3), tracer advection-diffusion (4), and continuity (5) using the hydrostatic and Boussinesq assumptions:

(1) Momentum Balance in X: $$\frac{\partial u}{\partial t}+\vec{u}\bullet\nabla u-fv=-\frac{\partial \phi}{\partial x}+\frac{\partial}{\partial z}\left((K_M+\nu)\frac{\partial u}{\partial z}\right)+F_u+D_u$$

(2) Momentum Balance in Y: $$\frac{\partial v}{\partial t}+\vec{u}\bullet\nabla v+fu=-\frac{\partial \phi}{\partial y}+\frac{\partial}{\partial z}\left((K_M+\nu)\frac{\partial v}{\partial z}\right)+F_v+D_v$$

(3) Momentum Balance in Z (Hydrostatic Approximation): $$\frac{\partial \phi}{\partial z}=-\frac{\rho(T,S,P)g}{\rho_0}$$

(4) Tracer Advective-Diffusive Equation: $$\frac{\partial C}{\partial t}+\vec{u}\bullet\nabla C=\frac{\partial}{\partial z}\left((K_M+\nu_\theta)\frac{\partial C}{\partial z}\right)+F_C+D_C$$

(5) Continuity Equation: $$\frac{\partial u}{\partial x}+\frac{\partial v}{\partial y}+\frac{\partial w}{\partial z}=0$$

where *(x, y, z)* were vertical coordinates, $\vec{u}=(u,v,w)$ was water velocity, *f* was the Coriolis parameter, φ was dynamic pressure, defined as pressure divided by , ρ_0, a reference density, K_m was eddy viscosity, *v* was molecular viscosity, and *g* was the gravitational acceleration. In Equations (1)-(4), '*D*' represented horizontal dispersion of tracers and momentum. For Equation (4), the tracer concentration, *C*, could represent an array of different tracers, which included temperature, *T*, salinity, *S*, and seven sediment classes for the Waipaoa shelf. The *F* terms represented forcing that included sources and sinks of momentum (F_u and F_v in Equations (1) and (2)), such as bottom friction, wind stress, or nudging to match the regional grid (see section 2.2.5), and tracers (F_c in Equation (4)), such as river discharge, sediment settling, and deposition. River discharge was treated as a point source for momentum, temperature,

salinity and suspended sediment. The density equation of state accounted for temperature, salinity, and sediment concentrations, C_s (Jackett and McDougall, 1995; Warner et al., 2008):

$$(6) \qquad \text{Density Equation of State: } \rho(T,S,C_s) = \rho(T,S) + C_s \left(\rho_s - \rho\right) \Big/ \rho_s$$

ROMS is similar to other community models, such as the Princeton Ocean Model (POM; Blumberg and Mellor, 1983, 1987) and Finite-Volume Coastal Ocean Model (FVCOM; Chen et al., 2003), but distinguishes itself through the features described here. It uses a curvilinear orthogonal grid in the horizontal and a stretched-terrain following grid in the vertical which allows it to carry high resolution in both the surface and bottom boundary layers (Haidvogel et al., 2000). The numerical schemes in ROMS include split barotropic-baroclinic modes (Leap-Frog – Adams-Moulton predictor-corrector scheme; Haidvogel et al., 2000; Haidvogel et al., 2008, Shchepetkin and McWilliams, 2005, 2009) and reduce the pressure-gradient truncation error (Haney, 1991; Beckmann and Haidvogel, 1993; Mellor et al., 1994, 1998) by redefining the pressure-gradient term (Ezer et al., 2002; Shchepetkin and McWilliams, 2003; Haidvogel et al., 2008). ROMS also provides high-order schemes for estimating both vertical and horizontal advection (Huang et al., 2008; Haidvogel et al., 2008). For horizontal advection of sediment and other tracers, ROMS provides the MP-DATA scheme (Multidimensional Positive Definite Advection Transport Algorithm; Smolarkiewicz and Margolin, 1988) to avoid numerical oscillations and negative concentrations, and reduce numerical dispersion (e.g. Warner et al., 2008; Hyatt and Signell, 2000). For vertical advection of sediment, the ROMS framework implemented the PPM (Piecewise Parabolic Method) so that relatively large timesteps can be used for faster settling sands without the introduction of instabilities (Colella et al., 1984; Liu et al., 1994; Warner et al., 2008). These numerical schemes and reasonably high spatial resolution are important for representing the high gradients typical of coastal

and estuarine settings without sacrificing computational efficiency (Hyatt and Signell, 2000; Huang et al., 2008; Ezer et al., 2002; Shchepetkin and McWilliams, 1998).

For application of ROMS to the Waipaoa shelf, numerical schemes and the model grid (Figure 2-1) were chosen to reduce error in numerical computations without sacrificing model efficiency. Table 2-2 lists the specific numerical schemes. A timestep of 15 seconds was used.

2.2.2 Surface boundary layer formulation

The surface boundary formulation in ROMS was adopted from the physically-based COARE (Coupled-Ocean Atmosphere Response Experiment) framework described in Fairall et al. (1996) and Fairall et al. (2003). In this one layer boundary model, momentum was transferred from the atmosphere to the ocean through wind and rain:

$$\overrightarrow{\tau_{surface}} = \rho_{air} C_d |\vec{W}| \vec{W} + 0.85 * R^* |\vec{W}| * sign(\vec{W}) \quad (7)$$

where ρ_{air} represented air density, $\vec{W}$ was mean wind velocity, and *R* was rainfall rate in kg m^{-2} s^{-1}. The surface drag coefficient, C_d, was calculated using:

$$C_d = W_*^2 \Big/ |\vec{W} + \overrightarrow{W_{gust}}|^2 \quad (8)$$

$$W_* = |\vec{W} + \overrightarrow{W_{gust}}|^2 \, \kappa \Big/ \left(\ln(Z_{obs} / Z_0) - \psi_w\right) \quad (9)$$

$$Z_0 = \alpha u_*^2 / g \quad (10)$$

Here, W_* was the Monin-Obukhov similarity scaling parameter based on Liu et al. (1979), $\overrightarrow{W_{gust}}$ represented wind gusts, κ was the von Karmen constant, Z_0 was a roughness length scale, α was the Charnock constant, and g was gravity. The height of wind observations $\left(\overrightarrow{W}\right)$ was Z_{obs}, and ψ_w was a stability function. The Charnock constant, and therefore Z_0, increased with wind stress since the ocean surface becomes rougher under energetic winds.

2.2.3 Bottom boundary layer formulation

This implementation of ROMS used the Sherwood, Signell and Warner (Warner et al., 2008; referred to as W08) bottom boundary layer parameterization, a physics-based approach that could account for form drag and ripples. This formulation, defined as 'SSW' within ROMS, was based on Madsen (1994; referred to as M94) that divided the bottom boundary layer into two sections: a combined wave-current boundary layer, and a current boundary layer. The model parameterized turbulence using the following eddy viscosity profile:

(11) M94 Equation 2, W08 Equation 49:

$$K_M = \begin{cases} \kappa u_{*wc,\max} z & for \quad z_0 < z < z_1 \\ \kappa u_{*_c} z & for \quad z_1 < z \end{cases}$$

where z_0 was the hydraulic roughness, and z_1 defined the upper boundary of the wave-current boundary layer. The von Karman constant was κ, while u_{*c} and $u_{*cw,max}$ were the current-induced and wave-current induced shear velocities. For this study, the hydraulic roughness, z_o, neglected ripples and biological features and was set equal to the grainsize roughness $z_{o,N}$:

(12) $\quad z_o = z_{o,N}$

(13) W08 Equation 44: $z_{o,N} = 2.5 \cdot D_{50}/30$

where D_{50} was the median grain size on the seabed. The model then used the bottom roughness, the eddy viscosity profiles, wave orbital velocities provided by input files, and currents, u_r, at reference height z_r (20 cm above the bed) estimated by the hydrodynamic model, to calculate the current-induced, $\vec{\tau}_c$, wave-induced, $\vec{\tau}_{w,\max}$, and combined maximum current-wave-induced, $\vec{\tau}_{cw,\max}$, bed stresses following Madsen, 1994 (referred to as M94).

(14) $\vec{\tau}_{cw,\max} = \vec{\tau}_c + \vec{\tau}_{w,\max}$

(15) M94 Equation 26: $u^2_{*cw,\max} = C_\mu u^2_{*w,\max}$

(16) M94 Equations 27 and 28: $$C_\mu = \left[1 + 2\left(\frac{u_{*c}}{u_{*w,\max}}\right)^2 \cos(\phi_{cw}) + \left(\frac{u_{*c}}{u_{*w,\max}}\right)^2\right]^{1/2}$$

(17) M94 Equation 29: $u_{*w,\max} = \frac{1}{2} f_{cw} u_b^2$

(18) M94 Equations 32 and 33, W08 Equation 48:

$$f_{cw} = C_\mu \exp\begin{cases} 0.3 & for \quad \left(\frac{C_\mu u_b}{k_N \omega}\right) < 0.2 \\ 7.02\left(\frac{C_\mu u_b}{k_N \omega}\right)^{-0.078} - 8.82 & for \quad 0.2 < \left(\frac{C_\mu u_b}{k_N \omega}\right) < 10^2 \\ 5.61\left(\frac{C_\mu u_b}{k_N \omega}\right)^{-0.109} - 7.30 & for \quad 10^2 < \left(\frac{C_\mu u_b}{k_N \omega}\right) < 10^4 \end{cases}$$

(19) $$u_{*c} = \frac{1}{2} u_{*cw,\max} \frac{\ln(z_r / z_{cw})}{\ln(z_{cw} / z_o)} \left(-1 + \sqrt{4\kappa \frac{\ln(z_{cw} / z_o)}{\ln(z_r / z_{cw})} \frac{u_r}{u_{*cw,\max}}}\right)$$

(20) $$z_{cw} = \begin{cases} k_N & for \quad \left(\frac{C_\mu u_b}{k_N \omega}\right) \le 8.0 \\ 2\frac{\kappa u_{*cw}}{\omega} & for \quad \left(\frac{C_\mu u_b}{k_N \omega}\right) > 8.0 \end{cases}$$

(21) $$k_N = 30 \cdot z_o$$

Here, $u_{*w,\max}$ was the wave-induced shear velocity, and k_N was bottom roughness length. Model input included the wave orbital velocity, u_b, and the angle between the waves and the currents, ϕ_{cw}. The wave friction factor, f_{cw}, increased with wave orbital velocity and period, and with C_μ (which increased as currents became more energetic compared to waves). The bottom boundary routine iterated through Equations (15) – (20) to find consistent values for $u_{*w,\max}$, u_{*c}, u_{*cw}, C_μ and f_{cw} that were then used to determine the dampening of circulation by bottom friction and evaluate sediment mobility.

2.2.4 Seabed model

As described in Warner et al. (2008) and summarized in Section 2.2.1, the model accounted for advection, diffusion, erosion and deposition of sediment. Both fluvial discharge and seabed erosion provided sediment to the water column, with erosion calculated following the Ariathurai and Arulanandan (1978) formulation for each sediment size class:

(22) $$F_c = E - \frac{\partial w_s C_{s,1}}{\partial z_s}$$

$$(23) \qquad E = \begin{cases} M(1-p)\dfrac{\tau_{cw,\max} - \tau_{crit}}{\tau_{crit}} & when \ \tau_{cw,\max} > \tau_{crit} \\ 0 & when \ \tau_{cw,\max} < \tau_{crit} \end{cases}$$

In Equation (22), F_c was the net entrainment of suspended sediment, where E represented erosion and the second term estimated settling to the bed based on settling velocity, w_s, and on $C_{s,1}$, the mass of suspended sediment per unit area of the bed in the near-bed grid cell. In Equation (23), M was the erosion rate parameter, p was porosity, or void fraction of the seabed, $\tau_{cw,max}$ was combined wave-current- bed shear stress from Equation (14), and τ_{crit} was a spatially-constant, time-invariant critical bed shear stress. Equations (22) and (23) were calculated for several sediment types, each having different input values for settling velocity and critical shear stress (see section 2.3.7). Note that these and other parameters (e.g. erosion rate parameter) were treated as constants for each sediment class, and so processes including flocculation (Syvitski et al., 1985), seabed consolidation (Parchure and Mehta, 1985) and bioturbation (Paterson, 1997) were not explicitly represented in the model. For the Waiapoa Shelf, different sediment types were used to distinguish material delivered by the river from particulates that originated on the seabed. Erosion was restricted by sediment mass conservation, and limited to the thickness of the active layer z_a following Harris and Wiberg (1997; their equation 1):

$$(24) \qquad z_a = \max\left[k_1(\tau_{cw,\max} - \tau_{crit}), 0\right] + k_2 D_{50} .$$

where k_1 and k_2 were constants set equal to 0.007 $m^2\ s^2\ kg^{-1}$and 6.0, respectively. As implemented for the Waipaoa shelf, active layer thicknesses on the mid-shelf rarely exceeded ~5-10 mm and increased in shallow areas and near the anticlines due to the relatively high bed stress and larger sediment grains

found there (Figure 2-2). Overall, seabed erodibility was determined by the availability within the active layer of sediment having a critical shear stress exceeded by the combined wave-current bed stress.

Sediment bed properties such as grain size distribution were stored for eight seabed layers that initially represented 1.6 m of sediment. Erosion and deposition of multiple sediment classes modified the grain size distributions stored for the sediment bed and the thickness of the seabed layers, as described in Warner et al. (2008). These changes impacted the upper few layers of the sediment bed, while the deeper layers served as a repository of sediment. The surficial seabed layer was ~1 cm across the shelf on average, but was thinner in areas of low deposition and where the active layer was thin. Choice of model formulations and parameters is further discussed in section 2.3.7.

2.2.5 Open Boundary Conditions

The Waipaoa shelf model grid was bounded by land only on the northwestern side (Figure 2-1), so a free-slip wall condition was used there. Specifically, a zero gradient condition was assumed for tracers and sea surface elevation, water velocities normal to land were zero, and a free-slip condition was used for the tangential velocities:

(25) Clamped OBC:

$$\frac{\partial \eta}{\partial n} = 0$$
$$\frac{\partial C}{\partial n} = 0$$
$$\vec{u} \bullet \hat{n} = 0$$

where $\hat{n}$ is direction perpendicular to the boundary. Along the other three edges, open boundary conditions (OBCs) for sea surface height, barotropic and baroclinic velocities, and tracer concentrations

accounted for tides, shelf waves, and the transient behavior of the river plume. Radiation conditions along the southwest, southeast, and northeast boundaries allowed waves to propagate through them without reflecting. Specifically, the Chapman (1985) and Flather (1976; Roed and Smesdtad, 1984) conditions were applied at the model boundaries for the free surface and barotropic momentum, respectively, to account for tides (Martinsen and Engedahl, 1987; Palma and Matano, 1998; Carter and Merrifield, 2007):

(26) Chapman OBC: $$\frac{\partial \xi}{\partial t} + \sqrt{g(h+\eta)}\frac{\partial \xi}{\partial x} = 0$$

(27) Flather OBC: $$\frac{\partial \bar{u}}{\partial t} + \sqrt{gh}\frac{\partial \bar{u}}{\partial x} = 0 \;;\; \frac{\partial \eta}{\partial t} + h\frac{\partial \bar{u}}{\partial x} = 0$$

where ξ is the variable of interest (e.g. velocity, the free surface, or tracer concentrations) unless otherwise specified. Velocity, $u_{obc}(t)$, and sea surface height, $\eta_{obc}(t)$, at the boundary, required as input, were specified using data provided by M. Hadfield (National Institute for Water and Atmosphere, New Zealand; NIWA) from a larger-scale model, ROMS-NZ, described below (Figure 2-3). Similarly, using the oblique radiation condition for baroclinic velocities and tracer concentrations reduced artificial reflections at the boundaries (Chapman, 1985; Palma and Matano, 2000; Marchesiello et al., 2001).

Following Marchesiello et al. (2001) and Lavelle and Thacker (2008), the model nudged current velocities, salinity, temperature, and suspended sediment concentrations near open boundaries toward values specified from a larger scale hydrodynamic model, ROMS-NZ (see Section 2.3.5). Model nudging occurred at locations within the interior of the grid first, followed by points on the open boundary:

(28a) Nudging, evaluated within grid interior:

$$\xi = \xi' + \frac{F_{grid}}{T_{R0}}\left(\xi_{obc} - \xi'\right)\Delta t$$

(28b) Nudging-Radiation OBC, evaluated at model boundary:

$$\frac{\partial \xi}{\partial t} + c_x \frac{\partial \xi}{\partial x} + c_y \frac{\partial \xi}{\partial y} = F_{grid}\left(\frac{1}{\mathrm{T}_R}\right)\xi_{obc}(t)$$

$$c_x = -\frac{\partial \xi}{\partial t}\frac{\partial \xi / \partial x}{(\partial \xi / \partial x)^2 + (\partial \xi / \partial y)^2}$$

$$c_y = -\frac{\partial \xi}{\partial t}\frac{\partial \xi / \partial y}{(\partial \xi / \partial x)^2 + (\partial \xi / \partial y)^2}$$

$$T_R = \begin{cases} T_{RO} & current\ \ velocities\ \ directed\ \ out\ \ of\ \ grid \\ \dfrac{T_{RO}}{F_{OBC}} & current\ \ velocities\ \ directed\ \ \mathrm{into}\ \ grid \end{cases}$$

Here, ξ' was the variable of interest before any nudging occurred, T_R was the relaxation timescale, and Δt was the timestep. The larger scale model provided $\xi_{obc}(t)$. The relaxation timescale decreased with decreasing T_{RO} and increasing F_{OBC}, enhancing nudging when currents flowed into the model grid. Based on sensitivity tests, T_{RO} and F_{OBC} were set to 2.5 days and 2.5. The constant F_{grid} specified spatial variability for nudging so that it decreased sinusoidally with distance from the open boundary, and was limited to those locations within 30 grid cells of open boundaries:

$$(29) \qquad F_{grid} = \begin{cases} 1-\sin\left(\frac{\pi}{2}\frac{j}{30}\right) & for \quad j \in [1,30] \\ 1-\sin\left(\frac{\pi}{2}\frac{J-j+1}{30}\right) & for \quad j \in [J-29,J] \\ 1-\sin\left(\frac{\pi}{2}\frac{I-i+1}{30}\right) & for \quad i \in [I-29,I] \\ 0 & otherwise \end{cases}$$

where I and J were the total number of grid cells in the NW-SE and SW-NE directions and coordinates (i,j) indicate location within the grid. Note that since ROMS-NZ did not include sediment, this meant that suspended sediment concentrations within 30 grid cells of the boundaries were nudged toward zero. This model nesting not only enabled the model to account for larger scale currents, but also reduced reflection of river plume salinity and suspended sediment concentrations at the boundaries, and increased model stability.

2.3 Model Initialization and Forcing

Observed and modeled datasets for bathymetry, winds, waves, river discharge, tides, currents, temperature, salinity, metrological conditions and sediment were used to initialize and force the model. Table 2-3 lists the specific datasets. All interpolations used linear Delaunay triangulation, unless specified below.

2.3.1 Model grid construction and bathymetry

Designed to include the river mouth, Poverty Bay, and the proximal continental shelf, the model grid (Figure 2-1) also encompassed the three depocenters identified by Miller and Kuehl (2010), Gerber et al. (2010), and Orpin et al. (2006). Use of a curvilinear horizontal grid and a stretched terrain-following

vertical grid allowed the model to resolve regions of interest (e.g. two depocenters landward of shelf anticlines) and the near-bed and near-surface areas that have high vertical gradients in sediment concentration or velocity. While our model achieved lower resolution within Poverty Bay than that used by Bever and Harris (submitted), it included more of the proximal continental shelf, allowing us to focus on shelf transport mechanisms.

Gridgen, a program that creates near-orthogonal grids, and Matlab were used to construct an appropriate model grid that had a horizontal resolution of about 450 m on the mid-shelf (see Figure 2-1). The grid was curved to reduce the number of terrestrial grid cells and to approximately parallel bathymetry to facilitate post-processing of data (i.e. across-shelf fluxes), and reduce model errors associated with nesting and along-isobath flow (Hadfield, pers. comm., 2012). In the unmasked (water) section of the grid, the angles of grid corners deviated from perpendicular by a maximum of 1.4^{o} and a mean of 0.13^{o}. Vertical resolution varied with depth, and was about 0.25 m , 2.2 m, and 0.78 m near the surface, mid water-column, and seabed where the water was 24 m deep at the entrance to Poverty Bay. In deeper areas of the shelf, resolution decreased so that, for example, surface, mid-water column and near-bed layers were 0.39 m, 4.8 m, and 1.6 m thick at 52 m depth near the Southern depocenter.

Four datasets that each had a different focus provided the basis for the model's bathymetry. Multibeam was used to map Poverty Bay in 2005 and 2006 by J. McNinch (then VIMS, now USACoE), while S. Kuehl (VIMS) provided multibeam data of the continental shelf and slope that had been obtained in 2005 on the *R/V Kilo Moana*. The NIWA dataset provided by S. Stephens (NIWA) contained complete, though low resolution, 10 m bathymetric contours of the continental shelf and slope. Finally, the historical gridded bathymetry from NIWA was the only data source near the entrance of Poverty Bay. The datasets

were all referenced with respect to the WGS 84 datum and the universal transverse Mercator horizontal projection, except for the historical gridded dataset, for which the projection was unknown.

Comparisons revealed systematic offsets between the datasets. In areas that overlapped (see Figure 2-4), the NIWA contours and Kuehl water depths were ~3 m and ~2 m shallower, respectively, than those from J. McNinch. The offsets were removed by adding 3 and 2 m to the NIWA contours and Kuehl data, which aligned them with the McNinch data from Poverty Bay. The deeper-water datsets were referenced to the McNinch data because bed stresses were most sensitive to bathymetry in shallow water and because 2-3 m was a smaller percentage of water column height in deeper areas compared to shallow areas. These three data sets were then combined for interpolation. Note that because the NIWA 10 m contours had lower resolution for much of the shelf, this dataset was relatively sparse compared to the gridded products. Thus, the gridded multibeam datasets dominated the model bathymetry where they provided coverage, while the NIWA contours filled in areas that were sparsely covered, primarily near the coastline and in the southwest and northeast portions of the grid.

After gridding, the model bathymetry was smoothed with a Shapiro (1975) filter to improve model stability (Haney, 1991; Beckmann and Haidvogel, 1993; Sikiric et al., 2009). Finally, water depths near the open boundaries of the model grid were tapered to match ROMS-NZ bathymetry to facilitate model nesting. Both water depth and land-ocean masking were identical to ROMS-NZ over the region where nudging occurred (see Section 2.2.5). This methodology avoided noticeable seams where the datasets abutted, and the bathymetry, slope and curvature of the model grid (Figure 2-1) was consistent with those of each individual dataset. The greatest uncertainty in bathymetry unfortunately lay at the entrance of Poverty Bay, where recent datasets on known projections did not provide much coverage.

2.3.2 Winds and Waves

Modeled wind and wave data were used as input to account for their spatial and temporal variability. Estimates from NZLAM and NZWAVE (see Figure 2-5) were used because they were calibrated against local as opposed to global data, and had relatively fine resolution. NZLAM, an implementation of the UK Meteorological (Met) Office's Unified Model (Davies et al., 2005), provided hourly estimates of wind velocity on a 12 km resolution grid. A local implementation of NOAA's Wave Watch 3 model (Tolman et al., 2001), NZWAVE produced output every three hours on a 12 km resolution grid. Wind velocities and wave estimates (significant wave height, mean wave direction, wave length, and mean wave period) from these two models were interpolated to the ROMS grid and used as input.

Since NZWAVE did not provide wave spectra, the bottom wave period was assumed to be equal to the surface average period. This assumption resulted in underestimations of bottom wave period, because high frequency waves within a wave spectrum decay with water depth, h, so that only the longer-period waves are felt at depth. Wave orbital velocities, u_b, were calculated using linear wave theory and the interpolated NZWAVE data and bathymetry from the model grid:

$$u_b = \pi H_{sig} \Big/ T \sinh(2\pi h / L) \tag{30}$$

Where H_{sig} was significant wave height, L is wave length and T is wave period.

2.3.3 River discharge

Waipaoa River water and sediment discharges were represented as a point-source entering Poverty Bay at a single grid cell located near the river mouth. Observations of river stage were collected hourly at Kanakania Bridge, ~80 km upriver, above tidal influences by G. Hall and D. Peacock at the Gisborne

District Council (GDC). For water and sediment input, recently-calibrated rating curves provided by the GDC were applied to the river stage and water discharge, respectively (see Figure 2-5). ROMS required that the vertical profile of the freshwater and sediment flux be specified at the point source. For the Waipaoa River, the profile was configured so that the freshwater and river sediment was delivered in the top half of the water column to represent estuarine circulation(see Figure 2-6).

2.3.4 Tides

Tidal velocities, amplitudes and phase components extracted from the Oregon State Tidal Prediction Software (OTPS) TPX07.1 global solution (Egbert et al., 1994; Egbert and Erofeeva, 2002) were used to specify estimated tidal currents and sea surface height at model open boundaries. OTPS accounted for eleven ocean tidal constituents, and was driven by satellite altimeter data (i.e. TOPEX/Poseidon and Jason). This model was previously used by Bever and Harris (submitted) to represent tides on the Waipaoa Shelf and Poverty Bay. Future work may instead use NZTIDE, provided by M. Hadfield and M. Uddstrom (NIWA), because it is a locally-calibrated tide model (Walters et al., 2001).

2.3.5 Baroclinic Currents, Temperature and Salinity

Current velocities, temperature and salinity at and near open boundaries of the Waipaoa grid were nudged toward values from ROMS-NZ, a larger scale baroclinic model adapted for northern New Zealand by M. Hadfield (NIWA; see Figure 2-3). ROMS-NZ provided estimates of current velocity, temperature and salinity every three hours on an about two kilometer grid. This one-way nesting of the Waipaoa shelf model within the lower resolution hydrodynamic model allowed larger-scale circulation (i.e. shelf waves and offshore eddies) to influence modeled Waipaoa shelf hydrodynamics. ROMS-NZ estimates agreed well with NIWA's established storm surge model River and Coastal Ocean Model (RiCOM;

Walters, 2005, 2006; Lane and Walters, 2009), and used a rectilinear grid, which facilitated interpolation of currents between grids (Hadfield, pers. comm., 2010).

Three-dimensional, time dependent current velocities, temperature and salinity estimates from ROMS-NZ were linearly interpolated to the Waipaoa shelf grid and used for model initialization and nudging at model boundaries. ROMS-NZ estimates were unavailable for some grid cells near the coast in the interior of the grid where the land-ocean masking differed between the two models. At these sites, current velocities were initialized to zero, and initial temperature and salinity estimates were set equal to values from adjacent grid cells. Since land-ocean masking was identical between model grids near the open boundaries, these approximations only affected model initialization and not nudging at open boundaries (see Section 2.2.5).

2.3.6 Atmospheric forcing

As discussed in section 2.3.2, wind velocities were interpolated from the estimates provided by NZLAM. ROMS also required as input estimates for air pressure, cloud cover, precipitation, relative humidity, shortwave radiation, and air temperature. Hourly records of these metrological data from the Gisborne, NZ airport were applied uniformly across the Waipaoa shelf, and obtained from NIWA's National Climate Database web system (Cliflo; http://cliflo.niwa.co.nz/).

2.3.7 Sediment characteristics

Model calculations accounted for a total of seven sediment types and eight seabed layers (see Table 2-4). Different sediment classes were used to store fluvial and bed sediment so that model analysis could differentiate between material from these two sources. Although model calculations included both

types of sediment, nearly all of the analysis presented in Chapter 3 focused on the transport and fate of the riverine material. Wadman and McNinch (2009), Wood (2006) and the January, 2010 cruise provided data used to develop the initial seabed sediment distributions (Figure 2-7). Grain size data were converted to percent sand and percent mud for all sites, and then spatially interpolated. Near the model open boundaries, there was no available grain size data and so grid cells with water depth deeper than 300 m or near the northeastern and southwestern boundaries were assumed to be mud. For the purpose of interpolation, the coastline was assumed to be composed of sand. Finally, the grain size distribution was constrained so that at least 10% of the seabed was composed of fast-settling material to enhance bed armoring based on Bever and Harris (submitted).

Four classes were used to represent sediment delivered fluvially. Their properties were informed by Hicks et al. (2004) and tripod estimates of effective settling velocity from the field site (obtained from A. Ogston and R. Hale, University of Washington). These sources estimated a median grain diameter of 8.5 μm in the Waipaoa river during floods and effective settling velocities ranging from <0.1 to ~ 1 mm s^{-1}, with a peak at ~0.1 mm s^{-1} during energetic shelf conditions at 40 m water depth. Since information regarding the distribution of sediment settling velocity in the river plume was unavailable, however, a range of reasonable sediment settling velocities (0.15 – 1 mm s^{-1}) was chosen. The fluvial sediment was logarithmically partitioned into these sediment classes following sensitivity tests that considered the sediment budgets for Poverty Bay and the continental shelf following a three month model run representing early 2010.

Sediment parameters (critical shear stress, erosion rate parameter) were chosen to match estimates from ADV (Acoustic Doppler Velocimeter) and OBS (Optical Backscatter Sensor) measurements from the

first two months of the tripod deployment (data obtained from A. Ogston and R. Hale, University of Washington) and Gust erosion chamber experiments conducted at the field site (data from J.P. Walsh, D.R. Corbett, and J. Kiker, East Carolina University; Kiker; 2012). Critical shear stress for riverine sediment was set to 0.1 Pa, consistent with tripod estimates of bed shear stress and sediment concentration, Gust chamber erodibility experiments (Kiker, 2012), and sediment transport models for other continental shelves that represented fluvial sediment (e.g. Ferre et al., 2010; Harris et al. 2008; Harris et al. 2005; Harris and Wiberg, 2002; Wiberg et al., 1994). Seabed sediment classes were assigned critical shear stress values that varied with grain size and source. Porosity was assumed constant across the shelf and was set equal to a relatively high value of 0.9 based on estimates of seabed elevation change from ADV backscatter. The erosion rate parameter (Equation (23)) was assigned a value of $M = 2 \times 10^{-4}$ kg m^{-2} s^{-1} based on OBS-derived suspended sediment concentrations. Although the model neglected seabed consolidation, spatially-variable sediment distributions and bed stresses created a gradient of high to low seabed erodibility from Poverty Bay to the depocenters, consistent with Gust erodibility estimates, as discussed in Chapter 3.

2.4 Computational Limits

Many decisions in the implementation of three-dimensional numerical ocean models must consider tradeoffs between the required accuracy, an acceptable level of spatial resolution and computational limits. The model described had a total of 118 x 287 horizontal grid cells, each with 20 vertical water column layers and 8 vertical sediment bed layers. A total of 9 tracer variables were estimated (salinity, temperature, and seven sediment classes), in addition to the momentum state variables. To provide estimates that overlapped with the Poverty Shelf field experiment, the modeled time period spanned

thirteen months, from January, 2010 – February, 2011. In setting up the model, sensitivity tests were run on a subset of this time period, the three months at the beginning of the longer model run.

ROMS has been parallelized using MPI (Message Passing Interface), which allowed us to run the model on the Virginia Institute of Marine Science's (VIMS') High Performance Computing (HPC) cluster using 16 nodes. The full thirteen month model run required 23 days to run to completion. Some choices of model implementation significantly slowed the computations, including the MPData algorithm for horizontal advection of tracers, and the nudging of currents and tracers near the open boundaries. These components of the model were, however, important for model stability.

Each thirteen month model run produced ~210 gigabytes (GB) of model output, which recorded hourly estimates of state variables including velocities and tracer concentrations for each grid point, as well as characteristics of the sediment bed.

2.5. Summary

This project built on previous efforts by using a nested hydrodynamic – sediment transport model to examine sediment fluxes on the Waipaoa Shelf. A three-dimensional sediment transport model accounting for a river plume, winds, waves, larger scale currents, and tides was developed and implemented for the Waipaoa Shelf, New Zealand. These processes were represented using the ROMS-CSTMS framework in conjunction with locally-validated observed and modeled datasets described above. By varying spatial and vertical resolution in the model, we focused on the area of interest and boundary layer processes while maintaining sufficient model efficiency.

References

Ariathurai, C.R and Arulanandan, K., 1978. Erosion rates of cohesive soils. Journal of Hydraulics Division, 104 (2): 279 – 282.

Beckmann, A. and Haidvogel, D. B., 1993. Numerical simulation of flow around a tall isolated seamount. part I: Formulation and model accuracy. Journal of Physical Oceanography, 23: 1736-1753.

Bever, A.J. and Harris, C.K., 2012. Storm and fair-weather driven sediment-transport within Poverty Bay, New Zealand, evaluated using coupled numerical models. Continental Shelf Research. *Submitted.*

Blumberg, A.F. and Mellor, G.L., 1987. A description of a three-dimensional coastal ocean circulation model. Coastal and estuarine sciences, 4: 1-16.

Blumberg, A.F. and Mellor, G.L., 1983. Diagnostic and prognostic numerical circulation studies of the South Atlantic Bight. Journal of Geophysical Research, 88 (C8): 4579-4592.

Carter, G.S. and Merrifield, M.A., 2007. Open boundary conditions for regional tidal simulations. Ocean Modelling, 18 (3-4): 194-209.

Chapman, D. C., 1985. Numerical treatment of cross-shelf open boundaries in a barotropic coastal ocean model. Journal of Physical Oceanography, 15: 1060-1075.

Chen, C. and Liu, H., 2003. An unstructured grid, finite-volume, three-dimensional, primitive equations ocean model: Application to coastal ocean and estuaries. Journal of atmospheric and oceanic technology, 20: 159-186.

Colella, P. and Woodward, P., 1984: The piecewise parabolic method (PPM) for gas-dynamical simulations. Journal of Computational Physics, 54: 174-201.

Davies, T., Cullen, M.J.P., Malcolm, A.J., Mawson, M.H., Staniforth, A., White, A.A. and Wood, N., 2005. A new dynamical core for the Met Office's global and regional modelling of the atmosphere. Quarterly Journal of the Royal Meteorological Society, 131: 1759-1782. doi: 10.1256/qj.04.101.

Egbert, G., Bennet, A., and Foreman, M., 1994. TOPEX/Poseidon tides estimated using a global inverse model. Journal of Geophysical Research, 99 (C12): 24821 – 24852.

Egbert, G.D., and Erofeeva, S.Y., 2002. Efficient inverse modeling of barotropic ocean tides. Journal of Oceanic Technology, 19(2): 183-204.

Ezer, T., Arango, H. and Shchepetkin, A., 2002. Developments in terrain-following ocean models: intercomparisons of numerical aspects. Ocean Modelling, 4: 249-267.

Fairall, C.W., Bradley, E.F., Rogers, D.P., Edson, J.B., and Young, G.S., 1996. Bulk parameterization of air-sea fluxes for Tropical Ocean-Global Atmosphere Coupled-Ocean Atmosphere Response Experiment. Journal of Geophysical Research, 101 (C2): 3747-3764.

Fairall, C.W., Bradley, E.F., Hare, J.E., Grachev, A.A. and Edson, J.B., 2003. Bulk parameterization of air-sea fluxes: Updates and verification for the COARE Algorithm. Journal of Climate, 16: 571-591.

Ferre, B., Sherwood, C.R. and Wiberg, P.L., 2010. Sediment transport on the Palos Verdes shelf, California. Continental Shelf Research, 30: 761-780.

Flather, R.A., 1976. A tidal model of the north-west European continental shelf. Memoires Societe Royale des Sciences de Liege, 6 (10): 141-164.

Gerber, T. P., Pratson, L. F., Kuehl, S., Walsh, J. P., Alexander, C., and Palmer, A., 2010. The influence of sea level and tectonics on late Pleistocene through Holocene sediment storage along the high-sediment supply Waipaoa continental shelf. Marine Geology, 270(1-4): 139-159.

Haidvogel, D. B., Arango, H. G., Hedstrom, K., Beckmann, A., Malanotte-Rizzoli, P., and Shchepetkin, A. F., 2000. Model evaluation experiments in the North Atlantic basin: Simulations in nonlinear terrain-following coordinates. Dynamics of Atmospheres and Oceans, 32(3-4): 239-281.

Haidvogel, D. B., Arango, H., Budgell, W. P., Cornuelle, B. D., Curchitser, E., Di Lorenzo, E., et al., 2008. Ocean forecasting in terrain-following coordinates: Formulation and skill assessment of the regional ocean modeling system. Journal of Computational Physics, 227(7): 3595-3624.

Haney, R. L., 1991. On the pressure gradient force over steep topography in sigma coordinate ocean models. Journal of Physical Oceanography, 21: 610-619.

Harris, C. K., Sherwood, C.R., Signell, R.P., Bever, A.J., and Warner, J.C., 2008. Sediment dispersal in the northwestern Adriatic Sea. Journal of Geophysical Research, 113: C11S03. doi: 10.1029/2006/JC002868.

Harris, C. K., Traykovski, P., and Geyer, W. R., 2005. Flood dispersal and deposition by near-bed gravitational sediment flows and oceanographic transport : A numerical modeling study of the eel river shelf, northern California. Journal of Geophysical Research, 110: C09025. doi: 10.1029/2004JC002727.

Harris, C.K. and Wiberg, P., 1997. Approaches to quantifying long-term continental shelf sediment transport with an example from the northern California STRESS mid-shelf site. Continental Shelf Research, 17: 1389-1418.

Harris, C. K. and Wiberg, P., 2002. Across-shelf sediment transport: Interactions between suspended sediment and bed sediment. Journal of Geophysical Research, 107 (C1): 3008. doi: 10.1029/2000JC000634.

Hicks, D. M., Gomez, B. and Trustrum, N. A., 2004. Event suspended sediment characteristics and the generation of hyperpycnal plumes at river mouths: East coast continental margin, north island, New Zealand. The Journal of Geology, 112(4): 471-485.

Huang, H., Chen, C., Cowles, G.W., Winant, C.D., Beardsley, R.C., Hedstrom, K.S., and Haidvogel, D.B., 2008. FVCOM validation experiments: Comparisons with ROMS for three idealized barotropic test problems. Journal of Geophysical Research, 113 (7); C07042. doi:10.1029/2007JC004557.

Hyatt, J. and Signell, R.P., 2000. Modeling surface trapped river plumes: A sensitivity study. In: M.L. Spaulding and A.F. Blumberg (Editors). 6th International Conference on Estuarine and Coastal Modeling. 3-5 November 1999. New Orleans, LA.

Jackett, D.R. and McDougall, T.J., 1995. Minimal adjustment of hydrographic profiles to achieve static stability. Journal of Atmospheric and Oceanic Technology, 12: 381-389.

Kiker, J.M., 2012. Spatial and temporal variability in surficial seabed character, Waipaoa River Margin, New Zealand. M.S. Thesis, East Carolina University, Greenville, NC.

Lane, E. M., and Walters, R. A., 2009. Verification of RiCOM for storm surge forecasting. Marine Geodesy, 32(2): 118-132.

Lavelle, J.W. & Thacker, W.C., 2008. A pretty good sponge: Dealing with open boundaries in limited-area ocean models. Ocean Modelling, 20: 270-292.

Liu, W. T., Katsaros, K. Bl. and Businger, J.A., 1979. Bulk parameterization of Air-Sea Exchanges of Heat and Water Vapor Including the Molecular Constraints at the Interface. Journal of the Atmospheric Sciences, 36: 1722-1735.

Liu, X.D., Osher, S. and Chan, T., 1994: Weighted essentially nonoscillatory schemes, J. Comp. Phys., 115, 200-212.

Madsen, O.S., 1994. Spectral wave-current bottom boundary layer flows. Proceedings of the 24th International Conference on Coastal Engineering, ASCE, Kobe 1:384-398.

Marchesiello, P., McWilliams, J. C., & Shchepetkin, A., 2001. Open boundary conditions for long-term integration of regional oceanic models. Ocean Modelling, 3(1-2): 1-20.

Martinsen, E. A., & Engedahl, H., 1987. Implementation and testing of a lateral boundary scheme as an open boundary condition in a barotropic ocean model. Coastal Engineering, 11(5-6): 603-627.

Mellor, G.L., Oey, L.-Y. and Ezer, T., 1994. The pressure gradient conundrum of sigma coordinate ocean models. Journal of Atmospheric and Oceanic Technology, 11: 1126-1134.

Mellor, G.L., Oey, L.-Y., and Ezer, T., 1998. Sigma coordinate pressure gradient errors and the seamount problem. Journal of Atmospheric and Oceanic Technology, 15: 1122-1131.

Miller, A. J., and Kuehl, S. A., 2010. Shelf sedimentation on a tectonically active margin: A modern sediment budget for Poverty continental shelf, New Zealand. Marine Geology, 270(1-4): 175-187.

Orpin, A. R., Alexander, C., Carter, L., Kuehl, S., and Walsh, J. P., 2006. Temporal and spatial complexity in post-glacial sedimentation on the tectonically active, Poverty Bay continental margin of New Zealand. Continental Shelf Research, 26(17-18): 2205-2224.

Palma, E. D., and Matano, R. P., 1998. On the implementation of passive open boundary conditions for a general circulation model: The barotropic mode. Journal of Geophysical Research, 103(C1): 1319-1341.

Palma, E.D., and Matano, R.P., 2000. On the implementation of open boundary conditions for a general circulationmodel: The three-dimensional case. Journal of Geophysical Research, 105 (C4): 8605-8627.

Parchure, T. M., and Mehta, A. J., 1985. Erosion of soft cohesive sediment deposits. Journal of Hydraulic Engineering, 111(10): 1308-1326.

Paterson, D.M., 1997. Biological mediation of sediment erodibility: ecology and physical dynamics. In N. Burt, R. Parker, and J. Watts (Eds.), Cohesive Sediments. Proceedings of the 4th Nearshore and Estuarine Cohesive Sediment Transport Conference, 11-15 July 1994, pp. 215-231.

Roed, L.P. and Smedstad, O.M., 1984. Open boundary conditions for forced waves in a rotating fluid. SIAM Journal Sci. Stat. Comput, 5: 414-426.

Tolman, H. L., Balasubramaniyan, B., Burroughs, L. D., Chalikov, D. V., Chao, Y. Y., Chen, H. S., et al., 2002. Development and implementation of wind-generated ocean surface wave modelsat NCEP*. Weather and Forecasting, 17(2): 311-333.

Shapiro, R., 1975. Linear filtering. Mathematics of Computation, 29(132): 1094-1097.

Shchepetkin, A. F. and J. C. McWilliams, 1998. Quasi-monotone advection schemes based on explicit locally adaptive dissipation. Monthly Weather Review, 126: 1541-1580.

Shchepetkin, A. F. and J. C. McWilliams, 2003: A method for computing horizontal pressure-gradient force in an oceanic model with a nonaligned vertical coordinate, Journal of Geophysical Research, 108 (C3): 3090. doi:10.1029/2001JC001047 .

Shchepetkin, A. F. and McWilliams, J. C., 2005. The regional oceanic modeling system (ROMS): A split-explicit, free-surface, topography-following-coordinate oceanic model. Ocean Modelling, 9(4): 347-404.

Shchepetkin, A. F. and McWilliams, J. C., 2009. Correction and commentary for "Ocean forecasting in terrain-following coordinates: Formulation and skill assessment of the regional ocean modeling system" by Haidvogel et al., J. comp. phys. 227, pp. 3595–3624. Journal of Computational Physics, 228(24): 8985-9000.

Sikiric, M. D., Janekovic, I., and Kuzmic, M., 2009. A new approach to bathymetry smoothing in sigma-coordinate ocean models. Ocean Modelling, 29: 128-136.

Smolarkiewicz, P. K., and Margolin, L. G., 1998. MPDATA: A finite-difference solver for geophysical flows, Journal of Computational Physics, 140(2): 459-480.

Syvitski, J.P.M, Asprey, K.W., Clattenburg, D.A., and Hodge, G.D., 1985. The prodelta environment of a fjord: suspended particle dynamics. Sedimentology, 32: 83-107.

Wadman, H.M. and McNinch, J.E., 2009. Sediment segregation and dispersal across the land-sea interface: Waipaoa sedimentary system, New Zealand, Integration and Synthesis of MARGINS Sediment Source-to-Sink Research Workshop, Gisborne, New Zealand.

Walters, R. A., 2005. Coastal ocean models: Two useful finite element methods. Continental Shelf Research, 25: 775-793.

Walters, R. A., 2006. Design considerations for a finite element coastal ocean model. Ocean Modelling, 15: 90-100.

Walters, R. A., Goring, D. G., and Bell, R. G., 2001. Ocean tides around New Zealand. New Zealand Journal of Marine and Freshwater Research, 35(3): 567-579.

Warner, J. C., Sherwood, C. R., Signell, R. P., Harris, C. K. and Arango, H. G., 2008. Development of a three-dimensional, regional, coupled wave, current, and sediment-transport model. Computers & Geosciences, 34(10): 1284-1306.

Wiberg, P. L., Drake, D. E., and Cacchione, D. A., 1994. Sediment resuspension and bed armoring during high bottom stress events on the northern California inner continental shelf: Measurements and predictions. Continental Shelf Research, 14(10-11): 1191-1219.

Wood, M. P., 2006. Sedimentation on a high input continental shelf at the active Hikurangi margin. M.S. thesis, Victoria University of Wellington, Wellington, New Zealand.

Tables

Table 2-1: Parameters in ROMS-CSTMS as described in Chapter 2

Parameter	Meaning	Unit
C	Tracer concentration	Amount of tracer (degrees celsius, psu, or kg of sediment) per cubic meter of water
C_d	Surface layer drag coefficient	non-dimensional
C_s	Suspended sediment concentration	kg m^{-3}
$C_{s,1}$	Suspended sediment concentration per unit area of the bed in the bottom water column grid cell	kg m^{-2}
C_μ	Coefficient for wave-current interaction in bottom boundary layer	non-dimensional
c_x, c_y	Phase speeds for oblique radiation boundary condition	m s^{-1}
D	Dispersion	m s^{-2}
D_{50}	Median grain diameter	m
E	Erosion	kg m^{-2} s^{-1}
f	Coriolis parameter	s^{-1}
f_{cw}	Wave friction factor	non-dimensional
F	Forcing term in ROMS momentum and tracer advective-diffusion equations. Can include, but is not limited to, sediment settling between vertical layers, surface stress, and river discharge	m s^{-2}
F_c	Source of sediment to the water column due to seabed deposition and erosion	kg m^{-2} s^{-1}
F_{grid}	Constant specifying spatially-variable nudging at open boundaries	non-dimensional
F_{OBC}	Constant specifying changes to nudging at open boundaries based on direction of currents	non-dimensional
g	Gravitational constant	m s^{-2}
H_{sig}	Significant wave height	m
h	Water depth	m
I	Number of grid cells in NW-SE direction	non-dimensional
i	Index for model grid in NW-SE direction	non-dimensional
J	Number of grid cells in SW-NE direction	non-dimensional
j	Index for model grid in SW-NE direction	non-dimensional
K_M	Eddy viscosity	m^2 s^{-1}

k_1 , k_2	Coefficients for active layer formulation (0.007 and 6.0, respectively)	$m^2\ s^2\ kg^{-1}$; non-dimensional
k_N	Bottom roughness for bed shear stress calculations	m
L	Wave length	m
M	Erosion rate parameter	$kg\ m^{-2}\ s^{-1}$
p	Seabed porosity	non-dimensional
R	Rainfall rate	$kg\ m^{-2}\ s^{-1}$
S	Salinity	psu
T	Wave period	s
T_R	Relaxation timescale for nudging at open boundaries	s
T_{RO}	Relaxation constant for nudging at open boundaries	non-dimensional
t	Time	s
u	Current velocity in x direction	$m\ s^{-1}$
$\overline{u}$	Depth-averaged velocity	$m\ s^{-1}$
u_{obc}	Prescribed value for vertically averaged velocity in open boundary equations	$m\ s^{-1}$
u_b	Wave orbital velocity	$m\ s^{-1}$
u_r	Near-bed current speed at reference height z_r	$m\ s^{-1}$
u_{*c}	Current-induced shear velocity	$m\ s^{-1}$
$u_{*cw,max}$	Maximum combined wave-current shear velocity	$m\ s^{-1}$
$u_{*w,max}$	Maximum wave-induced shear velocity	$m\ s^{-1}$
v	Current velocity in y direction	$m\ s^{-1}$
$\overrightarrow{W}$	Mean wind velocity	$m\ s^{-1}$
$\overrightarrow{W_{gust}}$	Wind gusts	$m\ s^{-1}$
W_*	Monin-Obukhov similarity scaling parameter	$m^2\ s^{-2}$
w_s	Sediment settling velocity	$m\ s^{-1}$
x, y	Horizontal coordinates	non-dimensional
Z_0	Roughness length for atmospheric boundary layer	m
Z_{obs}	Height of observations above ocean surface	m
z	Vertical coordinate in water column	non-dimensional
z_0	Hydrodynamic roughness	m
$z_{0,N}$	Bottom roughness due to sediment grains	m
z_1	Upper boundary of wave-current boundary layer in bottom boundary formulation	m
z_a	Thickness of seabed active layer	m
z_{cw}	Thickness of wave boundary layer for	m

	calculations of bed shear stress	
z_r	Reference height for near-bed currents	m
z_s	Vertical coordinate in seabed	m
α	Charnock constant	non-dimensional
η	Sea surface height	m
η_0	Prescribed value for sea surface height in open boundary equations	m
κ	vanKarmen constant	Non-dimensional
ν	Seawater viscosity	$m^2 s^{-1}$
ξ	Variable of interest in boundary condition equations	Same units as velocity, sea surface height, temperature, salinity, or sediment concentrations
ξ_{obc}	Prescribed value for variable of interest in open boundary condition equations	Same units as velocity, sea surface height, temperature, salinity, or sediment concentrations
ρ	Water density	$kg\ m^{-3}$
ρ_0	Reference water density	$kg\ m^{-3}$
ρ_{air}	Air density	$kg\ m^{-3}$
ρ_s	Sediment density	$kg\ m^{-3}$
$\overrightarrow{\tau_{w,\max}}$	Maximum wave-induced bed shear stress over a wave period	Pa
$\overrightarrow{\tau_c}$	Current-induced bed shear stress	Pa
$\overrightarrow{\tau_{cw,\max}}$	Maximum wave-current induced bed shear stress over a wave period	Pa
τ_{crit}	Critical shear stress for seabed	Pa
$\overrightarrow{\tau_{surface}}$	Shear stress at ocean surface	Pa
ϕ	Dynamic pressure (Pressure divided by a reference density)	$m^2 s^{-2}$
ϕ_{cw}	Angle between waves and currents in bottom boundary layer	Radians
ψ_w	Stability function for atmospheric boundary layer	non-dimensional
ω	Angular wave frequency	1/s

Table 2-2: Numerical Schemes for Waipaoa Shelf Model

Descriptions and citations of numerical schemes provided in Section 2.2.1.

Process	Numerical Scheme
Advection of momentum (Vertical, 3D)	4^{th} order, centered
Advection of momentum (Horizontal, 3D)	3^{rd} order, upstream
Advection of tracers	MPData
Vertical Sediment Settling	PPM

Table 2-3: Datasets used for model initialization and forcing

Type of Data	Data Description and Source
Bathymetry to construct model grid	• Multibeam surveys (McNinch et al., 2008; Gerber et al., 2010 provided by S. Kuehl) • Bathymetric contours provided by S. Stephens (NIWA) • Historical gridded bathymetry (pers. Comm. NIWA) • Modeled bathymetry of New Zealand ROMs model (ROMS-NZ; Hadfield, 2010)
Currents, temperature and salinity at open boundaries, and for model initialization	• Baroclinic version of ROMS-NZ, provided by M. Hadfield
Wave height, direction, and period	• NIWA's New Zealand Wave (NZWAVE) model (NZWAVE, an implementation of NOAA's Wave Watch III model; Tolman et al., 2002)
Wind stress	• NIWA's New Zealand Limited Area Model (NZLAM, an implementation of the UK Met Office's Unified Model; Davies et al., 2005)
Tidal components: open boundary sea surface height and tidal velocities	• Tidal velocities, amplitudes and phase components from the Oregon State Tidal Prediction Software TPX07.1 global solution (OTPS; Egbert et al., 1994; Egbert and Erofeeva, 2002)
Metrological data	• Air pressure, cloud cover, precipitation, relative humidity, shortwave radiation, air temperature from NIWA's National Climate Database web system (Cliflo; http://cliflo.niwa.co.nz/) at Gisborne airport
River discharge of freshwater and sediment	• River gauge measurements provided by G. Hall and D. Peacock (Gisborne District Council, New Zealand)
Sediment properties of fluvial and seabed material (diameter, settling velocity, critical stress for erosion)	• Hicks et al., 2004 • Wood, 2006. • ADV and OBS data provided by A. Ogston and R. Hale
Seabed characteristics for comparison to model estimates	• Radiometric and x-ray analysis of cores (by J.P. Walsh, R. Corbett, and J. Kiker of ECU; A. Orpin of NIWA; and T. Kniskern of VIMS)

Table 2-4: Sediment characteristics for all sediment classes

Grain Size Class	Sediment Source	% of Riverine Load	Settling Velocity (mm s^{-1})	Critical Shear Stress (Pa)	D_{50}(μm)	D_{50}(phi)
1	Seabed	--	2.4	0.1	63	4.0
2	Seabed	--	65.0	0.28	500	1.0
3	Seabed	--	125.0	0.53	1000	0.0
4	River	53	0.15	0.1	16	6.0
5	River	27	0.3	0.1	22	5.5
6	River	13	0.5	0.1	30	5.1
7	River	7	1.0	0.1	40	4.6
For all grain size classes: Sediment density: 2650 kg/m^3 Erosion rate: 2×10^{-4} $kg/m^2/s$ Porosity: 0.9						

Figures

Figure 2-1: Study site on North Island, New Zealand

A. Adapted from Miller and Kuehl, 2009. Spatial distribution of ^{210}Pb accumulation rates (cm y^{-1}) with labels for Waipaoa River (red arrow), Poverty Bay, Poverty Gap, Lachlan Anticline (L.A.), Ariel Anticline (A.A.), and depocenters (Dep.). Grey bathymetric contours indicate every 10 m. ***B.*** Waipaoa Shelf map showing tripod locations (brown) and multi-core stations (black) from the first research cruise. Grey and black bathymetric contours indicate every 10 m up to 100 m depth and every 50 m up to 150 m depth. Inset shows location of study site in New Zealand. ***C.*** Waipaoa model grid showing bathymetry with gridlines. Each box encompasses 25 grid cells. Model boundaries labeled 'NW', 'SW', 'SE', 'NE'. ***D.*** Waipaoa model grid showing details of shelf bathymetry without gridlines. Grey and black bathymetric contours indicate every 10 m up to 100 m depth and every 50 m up to 150 m depth.

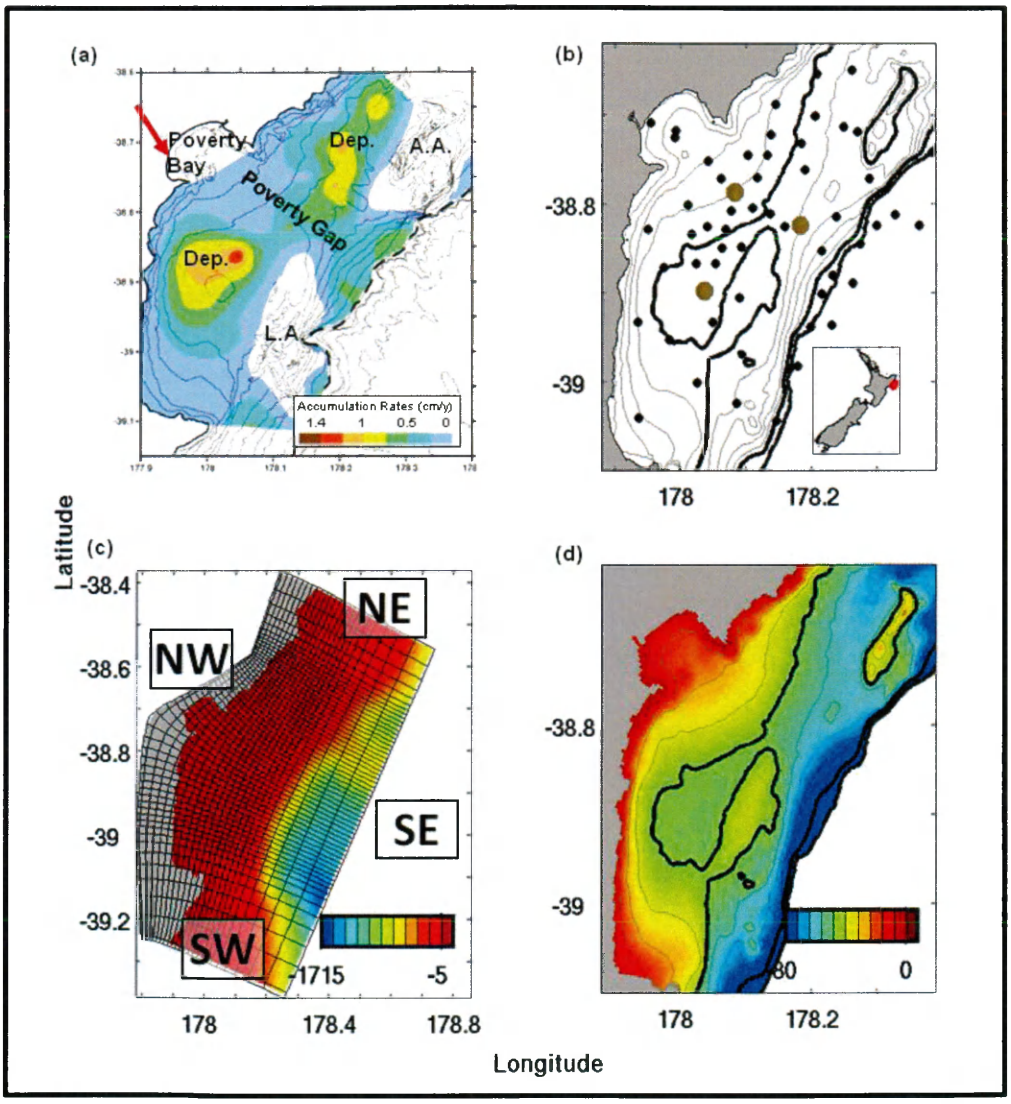
(a)
Poverty Bay
Dep.
A.A.
Poverty Gap
Dep.
L.A.
Accumulation Rates (cm/y)
1.4 1 0.5 0
(b)
-38.8
-39
178
178.2
(c)
Latitude
-38.4
-38.6
-38.8
-39
-39.2
NE
NW
SE
SW
-1715
-5
178
178.4
178.8
(d)
-38.8
-39
0
178
178.2
Longitude

Figure 2-2: Sediment within active layer

Shows time-averaged (a) mass of sediment within the active layer and (b) mass of riverine sediment within the active layer. Colorbar in (b) is for both panels. To obtain estimated active layer thickness in millimeters, assuming a sediment density of 2650 kg m^{-3} and a porosity of 0.9, multiply the figure's colorbar by 3.8 m^3 kg^{-1}.

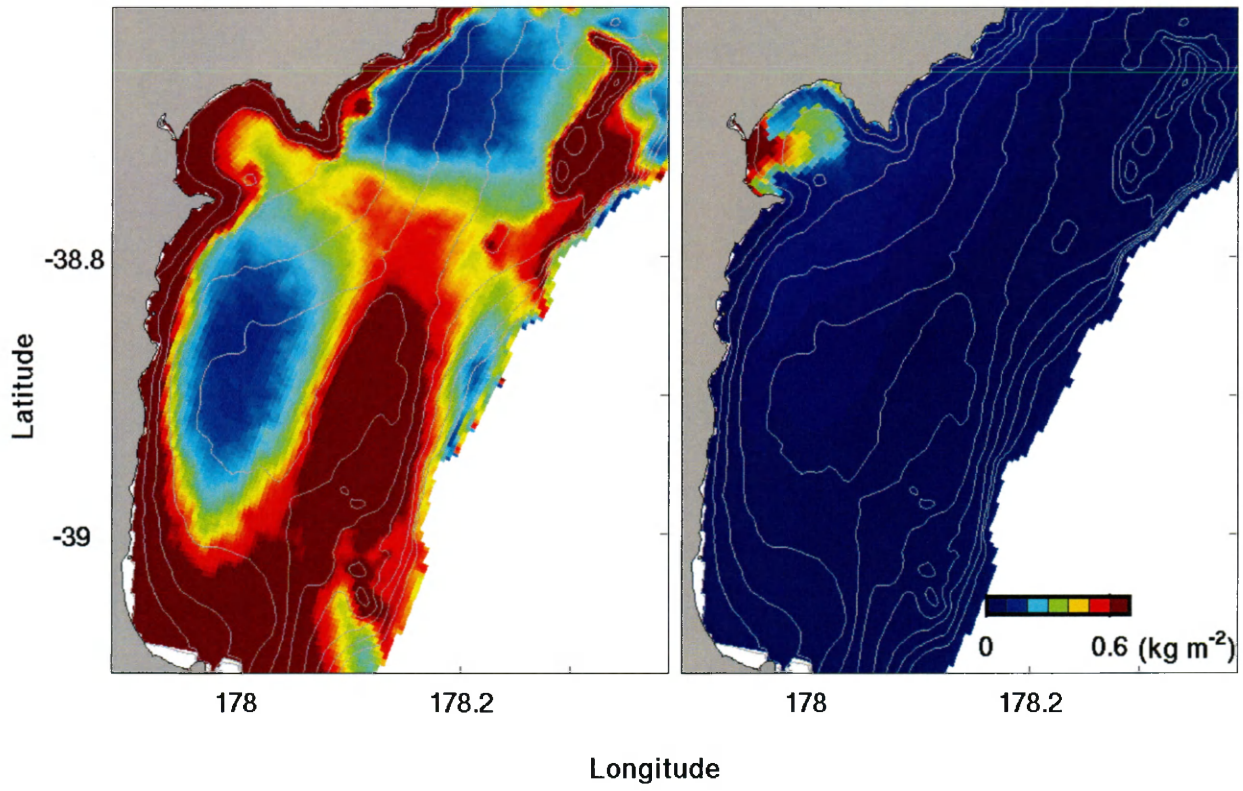

Figure 2-3**: Bathymetric map of the larger-scale model NZ-ROMS**

Bathymetric map of larger grid used by NZ-ROMS covering the eastern half of North Island, New Zealand. Black box shows approximate extent of the Waipaoa shelf model. Note that the X direction is oriented Northeast, the Y direction is oriented to the Northwest, and bathymetry is given in meters. Figure slightly modified by one provided by Mark Hadfield, NIWA.

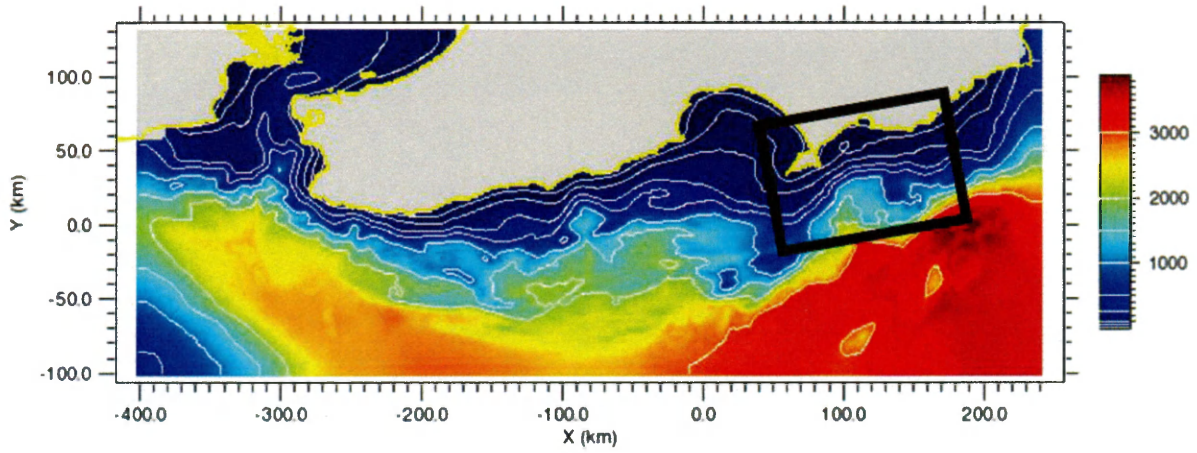

Figure 2-4: Coverage of bathymetric datasets near Poverty Bay mouth

The NIWA contours also act as 10 m bathymetric contours. Note that the NIWA contours and multibeam data provided by S. Kuehl extend onto the continental shelf and slope.

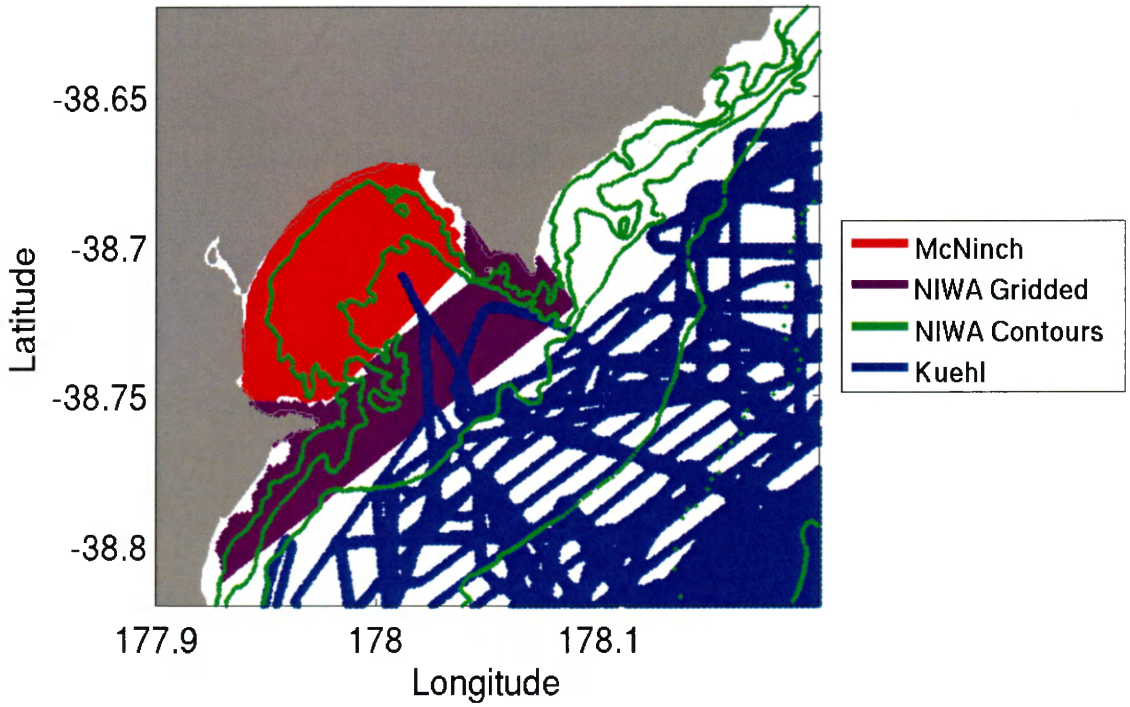

Figure 2-5: Timeseries of weather conditions on Waipaoa Shelf

(a) River and (b) sediment discharge from Gisborne District Council, New Zealand, (c) modeled significant wave height from NZWAVE, (d) modeled wind speed from NZLAM, and (e) modeled depth-averaged tidally-filtered current speed from ROMS-NZ. Wave and wind time-series are averages over the model domain. Currents are model estimates made for a location near the shallow tripod site (see Figure 1b). Grey boxes identify events analyzed in Chapter 3.

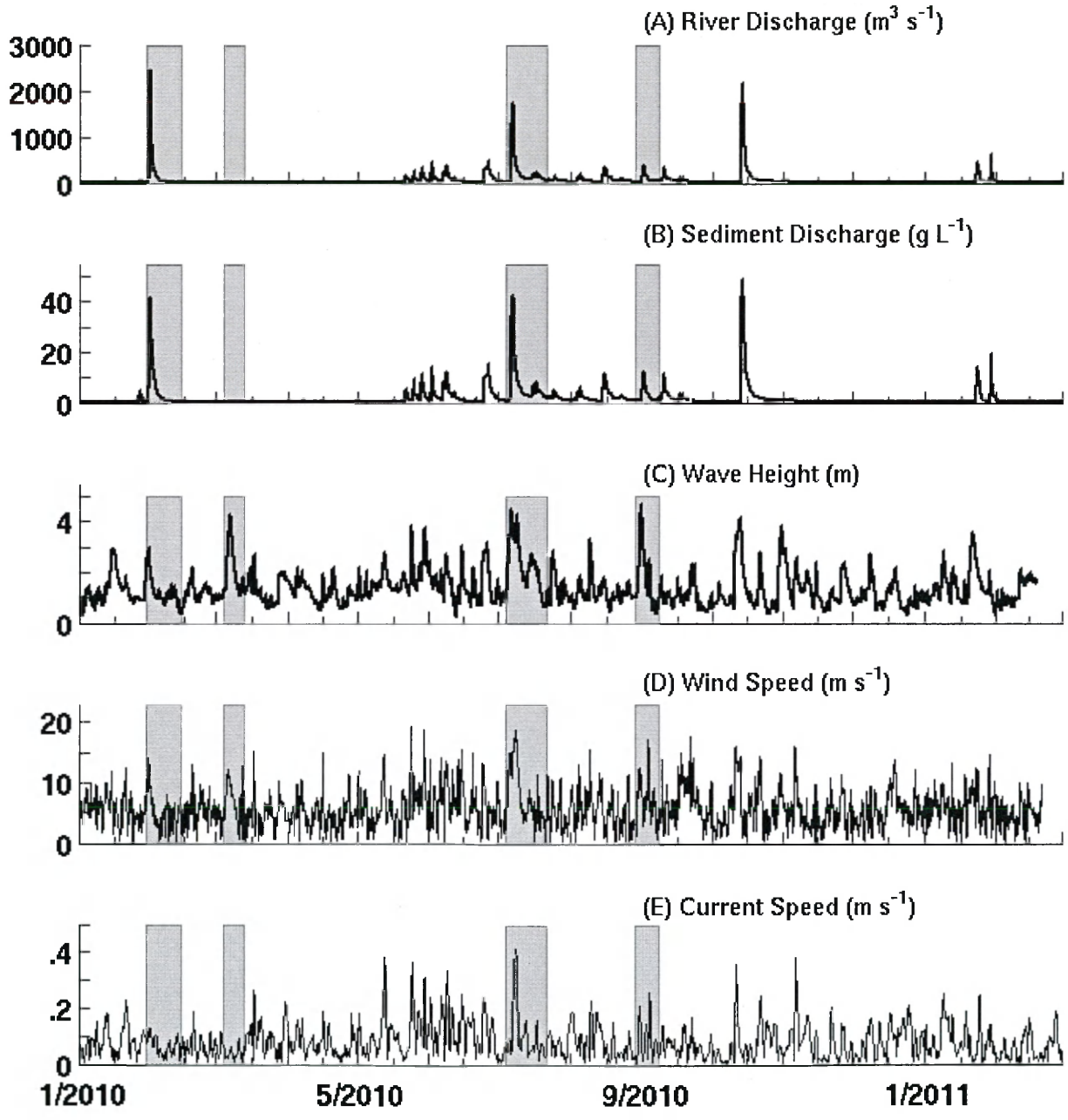
(A) River Discharge (m^3 s^{-1})
3000
2000
1000
0
(B) Sediment Discharge (g L^{-1})
40
20
0
(C) Wave Height (m)
4
0
(D) Wind Speed (m s^{-1})
20
10
0
(E) Current Speed (m s^{-1})
.4
.2
0
1/2010
5/2010
9/2010
1/2011

Figure 2-6: Vertical profile of river input

Shows the partitioning of momentum, fresh water, and river sediment at river mouth.

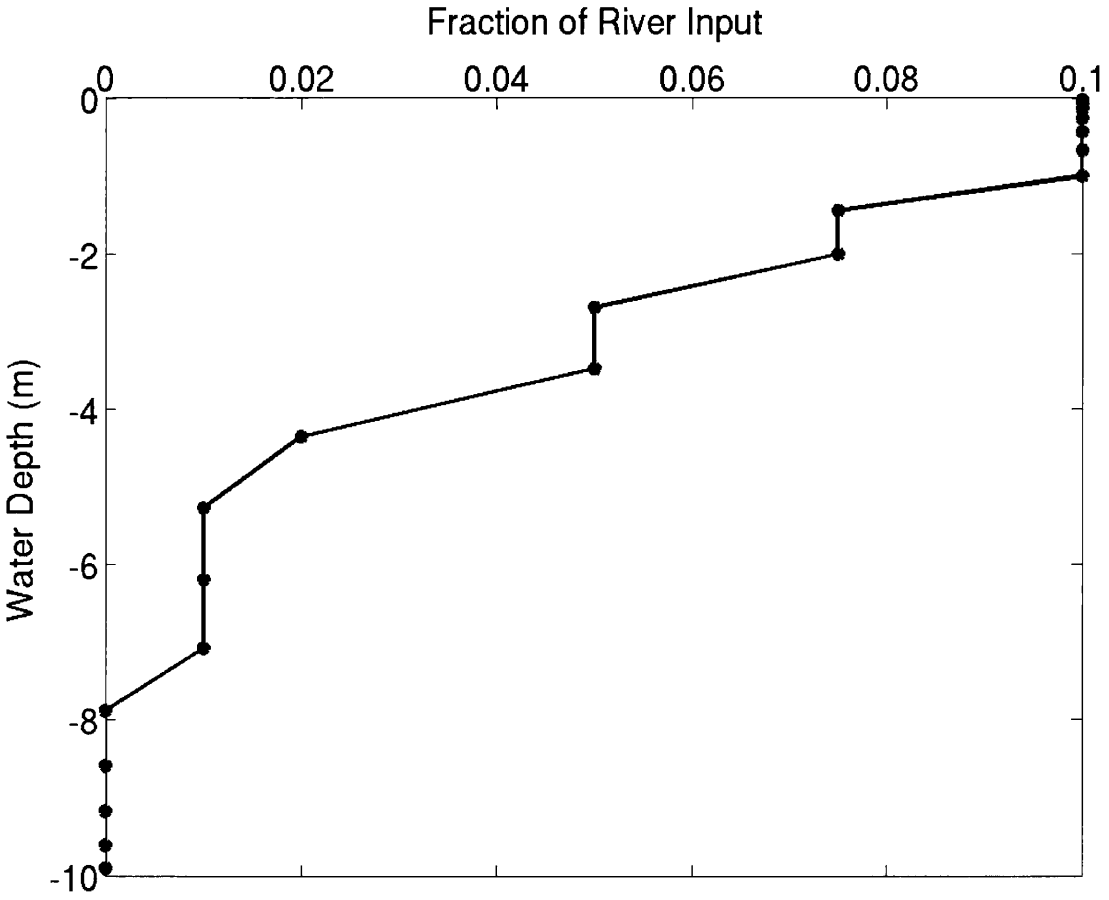

Figure 2-7: Initial sediment distribution

Shows (a) median grain size, and fraction of (b) mud and (c) sand, respectively.

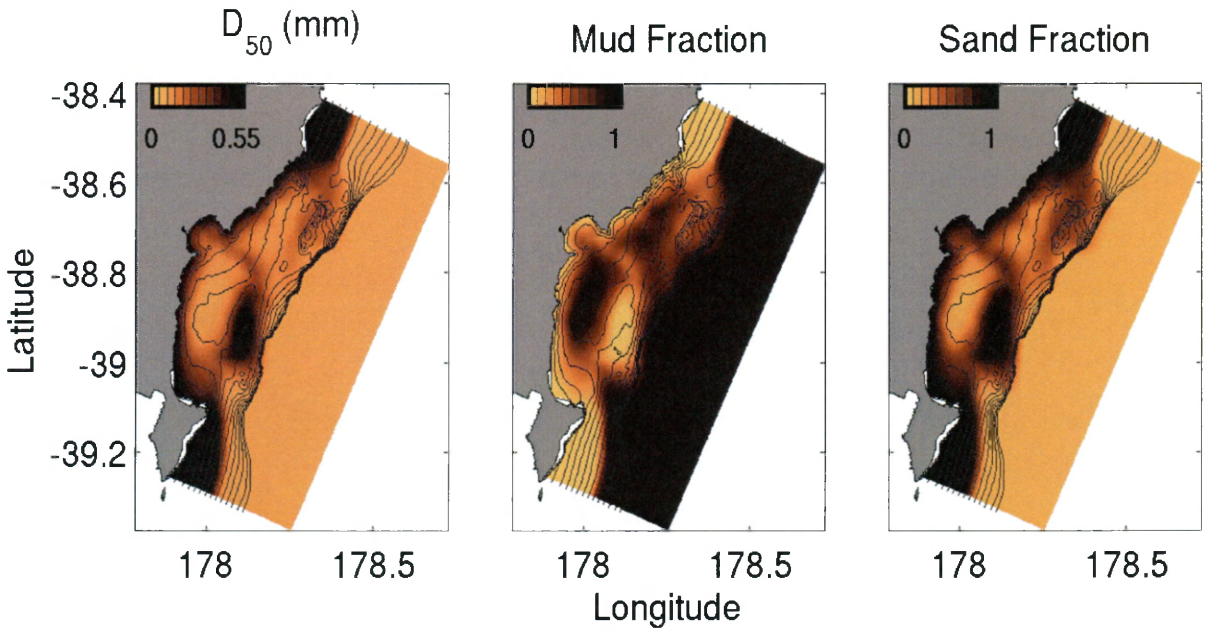

CHAPTER 3: Event – to – Seasonal Sediment Dispersal on the Waipaoa River Shelf, New Zealand: a Numerical Modeling Study

3.1 Abstract

The formation of the geologic record offshore of small mountainous rivers is event-driven and, compared to other environments, results in relatively complete sequences. One such river, the Waipaoa in New Zealand, has been studied from its terrestrial source to its oceanic sink over timescales spanning storms, seasons, and the Holocene. This study complemented other efforts by comparing the formation of riverine deposits on the Waipaoa Shelf during episodic flood and wave events to accumulation patterns created over thirteen months. Sediment fluxes and fate were estimated using a numerical hydrodynamic and sediment transport model (ROMS-CSTMS). During the study period (January 2010 – February 2011), event sedimentation on the Waipaoa shelf differed from accumulation patterns, especially over relatively short timescales. Initial deposition generally occurred near the river mouth and along the coast in water shallower than 30 m. In the days to months following a flood pulse, waves reworked this deposit, preferentially resuspending sediment from shallow depths and redistributing it toward deeper areas having lower near-bed wave stresses, including shelf depocenters and offshore. Overall, accumulation depended on characteristics of oceanographic transport (wave energy, current velocities) as well as source (flood size, sediment size distribution).

3.2 Motivation

Flood deposits comprise significant components of the geologic record on river-dominated margins, but may be reworked by physical and biological processes following emplacement (e.g. Wheatcroft et al.,

2007). This resuspension and redistribution of fluvial sediment can erase flood deposits from the stratigraphic record and reduce the role of flood deposits as carbon sinks (Wheatcroft and Drake, 2003; Blair et al. 2004). Although depositional and erosional processes act on a variety of timescales, Sadler (1981) showed that short-term accumulation rates typically exceed those representing longer timescales because the seabed does not directly record erosion and non-deposition. The marine geologic record is therefore incomplete (e.g. Orpin et al., 2009), complicating interpretation of seabed observations. Here, we complement previous studies by investigating how patterns of fluvial accumulation, or net deposition, change on short timescales, from days to months.

Recent studies have shown that geologic records offshore of small mountainous rivers, such as the Waipaoa River, New Zealand, may have relatively good fidelity (e.g. Sommerfield and Nittrouer, 1999; Wheatcroft et al., 2007; Blair et al., 2004; Brackley et al., 2010). Certain characteristics of these river-dominated active margins, e.g. the rivers' small drainage basins, high sediment yield, and steep slopes, help to coherently deliver flood signals from terrestrial events to the coastal ocean (Milliman and Syvitski, 1992; Wheatcroft, 2000). Upon reaching the continental shelf, steep slopes and energetic waves and currents may help transport sediment quickly to deeper sites where resuspension is less likely (Wheatcroft, 2000; Warrick and Milliman, 2003; Traykovski et al., 2000).

Despite the relatively good fidelity and terrestrial influence of stratigraphic records on river-dominated margins, these deposits reflect physical and biological reworking by oceanographic processes, in addition to flood magnitude and characteristics. Energetic waves and currents can resuspend fine sand

and mud to mid-shelf water depths and beyond (e.g. Bever et al., 2011; Ma et al., 2008; Drake and Cacchione, 1985), and sediment may be redistributed as dilute suspension (e.g. Sherwood et al., 1994; Drake, 1999, Harris and Wiberg, 2002), or gravity flows (Ma et al., 2008; Ma et al. 2010; Traykovski et al., 2000; Traykovski et al., 2007). Disturbances from benthic organisms may also modify sediment bed properties and erase deposit characteristics, e.g. through bioturbation (Drake, 1999; Bentley and Nittrouer, 2003; Wheatcroft, 1990).

The importance of biological and physical reworking for event layer preservation varies with depth into the seabed and water depth. For instance, both biological and physical processes act primarily on near-surface sediments, so rapid burial of event layers enhances the preservation of distinct beds in the geologic record (Wheatcroft, 1990; Bentley and Nittrouer, 2003; Wheatcroft and Drake, 2003). Similarly, wave orbital velocities attenuate with water depth, so waves more effectively resuspend sediment in shallow water (e.g. Harris and Wiberg, 2002). The spatial and temporal variations in all of these processes affect sediment fluxes, and are an important control on the preservation of flood beds. Thus, this study investigated the role of physical reworking on the formation of flood deposits on the Waipaoa River continental shelf, New Zealand.

3.2.1 Waipaoa Source-to-Sink Studies

NSF's MARGINS program chose the Waipaoa, a small mountainous river in New Zealand, as a Source-to-Sink study site for its high sediment yield, interesting marine geologic record, and because its offshore anticlines were thought to be conducive to preserving a relatively complete geologic record (see Figure 3-1, Carter et al., 2010; Foster and Carter, 1997; Gomez et al., 2004, Hicks et al., 2000; Milliman and

Farnsworth, 2011). The Waipaoa River has one of the Earth's highest sediment yields, about 6800 tons km^{-2} yr^{-1} (Milliman and Farnsworth, 2011; Griffiths and Glasby, 1985; Hicks et al., 2004), with even larger yields of 17,340 tons km^{-2} yr^{-1} in its upstream catchment (Walling and Webb, 1996). Previous studies, described further in Section 3.2.2, observed temporary storage of fluvial sediment in Poverty Bay (Bever et al., 2011; Bever and Harris, submitted) and also long-term accumulation in shelf depocenters (Miller and Kuehl, 2010; Gerber et al., 2010). Past studies also indicated that physical processes (e.g. resuspension by waves, gravity-driven transport) likely affected variations (e.g. grain size, carbon signature) within the Waipaoa shelf geologic record (Bever, 2010; Brackley et al., 2010; Carter et al., 2010). However, transport processes have only recently been studied on the Waipaoa shelf. Questions remain about how physical processes drive sedimentation and how short-term deposition differs from long-term accumulation.

The Waipaoa Shelf Initiative was funded to look at the formation, reworking, and preservation of flood deposits on the continental shelf over the course of a year (Walsh et al., 2009; Kniskern, 2010). From January 2010 – February 2011, the Waipaoa Shelf Initiative led four scheduled research cruises and one rapid response following the January 31, 2010 flood to deploy tripods and collect seabed and hydrodynamic observations (see Figure 3-1b). Measurements included current velocities, wave properties, suspended sediment concentrations, seabed elevation, and seabed radioisotope profiles. This numerical modeling study complemented the measurements made during the field program by analyzing estimated sediment fluxes and deposition during two floods, subsequent wave events, and the thirteen month field season in its entirety.

3.2.2 Waipaoa Sedimentary System (WSS)

The Waipaoa River, a small mountainous river with a highly erodible catchment, delivers sediment to the coastal ocean primarily during floods (Orpin et al., 2006; Hicks et al., 2000). Sediment sources vary depending on river conditions and precipitation, with landsliding and gullying dominating during high- and low-flow conditions, respectively (Hicks et al., 2000). Primarily muds (D_{50} = 8.5 μm during floods) are transported in suspension, although sands comprise about one percent of the load (Hicks et al., 2004; Orpin et al., 2006). Despite a very high sediment yield, hyperpycnal plumes do not seem to occur very often, with an approximate recurrence interval of ≥ 40 years (Hicks et al., 2004). Large floods occurred during the Waipaoa Shelf Initiative's field program on January 31 and July 6, 2010, however, representing the 5th and 14th largest discharges in the forty-four years of observations provided by the Gisborne District Council (GDC). Riverine sediment concentrations during their peaks were estimated to slightly exceed 40 g L^{-1} based on recent rating curves provided by the GDC. On century-long timescales, about 25% of Waipaoa riverine sediment seems to remain on the shelf (Miller and Kuehl, 2010), but the sediment budget for shorter timescales has not been estimated.

Observed sedimentation on the shelf indicates that event-scale deposition differs from patterns of long-term accumulation. During the 2010 field season, for instance, recent depositional patterns varied among the five research cruises. Depending on the timing of the research cruise relative to recent conditions, ^{7}Be ($\tau_{1/2}$ = 53.3 days) inventories indicated high deposition near the river mouth in Poverty Bay, on the inner to mid shelf near the entrance to Poverty Bay, and/or in depocenters identified by Miller and Kuehl (2010) and Orpin et al. (2006). Similarly, numerical model estimates indicated that some portion of riverine sediments delivered by floods would be retained in Poverty Bay for several

days before swell wave events resuspended them, and allowed currents to transport them to the shelf (Bever and Harris, submitted). Over century to Holocene timescales, grain size measurements, ^{210}Pb ($\tau_{1/2}$ = 22.3 years) accumulation rates, and geophysical mapping identified two mid-shelf (40 – 70 m) depocenters bordered by anticlines on their seaward edge, and separated from each other by an area of low accumulation called Poverty Gap; (see Figure 3-1) (Foster and Carter, 1997; Miller and Kuehl, 2010; Orpin et al., 2006). Even in areas of high accumulation, however, event layers may be destroyed by biological reworking, and Rose and Kuehl (2010) found biologically-dominated seabed facies ~25 km from the river mouth to the shelf break.

The weather systems and hydrodynamics driving sediment suspension and transport on this margin are highly variable. Energetic waves and winds on the Waipaoa shelf generally coincide with southward-travelling storms that also cause river floods (Orpin et al., 2006). Although winds are predominantly from the north-northwest (seaward), winds associated with these storms are typically easterly (landward) and then rotate and become westerly (seaward) (Stephens et al., 2000; Orpin et al., 2006). While winter is the stormy season, some of the largest historical floods have happened during other times of year (Orpin et al., 2006). For example, the largest recorded flood, Cyclone Bola, occurred in March, 1988 and one of the biggest floods of our study period was in late January, 2010.

During the 2010 field season, shelf current velocities generally flowed along shore. The tripod deployed at 40 m water depth recorded time- and depth-averaged velocities of 1.6 cm/s to the NE and a mean speed of 26.3 cm/s that switched direction often (data obtained from A. Ogston and R. Hale, University

of Washington). Several factors may influence currents, including a northward coastal current, coastally-trapped waves, and southward-traveling eddies (Chiswell, 2000; Wood, 2006; Hadfield, pers. comm., 2010; Stephens et al., 2000; Chiswell and Roemmich, 1998; Chiswell, 2005). In Poverty Bay, the river plume drives counter-clockwise circulation (Stephens et al., 2000; Healy et al., 1998; Bever et al., 2011). Waves generally travel from the southeast into Poverty Bay, and have average periods of 9-10 seconds, and significant wave heights of 0.8 – 0.9, although longer-period swell waves also propagate onto the shelf from the Southern Ocean (Bever et al., 2011; Smith, 1999). Waves dominate bed shear stresses at the study site, which were estimated to exceed 0.1 Pa (a typical threshold for suspension of fine-grained sediment on continental shelves; Ferre et al., 2010; Wiberg et al., 1994; Kachel and Smith, 1989) 58% of the time at the Southern Depocenter tripod during the 2010 deployments (bed stress data provided by A. Ogston and R. Hale, University of Washington).

In context, the 2010 field season was a relatively wet year for the WSS (Orpin, pers. comm., 2011), with multiple floods and periods of high discharge (wet storms) in addition to wave events that did not coincide with precipitation or discharge (dry storms). These events included a flood with relatively low waves on January 31, 2010, a series of subsequent dry wave events with peak shelf sediment fluxes on March 7, 2010, a flood with high waves on July 6, 2010, and a series of wet wave events with peak shelf sediment fluxes on August 31, 2010 (Figure 3-2). We used the numerical model to compare shorter-term sedimentation patterns during these events to each other and the year as a whole.

3.3 Objectives

This study addressed the following questions:

- How did shelf suspended sediment fluxes and deposition vary during a flood coinciding with relatively low waves, a series of subsequent dry wave events, a flood coinciding with high waves, and a series of subsequent wet wave events?
- How did event deposition contribute to sediment accumulation over the thirteen month study period? To what extent were initial flood deposits reworked by waves and currents?

3.4 Methods

To investigate sediment transport and deposition on the Waipaoa River continental shelf, a numerical circulation and sediment transport model, ROMS – CSTMS (Regional Ocean Modeling System – Community Sediment Transport Modeling System) was developed for the Waipaoa shelf. Model results for January 1, 2010 – February 15, 2011 were compared to data collected during the 2010 field season. Estimates of sediment flux and deposition during floods, wave events, and the year as a whole were analyzed. This section briefly reviews the formulation of the model that was described in detail in Chapter 2, and provides details of the model run implementation and analysis.

3.4.1 Model Description

ROMS, an open-source community-developed model, solves the Navier-Stokes, continuity, and tracer advective-diffusion equations (Haidvogel et al., 2000; Haidvogel et al., 2008; Shchepetkin and McWilliams, 2005, 2009). To implement ROMS for the Waipaoa shelf, a model grid was developed using multibeam estimates of bathymetry from J. McNinch (USACoE) and from S. Kuehl (VIMS; Gerber et al.,

2010), bathymetric contours and gridded bathymetry provided by NIWA, and modeled bathymetry from a lower resolution model, ROMS-NZ, provided by Mark Hadfield (NIWA; Figure 3 -1c, d). In the area of interest near shelf depocenters, horizontal grid resolution was ~450 m. Vertical grid resolution varied with water depth and location in the water column. Resolution increased in shallow water, near the bed, and near the water surface. At 50 m depth, for example, grid cells ranged from 0.24 – 4.6 m in thickness, and were 1.4 m thick at the bed.

The ROMS implementation relied on a variety of observations and model estimates (see Figure 3-2, Table 3-1). Model inputs included wind velocities from NZLAM (NZ Local Area Model; see Davies et al., 2005), and wave properties from NIWA's NZWAVE model, a local implementation of Tolman et al. (2002). To account for larger scale shelf currents, prevent reflection of the river plume on open boundaries, and ensure model stability, the model was nested within ROMS-NZ, a larger scale New Zealand circulation model developed by M. Hadfield (NIWA). Radiation boundary conditions were used for the free surface elevation (Chapman, 1985) and depth-averaged current velocities (Flather, 1976). An oblique radiation – nudging boundary condition for depth-varying current velocities, salinity, and temperature was used, moving these variables toward values obtained from ROMS-NZ following Marchesiello et al. (2001) and Lavelle and Thacker (2008). Nudging was strongest at the open boundary and decreased sinusoidally to zero within 30 grid cells of the boundary.

CSTMS, an open-source community model developed in conjunction with ROMS, was used to estimate suspended sediment transport and deposition. As described in Warner et al. (2008), the model

accounted for advection, diffusion, erosion and deposition of sediment. Both fluvial discharge and seabed erosion provided sediment sources to the water column. Seabed erosion was calculated following the Ariathurai and Arulanandan (1978) formulation:

$$E = M(1-p)\frac{(\tau_{bed} - \tau_{crit})}{\tau_{crit}}$$

where M was the erosion rate parameter, p was seabed porosity, τ_{bed} was bed shear stress, and τ_{crit} was critical bed shear stress. Erosion was also restricted by the thickness of the active layer following Harris and Wiberg (1997). Wave- and current- induced bed stress was calculated following Madsen (1994). The density equation of state included sediment concentration to account for gravity-driven transport, but vertical resolution was insufficient to resolve a wave-current boundary layer or thin near-bed fluid mud such as has been seen on other shelves (Wright and Friedrichs, 2006).

The calculations accounted for seven sediment types and eight seabed layers (see Table 3-2). Three sources provided data used to develop the initial seabed sediment distributions: Wadman and McNinch (2009), Wood (2006) and the January, 2010 cruise (see Figure 3-1b). Four classes were used for sediment delivered fluvially. Guidance in assigning their properties was sought from data from Hicks et al. (2004) and estimates of effective settling velocity from the tripod at 40 m water depth (obtained from A. Ogston and R. Hale, University of Washington). These sources estimated a median grain diameter of 8.5 μm in the Waipaoa river during floods and effective settling velocities ranging from < 0.1 to ~1 mm s^{-1}, with a peak at ~0.1 mm s^{-1} during energetic shelf conditions at 40 m water depth. Since information regarding the distribution of sediment settling velocity in the river plume was unavailable,

however, a range of reasonable values (0.15 – 1 mm s^{-1}) was chosen and the fluvial sediment was logarithmically partitioned into these sediment settling classes following sensitivity tests. Other parameters such as critical shear stress and erosion rate parameter were chosen to match estimates from Optical Backscatter Sensor (OBS) measurements from the first two months of the tripod deployment and Gust erosion chamber experiments from the 2010 field season (tripod data from A. Ogston and R. Hale, University of Washington; Gust data from J.P. Walsh, D.R. Corbett, and J. Kiker, East Carolina University; Kiker, 2012). Sediment and seabed parameters are discussed further in section 3.6.

3.4.2 Model Implementation and Analysis

ROMS-CSTMS was implemented for January 15, 2010 – February 15, 2011. Sensitivity tests of the first two months (January 15 – March 15, 2010) were used to choose parameters, and then the model was run and analyzed for the entire study period (see Section 3.5.1). Estimates of waves, currents and suspended sediment concentrations were quantitatively compared to tripod data from the thirteen month field season using the correlation, variability and means of the two time-series (statistics presented in Table 3-3; time-series presented in Figures 3-3, 3-4). This comparison used model estimates from the grid cell located closest to the tripod location. The observations, provided by A. Ogston and R. Hale, University of Washington, were derived from Acoustic Doppler Current Profiles (ADCP; current velocities), Acoustic Doppler Velocimeters (ADV; wave orbital velocity, wave frequency), and Optical Backscatter Sensors (OBS; suspended sediment concentrations). ROMS estimates of bed shear stress were compared to values derived following Madsen (1994) that relied on the tripods' observed velocities. More qualitative analyses compared spatial patterns of modeled deposition to seabed radioisotope inventories.

Spatial and temporal variations in sediment transport and deposition on the Waipaoa shelf were analyzed for the entire thirteen month field season, then transport during specific episodes were considered including two large floods, and subsequent wave events (Figure 3-2). The first flood peaked on January 31, 2010, and was characterized by relatively low waves. A period of dry wave events followed this flood, including large waves on March 7, 2010 when orbital velocities exceeded the thirteen-month average by a factor of 1.5 (Table 3-4). The second flood considered here, a more typical winter storm, peaked on July 6, 2010, with high waves coinciding with peak discharge. A series of moderate discharge and wave events followed this, including an episode on August 31, where orbital velocities almost reached 1.5 times the thirteen-month average (Table 3-4). Sections 3.5.2 and 3.5.3 analyze estimated sediment transport and sedimentation patterns during these individual events, and compare them to fluxes and accumulation over the thirteen month model run. Although model calculations included both fluvial and seabed sediments, the analysis presented here focused on the transport and fate of the riverine material, unless otherwise noted.

3.5 Results

The model was first evaluated with respect to both water column and seabed measurements. Then, the hydrodynamic climate and sediment dispersal patterns were described for the 2010 study period as a whole and for specific high-energy events.

3.5.1 Model Evaluation

Both the modeled and observed currents varied spatially and frequently reversed direction, but the model underestimated water speeds (Figures 3-4, 3-5). For the most part, depth- and time- averaged current velocities on the shelf were oriented to the NE; at the 40 m deep tripod location, velocities in the model were directed 26 degrees east of north, slightly inshore of measured velocities that were oriented 54 degrees east of north. Although the model underestimated peak water speeds at the three tripod locations (Table 3-3), it replicated the spatial patterns of the observed time- and depth- averaged current speeds, which increased from the depocenter tripod to the shallow tripod to the deep tripod. Modeled velocities along the slope / slope break were particularly fast, while low current speeds were estimated in the lee of Mahia Peninsula, over the Southern Depocenter and in Poverty Bay. While shelf currents were generally to the NE, a counterclockwise eddy formed within Poverty Bay, as seen in observations (Stephens et al., 2000, Healy et al., 1998, Bever et al., 2011) and previous model efforts (Bever and Harris, submitted). The model developed a persistent eddy over the Southern Depocenter, consistent with observations at the tripod there that depth-averaged currents were primarily directed to the northwest and south. In addition to spatial patterns, the model estimated frequent reversals of current direction influenced by flow from the larger-scale model and occurring on a timescale of days, similar to temporal behavior in the tripod measurements (Figure 3-4). Importantly, flow direction during events discussed in this chapter were consistent with observations, including the January 31 and July 6 floods, and March 7 and August 31 wave events. During the January flood, for example, estimated and measured currents, averaging a speed of 11.6 and 16.4 cm s^{-1}, respectively, switched direction from southward to northeastward as winds shifted on February 1, 2010.

Model estimates of waves, bed shear stresses, and sediment concentrations also captured the timing of episodic events, but underestimated measurements from the field season (Figure 3-3; Table 3-3). Underestimates of wave height and period from NZWAVE propagated to create bias in calculations of bed stress and suspended sediment concentrations. Although the models underestimated the magnitudes of waves, bed stress, and sediment concentrations these timeseries all peaked during observed wave events (Figure 3-3).

Seabed erodibility can be defined as the amount of sediment available for erosion at a given bed shear stress and the treatment of erodibility is a distinguishing factor between cohesive and non-cohesive models (see Sanford and Maa, 2001; Sanford, 2008). We used a non-cohesive formulation wherein the critical shear stress varied with sediment class, and assumed that sediments had critical bed stresses between 0.1 - 0.53 Pa. The bed erodibilty in the model therefore depended on the excess shear stress defined to be the difference between bed stress and critical stress for each size fraction. Though erosion during any one timestep was limited by the active layer thickness that scaled with excess shear stress (see Harris and Wiberg, 1997), in a general sense, we can assume that sediment classes having critical bed stress that exceeded the bed stress were erodible, and other classes were not. Erodibility was therefore under- and over- estimated during quiescent and energetic time periods, respectively. When bed stress fell beneath 0.1 Pa, no sediment could be resuspended in the model and so erodibility was therefore underestimated. Similarly, all sediment classes could be resuspended once bed stress exceeded 0.53 Pa, causing the model to overestimate seabed erodibility during energetic periods. Another way to evaluate the bed erodibility is to consider the degree to which the seabed was mobilized in the model, and the variability of modeled seabed thickness for each grid location gives an idea of how

responsive that site was to the applied bed stresses (Figure 3-6). This showed that seabed mobility was highest where fluvial deposition occurred, with "hot spots" for erosion being near the bay mouth. The gradient of high to low seabed erodibility from Poverty Bay to the depocenters compared well to erodibility estimates from Gust chamber experiments (data provided by Kiker, 2012) where the most erodible sediments were also found in Poverty Bay and the mouth of the bay (see Figure 3-7).

Patterns of erosion and deposition estimated by the model have been evaluated using seabed observations of ^{7}Be inventories (Corbett et al., 2012; Kiker, 2012; Kniskern et al., 2012; Kniskern et al., in prep; see Figures 3-8, 3-9). Overall, both the observations and model estimates exhibited high spatial and temporal variability. Areas of deposition often occurred in close proximity to areas where little or no sedimentation was detected or estimated, and the shape of the depositional footprint changed between each research cruise (Figure 3-8, 3-10, 3-11a). Both observations and model estimates generally showed enhanced deposition to either side of Poverty Gap, landward of shelf anticlines. During every research cruise, radioisotope signatures were also high in some part of Poverty Gap, consistent with model estimates that showed sediment deposits there, particularly following periods of high discharge. Often, these high radioisotope signatures and model estimates of deposition were observed at ~40 m and ~30 m in Poverty Gap, respectively. However, model estimates of deposition were generally located in shallower water than observed ^{7}Be inventories, and over-estimated accumulation in Poverty Bay, as discussed in section 3.6.

The January 31, 2010 flood accounted for most of the sediment delivered to the shelf between the research cruises in January and February, 2010, and it is worthwhile to compare model estimates of event deposition to seabed changes between the two cruises. Depositional patterns from the January 31 flood, evaluated using net gains in ^{7}Be inventories between the January 15 and February 15, 2010 research cruises, indicated riverine sediment deposited across much of the shelf (Kniskern et al., in prep.; Figure 3-9). Event deposition occurred from the northern depocenter, across Poverty Gap near the 30 and 40 m isobaths, to parts of the southern depocenter. Net losses of ^{7}Be, corrected for decay, were observed during this sampling interval in other parts of the southern depocenter and in Poverty Gap between 45 and 100 m water depth. Model estimates captured aspects of this sedimentation, including high deposition behind the northern depocenter and near the 30 m isobath in Poverty Gap (Figure 3-10a, 3-11a). However, model results indicated increased retention of sediment in Poverty Bay relative to the shelf. Also, model calculations showed millimeters of deposition in deeper areas of Poverty Gap (50 and 85 m water depth), whereas net losses of ^{7}Be indicated erosion there during this time. Also, estimated deposition near the Southern depocenter was less than 1 mm thick, while ^{7}Be was observed in sediment layers as deep as 8 cm there (Kniskern et al., 2012; Kniskern et al., in prep.). High spatial variability of shelf depositional patterns (Kiker, 2012; Corbett et al., 2012; Kniskern et al., in prep.; Kniskern et al., 2012), bioturbation, and processes discussed in section 3.6 may contribute to discrepancies.

3.5.2 Overall hydrodynamic climate and sedimentation during 2010 field season

This section analyzes system behavior as a whole, throughout the 13-month model run to gain insight into the cumulative effects of multiple flood, wind, and wave events superimposed on background conditions.

3.5.2.1 Effect of wave resuspension

Throughout the model run, wave events resuspended material previously deposited during floods, especially in shallow water. Waves traveled from the southeast onto the shelf, with an average wave height and period of 1.5 m and 8.16 s, estimated by NZWAVE. Wave-induced bed shear stresses exceeded those induced by currents by an order of magnitude (Figure 3-12), and therefore dominated the resuspension of sediment. Bathymetry exerted strong controls on wave orbital velocities and bed stresses, which were higher in Poverty Bay, Poverty Gap and the anticlines than in the long-term depocenters (Figure 3-12). Bed shear stress exceeded 0.1 Pa, an approximate threshold for resuspending sediment, 87, 38, and 19 % of the time at water depths of 20, 40 and 60 m. Even during moderate wave events, bed stresses exceeded 0.1 Pa across the shelf, including areas deeper than 150 m, although bed stresses and resuspension were still lower in deeper regions.

3.5.2.2 Effect of currents

Although waves dominated bed stresses, current velocities controlled sediment flux direction and strongly influenced its magnitude (Figure 3-10). Currents in the model were, on average, directed toward the northeast, but switched direction often, similar to what has been observed during tripod deployments (Figure 3-4). The strongest shelf currents traveled along the shelf break and along

isobaths, passing seaward of the southern anticline, through Poverty Gap, and inshore of the northern anticline (Figure 3-5). These currents dispersed sediment along-shelf in both directions, although velocities during most times of high river discharge (except the January 31 flood) were persistently northeastward (Figures 3-4; 3-10a, d; 3-13), consistent with observations. As discussed in Section 3.5.1, an eddy often formed landward of the Lachlan anticline, trapping sediment south of Poverty Gap in the vicinity of the Southern Depocenter.

3.5.2.3 Overall sediment fluxes

Resuspension by energetic waves encouraged transport of sediment toward depocenters on either side of Poverty Bay by preferentially eroding deposits in shallower areas like Poverty Bay and Poverty Gap. Dry wave events, when little freshwater and new sediment entered the model grid, were particularly effective at producing this pattern (Figure 3-10c). The effect of increased resuspension on sediment fluxes can also be seen by looking at the deposit footprint for sediment with different settling velocities. By the end of the model run, the deposit created by slower-settling sediment had two distinct shelf depocenters to either side of Poverty Gap (Figure 3-11b). Slower-settling sediment (w_s = 0.15 mm/s) was also deposited preferentially in deeper water, with 75% of the sediment remaining in Poverty Bay or on the shelf located in water depths exceeding 30 m. In contrast, sediment settling at 1 mm/s formed a narrower, shallower mudbelt in front of Poverty Bay that crossed Poverty Gap. This faster-sinking sediment also settled closer to shore, with shelf sediments equally split between the inner shelf (depth less than 30 m) and deeper areas.

3.5.2.4 Overall pattern of accumulation

Over the 13-month model run, net accumulation of fluvial sediment occurred in Poverty Bay and to either side of Poverty Gap between 30 and 55 m water depth, with reduced deposition in Poverty Gap. Settling velocity strongly influenced the shape of the deposit formed by fluvial material (Figure 3-11), and sediment budgets (e.g. Table 3-5; Figure 3-14) These budgets were calculated by summing all of the fluvial sediment deposited and suspended in Poverty Bay and on the shelf at the end of the model run (see Figure 3-13b). The mass of the riverine load transported off the proximal shelf was calculated by subtracting the sediment in Poverty Bay and on the shelf from the fluvial sediment input. Slower-settling material traveled farther from the river mouth, and more was exported from the Bay and the shelf. Overall, more than 90% of sediment settling at 1 mm/s remained in Poverty Bay, and almost all of the rest remained on the shelf. For comparison, only 30 – 40% of sediment settling at 0.15 mm/s remained in Poverty Bay, 10 – 30% was deposited on the shelf, and the remainder was carried to the northeast off of the proximal shelf.

3.5.3 Sedimentation during events

Sediment transport on this shelf was episodic and dominated by large fluxes that occurred during relatively short episodes (see, e.g. Figure 3-13). This section analyzes how transport and deposition during these energetic periods responded to oceanographic and meteorological conditions by examining four distinct events.

3.5.3.1 Sedimentation during a flood with relatively low waves

During the January 31 flood, the wind- and Coriolis- driven river plume superimposed on a larger-scale southwestward shelf current, influenced sediment transport and spread sediment over a wide area. Westward winds initially directed the river plume toward the southwest, but then winds weakened and the river plume turned toward the northeast during the time when much of the flood sediment entered the shelf from Poverty Bay. Further offshore on the mid- to outer- shelf, a large-scale isobath-parallel current entrained some water and sediment from the river plume and carried it southward.

The resulting deposit was focused in Poverty Bay and along the coast to the north, with a more diffuse deposit spread over the shelf south of Poverty Gap (Figure 3-10a). Little resupsension occurred during this flood, when wave orbital velocities and bed stresses were less than half the average values. Less than one percent of the riverine load escaped the shelf, though assumptions about sediment settling velocity strongly influenced estimates of the depositional footprint. Over 99% of sediment with settling velocity of 1 mm/s remained in Poverty Bay, while 30% of sediment settling at 0.15 mm/s was exported to the shelf. Of the sediment deposited on the shelf, 50 – 75% (depending on settling velocity) settled in areas shallower than 30 m, with faster settling sediment remaining close to the river mouth, and more slowly settling material reaching deeper water.

3.5.3.2 Waves redistribute January 31 flood deposit

In the months following the January 31 flood, waves resuspended the initial deposit, and sediment deposition shifted to deeper areas. The biggest fluxes occurred on March 7, 2010 (Figures 3-13, 3-14), when large waves resuspended sediment across the entire shelf. During this time, wave orbital

velocities and bed stresses on the shelf exceeded the thirteen month average by about a factor of two. Between 2% and 30% of the initial deposit, depending on the material's settling velocity, was exported from Poverty Bay onto the shelf (Figure 3-10b, 3-14). Currents strengthened by northward winds transported this material and resuspended shelf sediment to the north of Poverty Bay, and about 1% - 25% of each riverine sediment class was carried off the proximal shelf to the northeast.

In addition to the energetic March 7 waves, small to moderate waves reworked riverine sediments throughout the period from February 14, 2010 to May 15, 2010 (Figure 3-10c). Average wave orbital velocities and bed stresses during this time were low, equaling about the thirteen-month average, but the numerous moderate wave events augmented transport from the March 7 waves. These carried an additional 0 - 15%, depending on settling velocity, of the initial deposit from Poverty Bay to the shelf (Figure 3-14). Although average currents and highest fluxes were northward, currents switched direction on timescales of days to a week so the model estimated net deposition to either side of Poverty Bay's entrance. Net erosion of the January 31 flood deposit occurred in all areas shallower than ~20 m including Poverty Bay, the coastal region north of Poverty Gap, and to a lesser extent in Poverty Gap. Net deposition occurred in deeper areas adjacent to, and generally offshore of, the initial deposit and in areas that had no initial flood deposit such as the inner shelf to the south of Poverty Bay. These smaller wave events did not export much sediment from the proximal shelf, removing only <1 - 5% of the January 31 flood load (depending on sediment settling velocity).

3.5.3.3 Sedimentation during a flood with high waves

A large flood having peak discharge of over 1700 $m^3 s^{-1}$ and coinciding with energetic waves occurred on July 6, 2010. Transport within the river plume, directed northeastward by northward winds, dominated sediment fluxes during this flood. Waves, with orbital velocities about twice the thirteen month average, resuspended previously-deposited sediment, which was carried out of Poverty Bay and along-shore toward the northeast. In the surface layer, the river plume traveled out of Poverty Bay and then primarily continued northward along the coast. Near-bed currents were generally directed in the same direction as water column velocities, but had an increased offshore component in Poverty Bay and the inner shelf when sediment concentrations were high. A portion of the newly-delivered sediment in the plume, and some resuspended material were entrained by an eddy over the Southern Depocenter.

Net shelf deposition during the July 6 flood was influenced by the river plume, eddy over the Southern Depocenter and offshore near-bed currents. Deposits appeared to the north of the Waipaoa River (up to 40 m deep), landward of the Southern Depocenter (20 – 50 m water depth), and in the deeper portions of Poverty Bay and shallow areas of Poverty Gap (20 – 35 m water depth; Figure 3-10d). During this event, 50 - 100% of flood sediment was deposited in Poverty Bay, and up to 50% was transported off of the proximal shelf to the northeast, depending on settling velocity and fraction of the flux composed of older riverine material. Settling velocity again controlled the partitioning of sediment on the shelf, with about half of the faster-settling sediment that reached the shelf settling in depths shallower than 30 m, while about two-thirds of the slower-settling sediment settled in water deeper than 30 m.

3.5.3.4 Winter storms (discharge pulses and waves) redistribute flood deposit

In the months following the July flood, a series of smaller discharges that coincided with energetic waves delivered sediment to the shelf and changed the deposit footprint. The largest of these sediment fluxes occurred around August 31, 2010 (Figures 3-13, 3-14), when river discharge peaked at just under 400 $m^3 s^{-1}$, and wave orbital velocities exceeded the thirteen month average by a factor of about 1.5 (Table 3-4). Resuspension occurred across the shelf, and near-bed down-slope currents in the mouth of Poverty Bay and the inner shelf carried sediment toward deeper areas (Figure 3-10e). Newly-delivered sediments were carried northward by the river plume during the beginning of the flood, and then offshore as winds rotated from northward to southward. Depending on settling velocity, these winter storms transferred from <1% to 20% of the riverine sediment initially in Poverty Bay to the shelf. Poverty Bay, and to a lesser extent, parts of the inner – to – mid shelf experienced net erosion (Figure 3-10e). Net deposition occurred just outside of Poverty Bay and also along the coast to the northeast. The amount of riverine sediment on the shelf nearly doubled for all sediment sizes, with net deposition focused in areas deeper than 30 m or to the north along the inner shelf (Figure 3-10e).

In addition to the August 31 storm, a series of smaller river discharge and wave events redistributed and added to the original flood deposit. The discharges together delivered $2x10^9$ kg of sediment (~1/4 of the July 6 flood load) to Poverty Bay and the shelf. Net deposition occurred in parts of Poverty Bay, on the inner shelf to the south of Poverty Bay due to southwestward currents, and on the mid-shelf (30 – 50 m deep) to the north of Poverty Bay (Figure 3-10f). Net erosion occurred in the same parts of Poverty Bay and Poverty Gap that experienced high net deposition during the July 6 flood. Between July 20 and

September 30, 2010, the ratio of riverine sediment mass on the shelf to sediment mass in Poverty Bay increased from ~0.25 to ~0.35 for sediment settling at 0.15 mm/s.

3.6 Discussion

Wave processes and bathymetry helped explain the delivery of sediment to two distinct depocenters landward of shelf anticlines, and reduced accumulation in Poverty Gap. Attenuation of wave stresses with water depth added a seaward component to net flux since sediment was preferentially resuspended from shallow water. Zones of reduced wave-induced bed stresses occurred over bathymetric lows, and so sediment resuspension was discouraged there (Figure 3-12). These model results were consistent with observations showing that accumulation on century-long timescales occurs in shelf depocenters and not Poverty Gap (Miller and Kuehl, 2010).

Even moderate wave heights on the Waipaoa shelf created bed stress sufficient to resuspend shelf sediment and rework riverine deposits. Excluding floods, the highest sediment fluxes occurred during larger and more sustained wave events when bed stresses exceeded 1 Pascal at 40 m depth for at least a few days (Figure 3-2, 3-13). Sediment concentrations, and therefore fluxes, were also elevated following periods of high discharge which increased sediment availability for subsequent resuspension events.

Although waves preferentially resuspended sediment from shallow areas during all events, dry storms (including swell waves and local wind storms) were particularly effective at removing sediment from Poverty Gap and the inner shelf because they did not coincide with the input of new riverine sediment.

In contrast, newly delivered sediment during wet storms generally settled in or near Poverty Bay, including drapes of sediment over Poverty Gap (Figure 3-10d, e, f). The increased sediment availability near the river mouth and the relatively high bed stresses in shallow areas enhanced resuspension there (Figure 3-10), consistent with a seabed that grades from physically-dominated to biologically-dominated with distance from river mouth (Rose and Kuehl, 2010). The low background discharge of the Waipaoa River, however, limited spatial variability in salinity structure (unpublished CTD casts and model estimates) and likely limited strong spatial gradients in nutrient delivery, except during floods or to areas within a kilometer of the river mouth. Therefore, variations in ephemeral deposition and near-bed turbidity, due to fluvial supply and resuspension frequency, likely drive the transition of seabed facies from physically- to biologically- dominated.

While waves dominated bed shear stress (Figure 3-12), and thus determined the timing, and to some extent, magnitude of resuspension, current velocities influenced flux magnitude and determined net flux direction. Average currents during all events except the January flood were directed to the northeast, so buoyant sediment fluxes were also primarily in that direction. During the March 7 wave event, strong wind-driven northward currents were particularly effective at transporting sediment alongshore. In contrast, currents during the August 31 storm were directed eastward during peak waves and they were relatively weak because winds changed direction often, so fluxes were smaller and less sediment was carried off of the proximal shelf (Figure 3-14).

Model nesting within ROMS-NZ helped to stabilize the modeled currents and reduced reflection of the river plume at open boundaries during floods. Although estimated currents in both this model and ROMS-NZ were weaker than observed currents during 2010, model nesting produced fluctuations in along-shore current direction on the shelf at the same frequency as the observations. Both this study and Xue et al. (2012) found that model nesting increased along-shore currents and associated sediment fluxes.

Estimated fluxes of flood material depended strongly on the settling characteristics assumed for sediment (Figure 3-11). The sediment budget (see Table 3-5) was therefore very dependent on sediment settling velocity which was difficult to constrain with available data. Sand was not included because earlier models showed that it settled at the river mouth. For all settling velocities considered (w_s ranged from 0.15 to 1.0 mm/s), Poverty Bay retained a significant fraction of fluvial material over timescales of a single flood to months. On event timescales, the bay retained most of the faster-settling mud ($w_s > 0.5$ mm/s), while more of the slower-settling fractions ($w_s < 0.3$ mm/s) settled on shelf or were carried buoyantly off of the shelf (Figure 3-11; Table 3-5). Over the timespan of a year, initial flood deposits were redistributed. Although faster-settling material remained in Poverty Bay, some was exported to the shelf, while slower-settling mud on the shelf was either retained in the deeper areas, or carried off the proximal shelf (Figure 3-11).

Estimated deposits at the end of the thirteen-month study period (Figure 3-10g) were generally landward of the observed long-term depocenters (Figure 3-1a). One or more factors contributed to this.

First, although the temporal patterns of modeled bed stresses reflected the wave events observed during the field season, estimated stresses, suspended sediment concentrations and across-shelf currents were consistently lower than values derived from tripod observations, reducing modeled estimates of resuspension. For instance, doubling both the wave orbital velocities and across-shelf current speeds would roughly increase sediment fluxes by a factor of eight. Second, while this model accounted for gravity-driven transport, it lacked sufficient vertical resolution to the represent thin near-bed gravity flows observed on other shelves (e.g. Traycovski et al., 2000; Ma et al., 2008) which seem more capable of creating thick event beds than dilute suspensions (Harris et al., 2005). Future efforts may more thoroughly investigate the role of gravitational forcing on depositional patterns on the Waipaoa shelf, perhaps using a ROMS model having higher vertical resolution, or a gravity flow model similar to Ma et al. (2010) and Scully et al. (2003).

The model neglected seabed consolidation, which also would affect the sediment budget. Bed stresses in shallow water almost continuously resuspend sediment, slowing the consolidation of newly delivered muds. In deeper water, wave agitation is less frequent, and the seabed may consolidate between wave events. Supporting this theory, measurements of erodibility from the Waipaoa shelf (Kiker, 2012; Figure 3-7) indicated that erodibility was highest and most variable in Poverty Bay and Poverty Gap (Kiker, 2012; Figure 3-7). However, while the model indicated higher variability in seabed thickness near Poverty Bay than in deeper areas of the shelf (Figure 3-6), this trend was driven by deposition, not seabed consolidation. Accounting for seabed consolidation would therefore likely increase export from shallow regions and increase retention of sediment in deeper areas of the shelf.

Fluxes on other river-dominated margins have also been strongly correlated to oceanic conditions, but not necessarily to floods. Similar to the Waipaoa margin, flooding river plumes on both the nearby Waiapu River, New Zealand and the Eel River, California, USA, primarily delivered sediment along the coast to the inner shelf (Kniskern, 2007; Harris et al., 2005; Geyer et al., 2000). As winds weakened or switched direction following peak flood, river plumes at these three sites spread further offshore, reducing along-shelf fluxes (Kniskern, 2007; Harris et al., 2005; Geyer et al., 2000). In the hours to months following floods, energetic waves and currents then resuspended and redistributed sediment that had settled from the flood plume, with some portion transported as suspended load along-shore, away from the proximal shelf (Kniskern, 2007; Harris et al., 2005). During these times, however, gravity flows also carried sediment offshore on the Eel and Waiapu shelves (Ma et al., 2008; Kniskern, 2007; Traykovski et al., 2000; Harris et al., 2005), and may have played some role on the Waipaoa shelf, too (Hale et al., 2012; Moriarty et al., 2012).

Despite many similarities, the relative role of waves and currents on the shelves, and the timing of waves and currents relative to river floods differed among the three margins. Offshore of the Eel River, gravity flows were primarily wave-supported (Traycovski et al., 2000). While similar wave-supported gravity flows were important in shallow areas (water depth less than 60 m) of the Waiapu shelf, current-supported gravity flows could carry sediment to deeper water (Ma et al., 2010), and likely played a role on the Waipaoa shelf, too (Moriarty et al., 2012). Unlike the Eel margin, where floods usually coincided with energetic ocean conditions, the Waiapu and Waipaoa margins also experience floods in times of relatively low wave energy. During a Waiapu River flood with relatively low waves, sediment settled from the river plume and rapidly deposited on the inner shelf (Ma, 2009; Kniskern, 2007). This sediment

was only resuspended and moved to deeper water when waves became more energetic (Ma, 2009; Kniskern, 2007). This timing was similar to the January 31 flood and subsequent wave events discussed above for the Waipaoa shelf, and to Poverty Bay events described in Bever et al. (2011) and Bever and Harris (submitted).

Will shelf deposits from either the January 31 or July 7 floods be preserved? These events were the 5th and 14th largest floods in the forty-four year record, with discharge peaks of over 2400 and 1700 $m^3 s^{-1}$. Yet in both cases, waves resuspended sediment across the entire shelf within two months of the flood, reworking and redistributing the initial deposit (e.g. Figure 3-10, 3-11). Estimated riverine deposits on the shelf were thin (Figure 3-11) compared to field observations that indicated measurable ^{7}Be activities as deep as 0 - ~8 cm in the seabed two weeks after the January 31, 2010 flood (Kniskern et al., 2012). Storm waves, however, were estimated to be capable of resuspending sediment (from both the seabed and riverine sediment classes) from up to 1 – 10 cm deep in the seabed, depending on bed stresses and sediment availability. These model results indicate that only thick flood deposits would be capable of being preserved throughout a winter storm season. Bioturbation will also mix the seabed (Rose and Kuehl, 2008), especially in the summer (December - February). Thus, the physical structure of these flood deposits is likely compromised, although carbon or radioisotope signatures could persist.

3.7 Conclusion

Dispersal estimates for flood sediment depended strongly on the settling characteristics assumed for the material. Poverty Bay retained most of the faster-settling sediment (w_s ~ 0.5 – 1.0 mm/s) and only a low

percentage of this sediment was exported to the shelf several months after its delivery to the coastal ocean (Table 3- 5, Figure 3-11). Sediment dispersal from Poverty Bay and the shelf increased for slower-settling particles. Consolidation and swelling, neglected in this model, may also enhance export from shallow areas, where the seabed is more often mobilized, and facilitate retention on the shelf where energetic bed stresses occur less frequently, allowing the seabed to consolidate. Settling velocity also affected the shape of the flood deposit footprint. Deposits of slower settling material were more widespread than those composed of faster settling sediment because of the longer residence time in the water column.

Initial flood deposits were resuspended by waves and redistributed by currents on the Waipaoa shelf. During floods, both local winds and larger-scale currents influenced water column velocities and the path of the river plume. Energetic waves, whether occurring during or after a flood, resuspended fluvial sediment into the water column where they were dispersed as suspended load. Preferential resuspension of deposits from shallow locations encouraged accumulation in deeper water, near long-term depocenters.

Short term deposition as estimated by the numerical model, occurring over days to months, differed from long-term accumulation seen in geochronological records of ^{210}Pb. Hydrodynamic conditions varied among the flood and wave events studied, which greatly affected the shapes of resultant deposits, especially on shorter timescales. Estimates of sediment budget and deposit characteristics changed over time as shallow initial deposits were resuspended, and sediment accumulated in deeper

areas that had low bed stresses (Figure 3-12). Because transport to the final location of deposition seemed to occur in multiple steps, this implied that oceanographic transport mechanisms provide important controls on depositional patterns. That is, shelf deposition depended as much on oceanographic transport (waves and currents) as on source characteristics such as flood size and sediment distribution.

References

Ariathurai, C.R., and Arulanandan, K., 1978. Erosion rates of cohesive soils. Journal of Hydraulics Division, 104 (2): 279 – 282.

Bentley, S.J., and Nittrouer, C.A., 2003. Emplacement, modification, and preservation of event strata on a flood-dominated continental shelf: Eel shelf, Northern California. Continental Shelf Research, 23: 1465-1493.

Bever, A. J., 2010. Integrating space– and time-scales of sediment-transport for Poverty Bay, New Zealand. (PhD, Virginia Institute of Marine Science, College of William & Mary).

Bever, A. J., Harris, C. K., and McNinch, J. E., 2011. Hydrodynamics and sediment-transport in the nearshore of Poverty Bay, New Zealand: Observations of nearshore sediment segregation and *oceanic* storms. Continental Shelf Research, 31: 507-526.

Bever, A.J. and Harris, C.K., 2012. Storm and fair-weather driven sediment-transport within Poverty Bay, New Zealand, evaluated using coupled numerical models. *Submitted.*

Blair, N.E., Leithold, E.L., and Aller, R.C., 2004. From bedrock to burial: the evolution of particulate organic carbon across coupled watershed-continental margin systems. Marine Chemistry, 92: 141-156.

Brackley, H. L., Blair, N. E., Trustrum, N. A., Carter, L., Leithold, E. L., Canuel, E. A., et al., 2010. Dispersal and transformation of organic carbon across an episodic, high sediment discharge continental margin, Waipaoa sedimentary system, New Zealand. Marine Geology, 270(1-4): 202-212.

Carter, L., Orpin, A. R., and Kuehl, S. A., 2010. From mountain source to ocean sink – the passage of sediment across an active margin, Waipaoa sedimentary system, New Zealand. Marine Geology, 270(1-4): 1-10.

Chapman, D. C., 1985. Numerical treatment of cross-shelf open boundaries in a barotropic coastal ocean model. Journal of Physical Oceanography, 15, 1060-1075.

Chiswell, S. M., 2000. The Wairarapa coastal current. New Zealand Journal of Marine and Freshwater Research, *34*(2): 303-315.

Chiswell, S. M., 2005. Mean and variability in the Wairarapa and Hikurangi eddies, New Zealand. New Zealand Journal of Marine and Freshwater Research, *39*(1): 121-134.

Chiswell, S. M., and Roemmich, D., 1998. The east cape current and two eddies: A mechanism for larval retention? New Zealand Journal of Marine and Freshwater Research, 32(2): 385-397.

Corbett, D.R., Walsh, J.P., Orpin, A., Ogston, A., Kiker, J., Hale, R., Moriarty, J.M., and Harris, C.K., 2012. Spatial and temporal variability of surface seabed properties: Waipaoa River margin, New Zealand. Proceedings of the AGU Ocean Sciences Conference. Salt Lake City, UT: 20 – 24 February 2012.

Davies, T., Cullen, M. J. P., Malcolm, A. J., Mawson, M. H., Staniforth, A., White, A. A., et al., 2005. A new dynamical core for the met office's global and regional modelling of the atmosphere. Quarterly Journal of the Royal Meteorological Society, 131(608): 1759-1782.

Drake, D.E., 1999. Temporal and spatial variability of the sediment grain-size distribution on the Eel shelf: the flood layer of 1995. *Marine Geology*, *154:* 169-182.

Drake, D.E. and Cacchione, D.A., 1985. Seasonal variation in sediment transport on the Russian River shelf, California. Continental Shelf Research, *4*(5): 495 – 514.

Ferre, B., Sherwood, C.R. and Wiberg, P.L., 2010. Sediment transport on the Palos Verdes shelf, California. Continental Shelf Research, 30: 761-780.

Flather, R.A., 1976. A tidal model of the north-west European continental shelf. Memoires Societe Royale des Sciences de Liege, 6 (10): 141-164.

Foster, G., and Carter, L., 1997. Mud sedimentation on the continental shelf at an accretionary margin - Poverty Bay New Zealand. New Zealand Journal of Geology and Geophysics, 40: 157-173.

Gerber, T. P., Pratson, L. F., Kuehl, S., Walsh, J. P., Alexander, C., and Palmer, A., 2010. The influence of sea level and tectonics on late Pleistocene through Holocene sediment storage along the high-sediment supply Waipaoa continental shelf. Marine Geology, 270(1-4): 139-159.

Geyer, W.R., Hill, P., Milligan, T., and Traykovski, P., 2000. The structure of the Eel River plume during floods. Continental Shelf Research. *20*: 2067 – 2093.

Gomez, B., Carter, L., Trustrum, N. A., Palmer, A. S., and Roberts, A. P., 2004. El Niño–Southern oscillation signal associated with middle Holocene climate change in intercorrelated terrestrial and marine sediment cores, north island, New Zealand. Geology, 32(8): 653-656.

Griffths and Glasby, 1985. Input of river-derived sediment to the New Zealand continental shelf: I. Mass. Estuarine, Coastal, and Shelf Science, 21: 773-787.

Haidvogel, D. B., Arango, H. G., Hedstrom, K., Beckmann, A., Malanotte-Rizzoli, P., and Shchepetkin, A. F., 2000. Model evaluation experiments in the North Atlantic basin: Simulations in nonlinear terrain-following coordinates. Dynamics of Atmospheres and Oceans, 32(3-4): 239-281.

Haidvogel, D. B., Arango, H., Budgell, W. P., Cornuelle, B. D., Curchitser, E., Di Lorenzo, E., et al., 2008. Ocean forecasting in terrain-following coordinates: Formulation and skill assessment of the regional ocean modeling system. Journal of Computational Physics, 227(7), 3595-3624.

Hale, R., Ogston, A., Walsh, J.P and Orpin, A., 2012. Annual trends in sediment flux on the Waipaoa River margin, NZ. Proceedings of the AGU Ocean Sciences Conference. Salt Lake City, UT: 20 – 24 February 2012.

Harris, C. K., Traykovski, P., and Geyer, W. R., 2005. Flood dispersal and deposition by near-bed gravitational sediment flows and oceanographic transport : A numerical modeling study of the eel river shelf, northern California. Journal of Geophysical Research, 110(C09025).

Harris, C.K. and Wiberg, P., 1997. Approaches to quantifying long-term continental shelf sediment transport with an example from the northern California STRESS mid-shelf site. Continental Shelf Research, 17: 1389-1418.

Harris, C. K., and Wiberg, P., 2002. Across-shelf sediment transport: Interactions between suspended sediment and bed sediment. *Journal of Geophysical.Research, 107*: 3008.

Healy, T., Stephens, S., Black, K., Gorman, R., and Beamsley, B., 1998. Numerical and physical process studies for port of Gisborne redesign for the 21st century. Journal of Coastal Research Special Issue, *26:* 304-311.

Hicks, D. M., Gomez, B., and Trustrum, N. A., 2000. Erosion thresholds and suspended sediment yields, Waipaoa River basin, New Zealand. Water Resources Research, *36*(4): 1129-1142.

Hicks, D. M., Gomez, B., and Trustrum, N. A., 2004. Event suspended sediment characteristics and the generation of hyperpycnal plumes at river mouths: East coast continental margin, north island, New Zealand. The Journal of Geology, 112(4): 471-485.

Kachel, N.B. and Smith, J.D., 1989. Sediment transport and deposition on the Washington continental shelf. In M.R. Landry and B. M. Hickey (Eds.), Coastal oceanography of Washington and Oregon. Elsevier, New York: 287-348.

Kiker, J.M., 2012. Spatial and temporal variability in surficial seabed character, Waipaoa River Margin, New Zealand. M.S. Thesis, East Carolina University, Greenville, NC.

Kniskern, T.A., 2007. Shelf sediment dispersal mechanisms and deposition on the Waiapu River shelf, New Zealand. (PhD, Virginia Institute of Marine Science, College of William & Mary).

Kniskern, T.A., 2010. Investigating sediment dynamics on the Waipaoa River shelf, New Zealand: creating a framework to predict preservation on continental margins. A Postdoctoral Proposal. NSF Proposal.

Kniskern, T.A., Harris, C.K., Mitra, and S., Orpin, A., 2012. Flood deposition on the Waipaoa shelf, New Zealand. Proceedings of the AGU Ocean Sciences Conference. Salt Lake City, UT: 20 – 24 February 2012.

Kniskern, T.A., Mitra, S., Orpin, A., and Harris, C.K., in prep. Radioisotopic and biomarker characteristics of a post-flood event on the Waipaoa River shelf.

Lavelle, J.W. and Thacker, W.C., 2008. A pretty good sponge: Dealing with open boundaries in limited-area ocean models. Ocean Modelling, 20: 270-292.

Ma, Y., 2009. Continental shelf sediment transport and depositional processes on an energetic active margin: the Waiapu River Shelf, New Zealand. (PhD, Virginia Institute of Marine Science, College of William & Mary)

Ma, Y., Wright, L. D., and Friedrichs, C. T., 2008. Observations of sediment transport on the continental shelf off the mouth of the Waiapu river, New Zealand: Evidence for current-supported gravity flows. *Continental Shelf Research, 28*(4-5): 516-532.

Ma, Y., Friedrichs, C. T., Harris, C. K., and Wright, L. D., 2010. Deposition by seasonal wave- and current-supported sediment gravity flows interacting with spatially varying bathymetry: Waiapu shelf, New Zealand. *Marine* Geology, *275*(1-4): 199-211.

Madsen, O.S., 1994. Spectral wave-current bottom boundary layer flows. Proceedings of the 24th International Conference on Coastal Engineering, ASCE, Kobe 1:384-398.

Marchesiello, P., McWilliams, J. C., and Shchepetkin, A., 2001. Open boundary conditions for long-term integration of regional oceanic models. Ocean Modelling, *3*(1-2): 1-20.

McNinch, J. E., Wadman, H. M., and Perkey, D. W., 2008. Sediment segregation and dispersal across the land-sea interface: Waipaoa sedimentary system, New Zealand. AGU Ocean Sciences Meeting, San Francisco, Abstract 3174.

Miller, A. J., and Kuehl, S. A., 2010. Shelf sedimentation on a tectonically active margin: A modern sediment budget for Poverty continental shelf, New Zealand. Marine Geology, 270(1-4): 175-187.

Milliman, J.D. and Farnsworth, K.L., 2011. River Discharge to the Coastal Ocean: A Global Synthesis. Cambridge University Press, Cambridge.

Milliman, J. D., and Syvitski, J. P. M. 1992. Geomorphic/Tectonic control of sediment discharge to the ocean: The importance of small mountainous rivers. The Journal of Geology, 100(5): 525-544.

Moriarty, J.M, Harris, C.K., and Friedrichs, C.T., 2012. Gravity-driven transport on a relatively flat active margin with complicated bathymetry: the Waipaoa River continental shelf, NZ. Proceedings of the 16th International Conference on Physics of Estuaries and Coastal Seas, Manhatten, New York.

Orpin, A. R., Alexander, C., Carter, L., Kuehl, S., and Walsh, J. P., 2006. Temporal and spatial complexity in post-glacial sedimentation on the tectonically active, Poverty Bay continental margin of New Zealand. Continental Shelf Research, *26*(17-18): 2205-2224.

Orpin, A.R., 2010. Holocene sedimentary record from Lake Tutira: A template for upland watershed erosion proximal to the Waipaoa Sedimentary System, northeastern New Zealand. Marine Geology, 270: 11-29.

Rose, L. E., and Kuehl, S. A., 2010. Recent sedimentation patterns and facies distribution on the Poverty shelf, New Zealand. Marine Geology, 270(1-4): 160-174.

Sadler, P.M., 1981. Sediment Accumulation Rates and the Completeness of Stratigraphic Sections. Journal of Geology, 89(5): 569-584.

Sanford, L.P., 2008. Modeling a dynamically varying mixed sediment bed with erosion, deposition, bioturbation, consolidation, and armoring. Computers & Geosciences, 34: 1263-1283.

Sanford, L.P., and Maa, J.P.-Y., 2001. A unified erosion formulation for fine sediments. Marine Geology, 179: 9-23.

Scully, M.E., Friedrichs, C.T., and Wright, L.D., 2003. Numerical modeling of gravity-driven sediment transport and deposition on an energetic continental shelf: Eel River, northern California. Journal of Geophysical Research, 108: C4.

Shchepetkin, A. F., & McWilliams, J. C. (2005). The regional oceanic modeling system (ROMS): A split-explicit, free-surface, topography-following-coordinate oceanic model. Ocean Modelling, 9(4): 347-404.

Shchepetkin, A. F., & McWilliams, J. C. (2009). Correction and commentary for "Ocean forecasting in terrain-following coordinates: Formulation and skill assessment of the regional ocean modeling system" by Haidvogel et al., J. comp. phys. 227, pp. 3595–3624. Journal of Computational Physics, 228(24): 8985-9000.

Sherwood, C. R., Butman, B., Cacchione, D. A., Drake, D. E., Gross, T. F., Sternberg, R. W., Wiberg, P.L., and Williams III, A.J., 1994. Sediment-transport events on the northern California continental shelf during the 1990–1991 STRESS experiment. Continental Shelf Research, 14(10-11): 1063-1099.

Smith, R. K., 1988. Poverty Bay, New Zealand: A case of coastal accretion. New Zealand Journal of Marine and Freshwater Research, 22(1): 135-142.

Sommerfield, C.K. and Nittrouer, C.A., 1999. Modern accumulation rates and a sediment budget for the Eel shelf: a flood-dominated depositional environment. Marine Geology, 154: 227-241.

Stephens, S. A., Bell, R. G., and Black, K. P., 2000. Complex circulation in a coastal embayment: Shelf-current, wind and density-driven circulation in Poverty Bay, New Zealand. International Coastal Symposium (ICS 2000): Challenges for the 21st Century in Coastal Science, Engineering and Environment, Rotorua, New Zealand, *34:* 45-59.

Tolman, H. L., Balasubramaniyan, B., Burroughs, L. D., Chalikov, D. V., Chao, Y. Y., Chen, H. S., et al., 2002. Development and implementation of wind-generated ocean surface wave modelsat NCEP*. Weather and Forecasting, 17(2): 311-333.

Traykovski, P. Geyer, W.R., Irish,. J.D., and Lynch, J.F., 2000. The role of wave-induced density-driven fluid mud flows for cross-shelf transport on the Eel River continental shelf. Continental Shelf Research, 20: 2113-2140.

Traykovski, P., Wiberg, P.L., and Geyer, W.R., 2007. Observations and modeling of wave-supported sediment gravity flows on the Po prodelta and comparison to prior observations from the Eel Shelf. Continental Shelf Research, 27: 375-399.

Wadman, H.M., and McNinch, J.E., 2009. Sediment segregation and dispersal across the land-sea interface: Waipaoa sedimentary system, New Zealand, Integration and Synthesis of MARGINS Sediment Source-to-Sink Research Workshop, Gisborne, New Zealand.

Walling, D.E. and Webb, B.W., 1996. Erosion and sediment yield: a global overview. In: Erosion and sediment yield: global and regional perspectives. IAHS (International Association of Hydrological Sciences) Publications, vol. 236. Galliard Printers Ltd, Great Yarmouth, UK, 3-19.

Walsh, J.P, Corbett, R. Ogton, A. Harris, C.K. and Orpin, A., 2009. Collaborative research: formation, reworking and accumulation of sedimentary deposits, Waipaoa river shelf, New Zealand. NSF Proposal 0840887.

Warner, J. C., Sherwood, C. R., Signell, R. P., Harris, C. K., and Arango, H. G., 2008. Development of a three-dimensional, regional, coupled wave, current, and sediment-transport model. Computers & Geosciences, 34(10): 1284-1306.

Warrick, J. A., and Milliman, J. D., 2003. Hyperpycnal sediment discharge from semiarid southern california rivers: Implications for coastal sediment budgets. Geology, *31*(9): 781-784.

Wheatcroft, R.A., 1990. Preservation potential of sedimentary event layers. Geology, 18 (9): 843-843.

Wheatcroft, R. A., 2000. Oceanic flood sedimentation: A new perspective. Continental Shelf Research, 20(16): 2059-2066.

Wheatcroft, R.A., and Drake, D.E., 2003. Post-depositional alteration and preservation of sedimentary event layers on continental margins, I. The role of episodic sedimentation. Marine Geology (199): 123-137.

Wheatcroft, R. A., Wiberg, P. L., Alexander, C. R., Bentley, S. J., Drake, D. E., Harris, C. K., et al., 2007. Post-depositional alteration and preservation of sedimentary strata. In C. A. Nittrouer, J. A. Austin, M. E. Field, J. H. Kravitz, J. P. M. Syvitski & P. L. Wiberg (Eds.), Continental margin sedimentation: From sediment transport to sequence stratigraphy. International Association of Sedimentologists: 101-155.

Wiberg, P. L., Drake, D. E., and Cacchione, D. A., 1994. Sediment resuspension and bed armoring during high bottom stress events on the northern California inner continental shelf: Measurements and predictions. Continental Shelf Research, 14(10-11): 1191-1219.

Wood, M. P., 2006. Sedimentation on a high input continental shelf at the active Hikurangi margin. Unpublished M.S., Victoria University of Wellington.

Wright, L.D. and Friedrichs, C.T., 2006. Gravity-driven sediment transport on continental shelves: A status report. Continental Shelf Research, 26: 2092-2107.

Xue, Z., He, R., Liu, J.P., and Warner, J.C., 2012. Modeling transport and deposition of the Mekong River sediment. Continental Shelf Research, 37: 66 – 78.

Tables

Table 3-1: Datasets used for model initialization and forcing

Type of Data	Data Description and Source
Bathymetry to construct model grid	• Multibeam surveys (McNinch et al., 2008; Gerber et al., 2010 provided by S. Kuehl) • Bathymetric contours provided by S. Stephens (NIWA) • Historical gridded bathymetry (pers. Comm. NIWA) • Modeled bathymetry of New Zealand ROMs model (ROMS-NZ; Hadfield, 2010)
Currents, temperature and salinity at open boundaries, and for model initialization	• Baroclinic version of ROMS-NZ, provided by M. Hadfield
Wave height, direction, and period	• NIWA's New Zealand Wave (NZWAVE) model (NZWAVE, an implementation of NOAA's Wave Watch III model; Tolman et al., 2002)
Wind stress	• NIWA's New Zealand Limited Area Model (NZLAM, an implementation of the UK Met Office's Unified Model; Davies et al., 2005)
Tidal components: open boundary sea surface height and tidal velocities	• Tidal velocities, amplitudes and phase components from the Oregon State Tidal Prediction Software TPX07.1 global solution (OTPS; Egbert et al., 1994; Egbert and Erofeeva, 2002).
Metrological data	• Air pressure, cloud cover, precipitation, relative humidity, shortwave radiation, air temperature from NIWA's National Climate Database web system (Cliflo; http://cliflo.niwa.co.nz/) at Gisborne airport
River discharge of freshwater and sediment	• River gauge measurements provided by G. Hall and D. Peacock (Gisborne District Council, New Zealand)

Sediment properties of fluvial and seabed material (diameter, settling velocity, critical stress for erosion)	• Hicks et al., 2004 • Wood, 2006. • ADV and OBS data provided by A. Ogston and R. Hale
Seabed characteristics for comparison to model estimates	• Radiometric and x-ray analysis of cores (by J.P. Walsh, R. Corbett, and J. Kiker of ECU; A. Orpin of NIWA; and T. Kniskern of VIMS)

Table 3-2: Sediment characteristics for all sediment classes

Grain Size Class	Sediment Source	% of Riverine Load	Settling Velocity (mm s^{-1})	Critical Shear Stress (Pa)	D_{50}(μm)	D_{50}(phi)
1	Seabed	--	2.4	0.1	63	4.0
2	Seabed	--	65.0	0.28	500	1.0
3	Seabed	--	125.0	0.53	1000	0.0
4	River	53	0.15	0.1	16	6.0
5	River	27	0.3	0.1	22	5.5
6	River	13	0.5	0.1	30	5.1
7	River	7	1.0	0.1	40	4.6
For all grain size classes: Sediment density: 2650 kg/m^3 Erosion rate: 2×10^{-4} $kg/m^2/s$ Porosity: 0.9						

Table 3-3: Model evaluation statistics

Statistics calculated for all tripod deployments with available observations. There was no data for currents for the third deployment at the deep tripod, or for suspended sediment concentrations for any deployments at the deep tripod.

Parameter		**R**[1]	σ_{model} / $\sigma_{observations}$[2]	**Bias**[3]
Wave Orbital Velocity		0.63 – 0.85	0.84 – 1.35	-6.4 – -1.4 cm/s
Depth-Averaged Currents	Along-Shelf	0.02– 0.42	0.34 – 0.73	-0.9 – 2.8 cm/s
	Across-Shelf	0.38 – 0.82	0.37 – 0.57	-1.4 – 9.8 cm/s
Suspended Sediment Concentrations		0.35 – 0.68	0.11 – 1.57	-0.206 – 0.003 g/L

[1] Correlation Coefficient

[2] Ratio of the standard deviation of the model estimates to that of the observations

[3] Difference between the mean of the model estimates and mean of the observations

Table 3-4: Hydrodynamic conditions

Evaluated at the deep tripod at 60 m water depth for different time periods.

'Event'	Time Period	Wave Orbital Velocity (cm/s)	Bed Stress (Pa)	Current Magnitude (cm/s)	Mean Current Direction (degrees[1])	Wind Magnitude (m/s)	Mean Wind Direction (degrees[1])
Entire Field Season	15 Jan 2010 – 15 Feb 2011	4.30	0.06	10.4	69	6.6	-56
31 Jan Flood	30 Jan 2010 – 14 Feb 2010	2.94	0.03	11.6	-106	5.4	-173
6 Jul Flood	4 Jul 2010 – 22 Jul 2010	8.29	0.16	15.7	68	8.7	78
7 Mar Wave Event	4 Mar 2010 – 13 Mar 2010	7.94	0.11	9.4	81	7.6	81
31 Aug Wave Event	29 Aug 2010 – 8 Sep 2010	6.77	0.08	5.4	87	8.2	8.6
Period of Dry Wave Events	15 Feb 2010 – 19 May 2010	5.13	0.06	7.4	77	6.1	-89
Period of Wet Wave Events	22 Jul 2010 – 30 Sept 2010	4.36	0.05	6.3	84	6.9	-44

[1]Direction is given in degrees counterclockwise from east, toward which the currents and wind are traveling.

Table 3-5: Sediment budget for riverine sediments

Grain Size Class	% of Riverine Load	Settling Velocity (mm s^{-1})	Percent of Riverine Load Remaining in Poverty Bay[1]	Percent of Riverine Load Remaining on the Shelf (outside of Poverty Bay)[1]	Percent of Riverine Load Transported Offshore[1]
4	53	0.15	34	21	45
5	27	0.3	58	21	21
6	13	0.5	75	16	9
7	7	1.0	92	7	1

[1] Budgets were computed as follows: the total mass of suspended and deposited sediment in Poverty Bay and on the shelf (excluding Poverty Bay) was divided by the cumulative sum of sediment entering the model grid between 1 January 2010 and 15 February 2011. The remainder of sediment was assumed to be transported offshore.

Figures

Figure 3-1: Study site on North Island, New Zealand

A. Adapted from Miller and Kuehl, 2009. Spatial distribution of ^{210}Pb accumulation rates (cm y^{-1}) with labels for Waipaoa River (red arrow), Poverty Bay, Poverty Gap, Lachlan Anticline (L.A.), Ariel Anticline (A.A.), and depocenters (Dep.). Grey bathymetric contours indicate every 10 m. ***B.*** Waipaoa Shelf map showing tripod locations (brown) and multi-core stations (black) from the first research cruise. Grey and black bathymetric contours indicate every 10 m up to 100 m depth and every 50 m up to 150 m depth. Inset shows location of study site in New Zealand. ***C.*** Waipaoa model grid showing bathymetry with gridlines. Each box indicates 25 grid cells. ***D.*** Waipaoa model grid showing a close-up of shelf bathymetry without gridlines. Grey and black bathymetric contours indicate every 10 m up to 100 m depth and every 50 m up to 150 m depth.

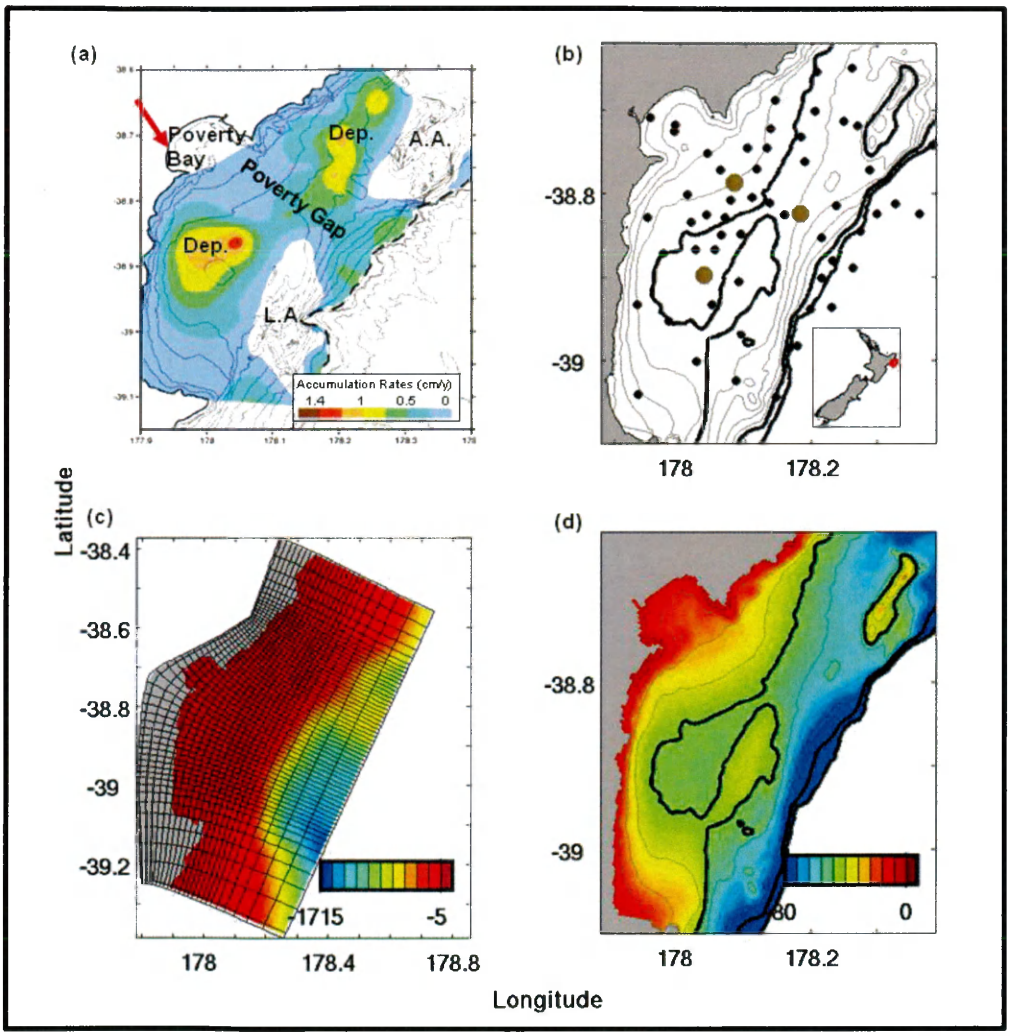
(a)
Poverty Bay
Dep.
A.A.
Poverty Gap
Dep.
L.A.
Accumulation Rates (cm/y)
1.4 1 0.5 0
(b)
-38.8
-39
178
178.2
(c)
Latitude
-38.4
-38.6
-38.8
-39
-39.2
1715
-5
178
178.4
178.8
(d)
-38.8
-39
0
178
178.2
Longitude

Figure 3-2: Timeseries of weather conditions on the Waipaoa Shelf

(a) River and (b) sediment discharge from Gisborne District Council, New Zealand, (c) modeled significant wave height from NZWAVE, (d) modeled wind speed from NZLAM, and (e) modeled depth-averaged tidally-filtered current speed from ROMS-NZ. Wave and wind time-series are averages over the model domain. Currents are estimates from the shallow tripod site (see Figure 1b). Grey boxes highlight the January flood (1/30/2010 – 2/14/2010), March wave event (3/4/2010 – 3/13/2010), July flood (7/4/2010 – 7/22/2010), and August wave event (8/29/2010 – 9/8/2010).

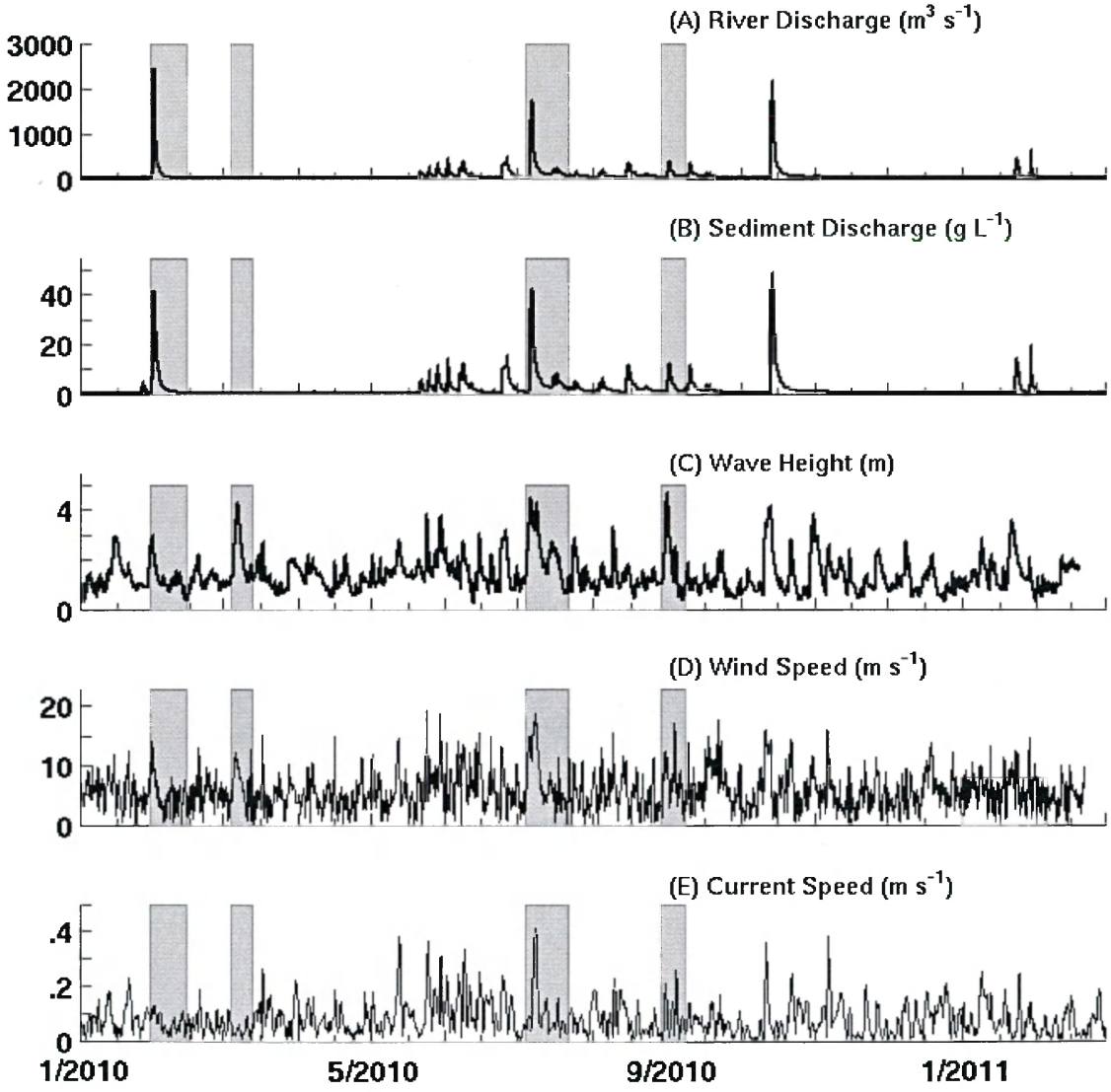
(A) River Discharge ($m^3 s^{-1}$)
3000
2000
1000
0
(B) Sediment Discharge ($g L^{-1}$)
40
20
0
(C) Wave Height (m)
4
0
(D) Wind Speed ($m s^{-1}$)
20
10
0
(E) Current Speed ($m s^{-1}$)
.4
.2
0
1/2010
5/2010
9/2010
1/2011

Figure 3-3: Timeseries of estimated waves, bed stress, SSC and seabed elevation

Timeseries of (a) significant wave height, (b) bottom wave period, (c) wave orbital velocity, (d) total wave- and current- induced bed shear stress, (e) suspended sediment concentrations and (f) seabed height at the shallow tripod calculated based on fluxes of fluvial and seabed material. Black lines indicate model estimates. Grey lines indicate ADV (wave height; bed shear stress) and OBS (suspended sediment concentration) observations collected by A. Ogston and R. Hale (University of Washington).

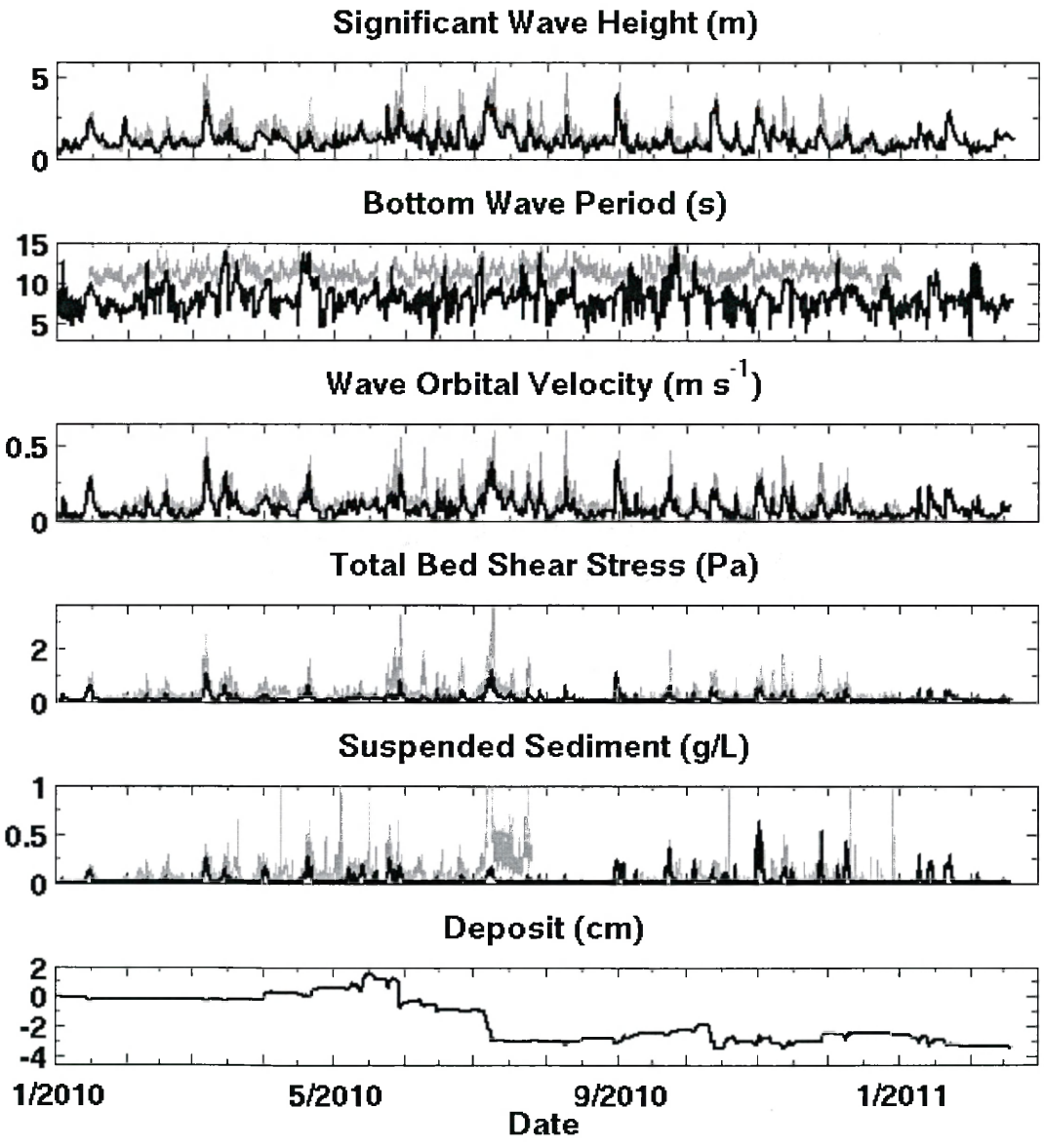
Significant Wave Height (m)
5
0
Bottom Wave Period (s)
15
10
5
Wave Orbital Velocity (m s-1)
0.5
0
Total Bed Shear Stress (Pa)
2
0
Suspended Sediment (g/L)
1
0.5
0
Deposit (cm)
2
0
-2
-4
1/2010
5/2010
9/2010
1/2011
Date

Figure 3-4: Time-series of estimated currents

(a) Along-isobath and (b) across-isobath depth-averaged and tidally-filtered currents at the shallow tripod. ADCP observations provided by A. Ogston and R. Hale (University of Washington). Grey boxes highlight the January flood (1/30/2010 – 2/14/2010), March wave event (3/4/2010 – 3/13/2010), July flood (7/4/2010 – 7/22/2010), and August wave event (8/29/2010 – 9/8/2010).

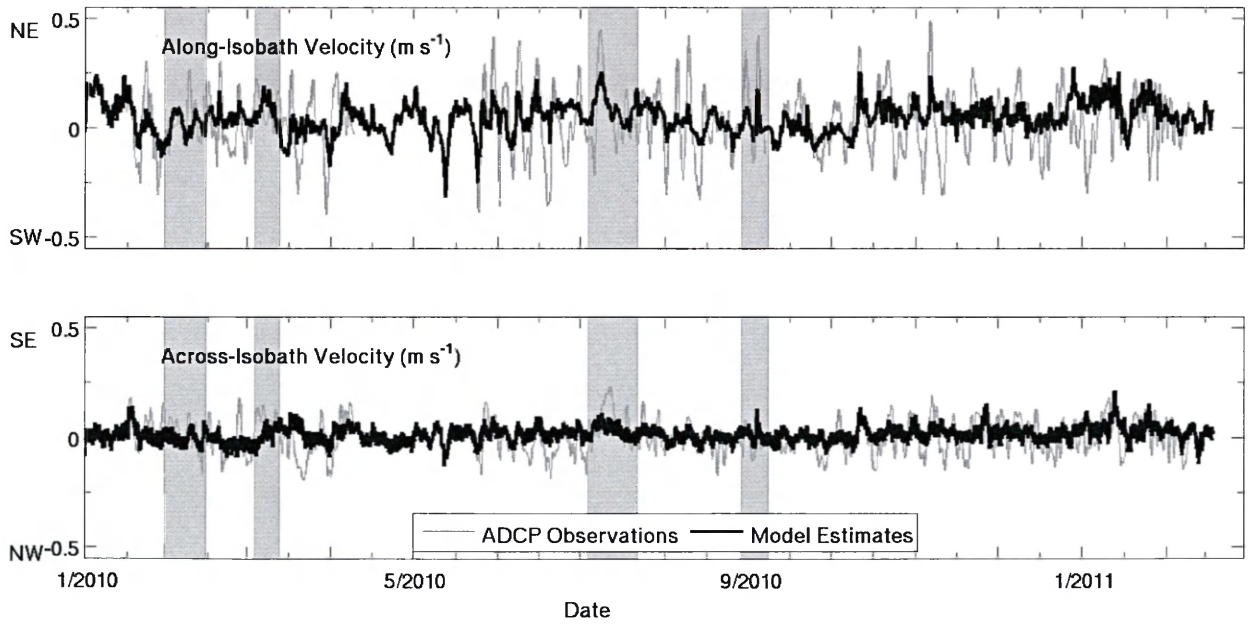

Figure 3-5: Map of estimated time-averaged depth-averaged currents

Water speed (shading) and direction (black arrows) are shown. Long blue arrows indicate direction of observed current velocities for all tripod deployments. Black bathymetric contours indicate every 10 m.

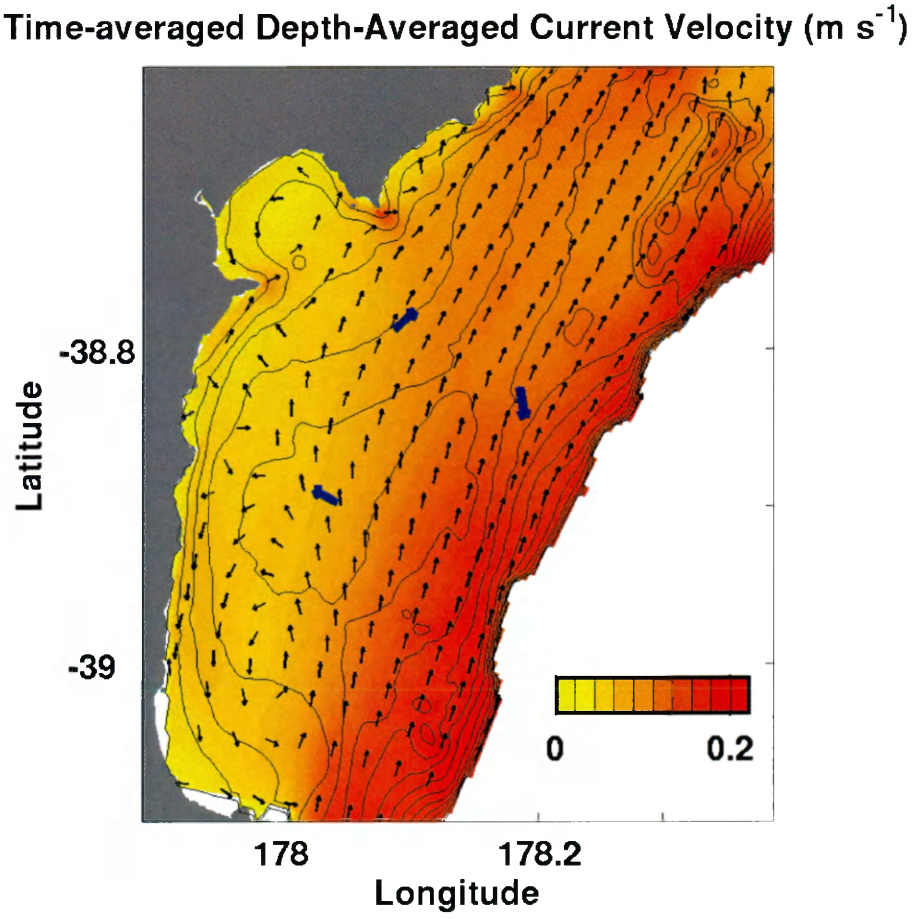

Figure 3-6: Seabed thickness variability

Time-averaged seabed thickness (left) and standard deviation of seabed thickness (right). Thickness calculations include both seabed and riverine sediment. Bathymetic contours show every 10 m water depth and highlight the 50 m, 100 m, and 150 m contours.

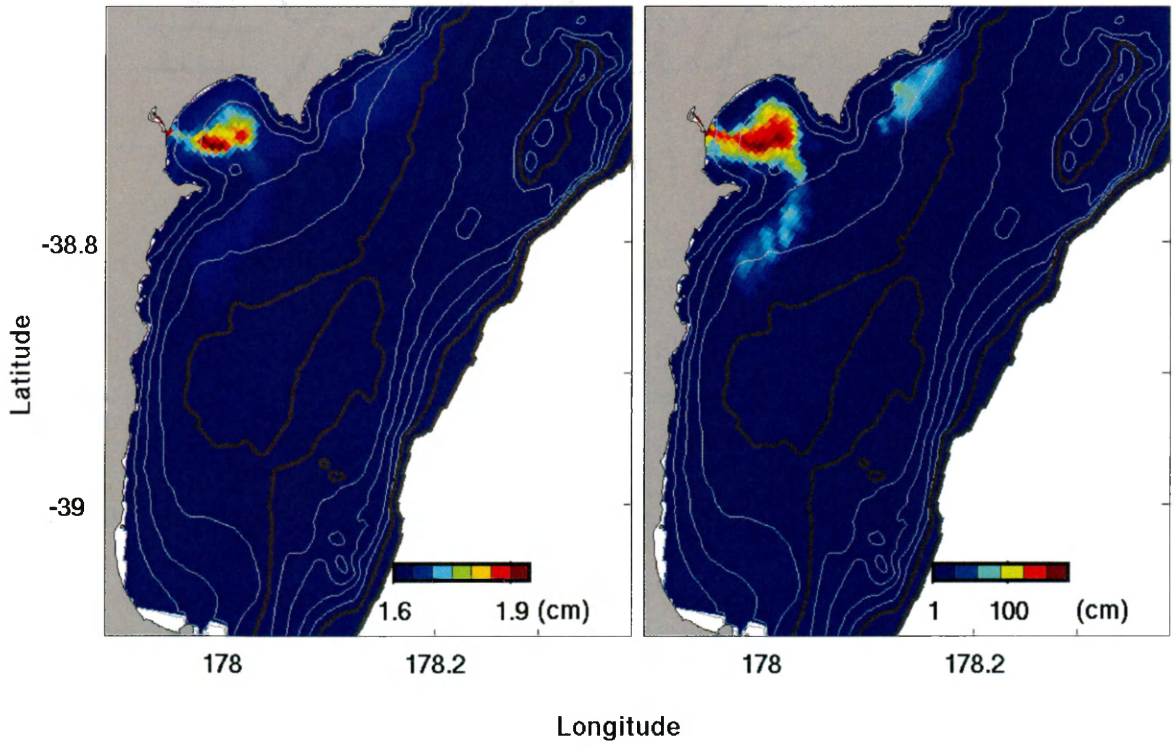

Figure 3-7: Observed seabed erodibility

From Kiker, 2012. Sediment erodibility measurements taken in January 2010 (C1), May 2010 (C2), September 2010 (C3), and February 2011 (C4). Grey bathymetric contours are every 10 m. until 100 m.

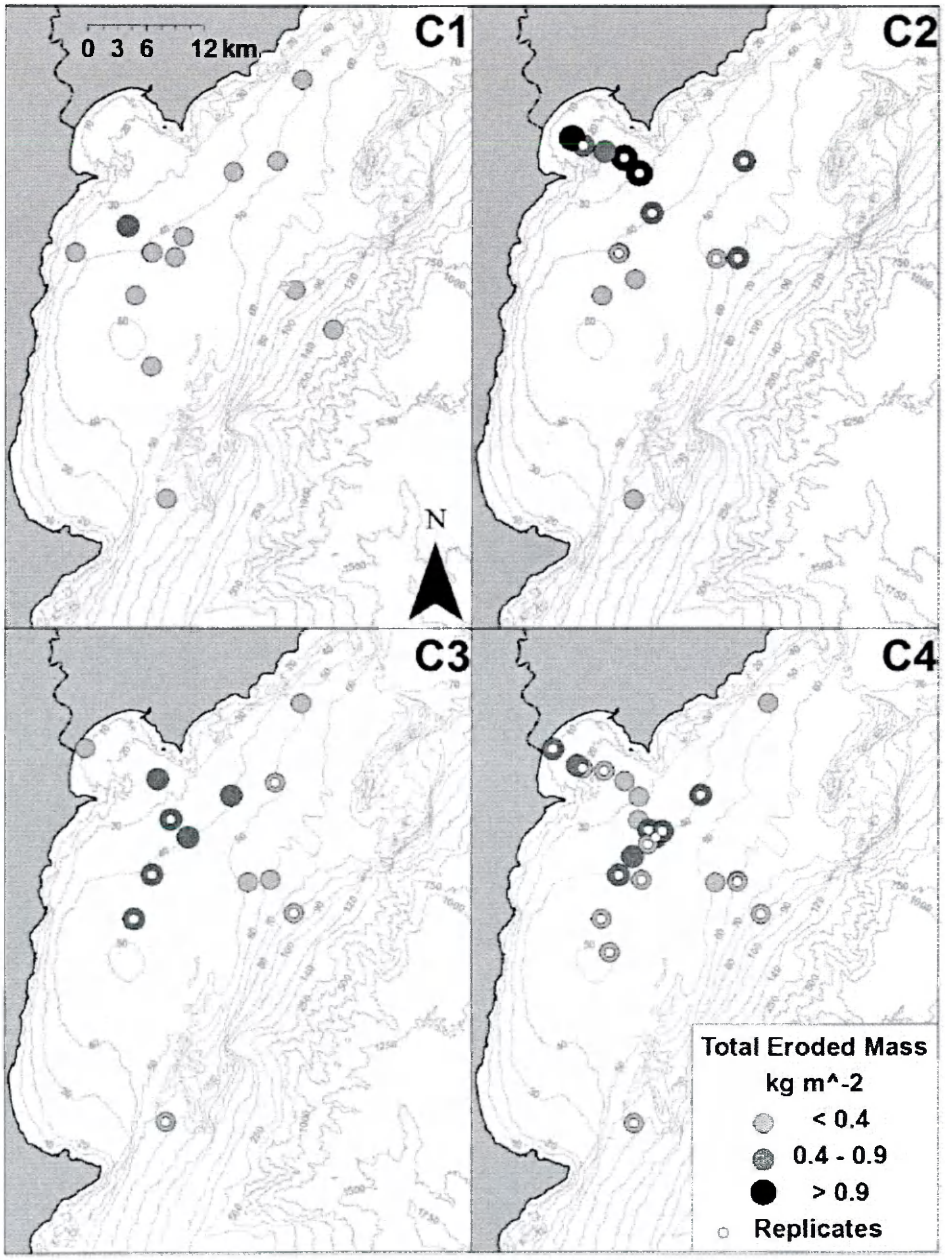

Figure 3-8: Observed ^{7}Be inventories

From (a) January, (b) May, and (c) September 2010 research cruises and the (d) February 2011 research cruises. Figure from Kiker, 2012.

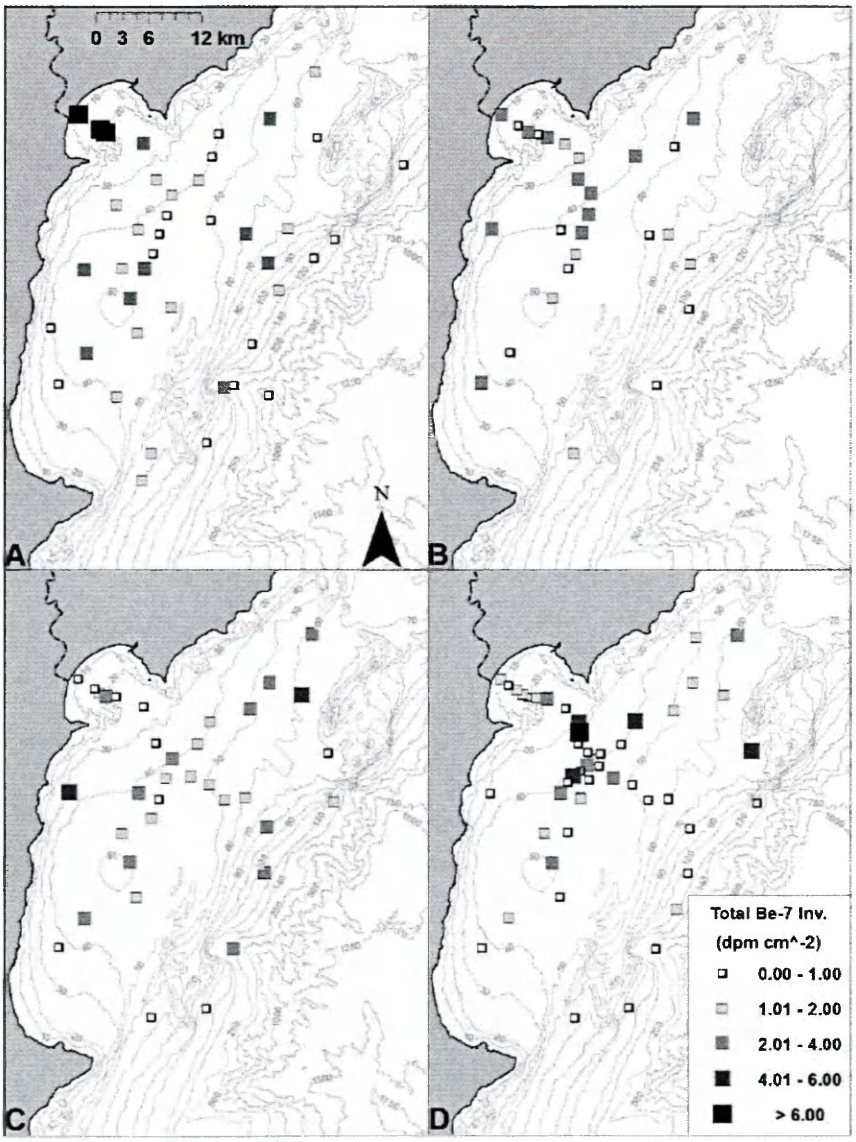

Figure 3-9: Net ^{7}Be inventories from 15 – 17 February 2010 to 13 - 20 January 2010

Positive values indicate fresh deposition and negative values indicate erosion. Figure provided by Tara Kniskern (VIMS; Kniskern et al, in prep).

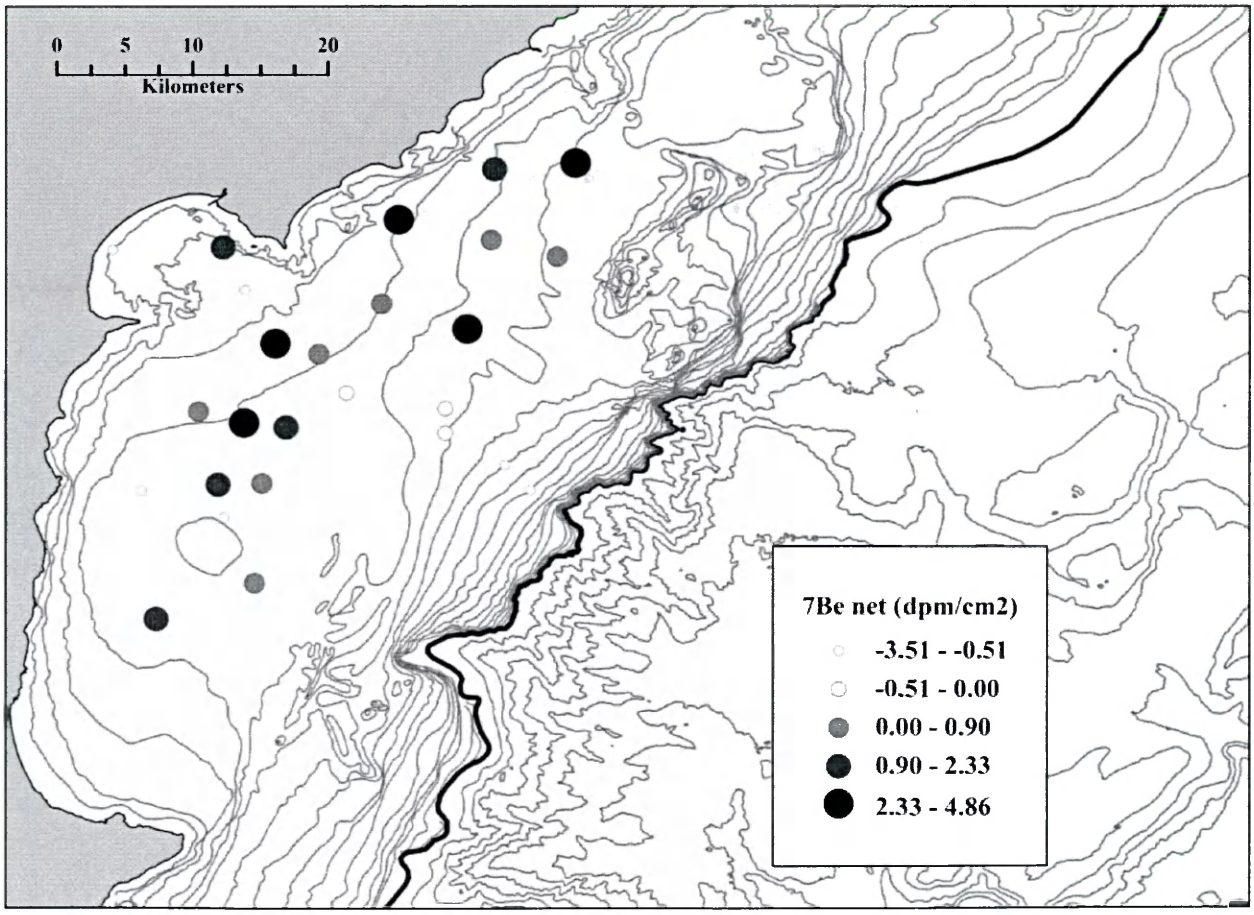

Figure 3-10: Cumulative sediment fluxes and hydrodynamic conditions for selected time periods

Left panels: Maps of cumulative deposition (positive) and erosion (negative) of riverine sediments during a specific time period. Deposition and erosion are shown for changes in seabed height greater than 1 mm. Flux arrows are shown for every 10 grid cells, and for fluxes greater than 2×10^6 kg m^2 except as noted. ***Right panels***: Representative snapshots of bottom orbital velocity (shading), surface (maroon arrows) and bottom (black arrows) currents, and wind (red arrow) during events. Currents are shown for every 10 grid cells. Time periods include (a) Cumulative sediment fluxes and deposition for January 30 – February 14, 2010. Snapshot of hydrodynamic conditions on February 2, 2010; (b) Cumulative sediment fluxes and deposition for March 4 – 13, 2010. Snapshot of hydrodynamic conditions on March 7, 2010; (c) Cumulative sediment fluxes and deposition for February 14 – May 15, 2010. Snapshot of hydrodynamic conditions on April 7, 2010; (d) Cumulative sediment fluxes and deposition for July 4 - 22, 2010. *Notice the change in scale from 4a,b,c,e and f.* Snapshot of hydrodynamic conditions on July 9, 2010; (e) Cumulative sediment fluxes and deposition for August 29 – September 8, 2010. Snapshot of hydrodynamic conditions on September 1, 2010; (f) Cumulative sediment fluxes and deposition for July 22 – September 30, 2010. Snapshot of hydrodynamic conditions on August 4, 2010; (g) Cumulative sediment fluxes and deposition for January 15, 2010 – February 15, 2011. *Flux arrows are shown for every 10 grid cells, for fluxes greater than* 20×10^6 *kg* m^2*. Notice the change in scale from 4a,b,c,e and f.*

(a) Cumulative sediment fluxes and deposition for January 30 – February 14, 2010. Snapshot of hydrodynamic conditions on February 2, 2010.

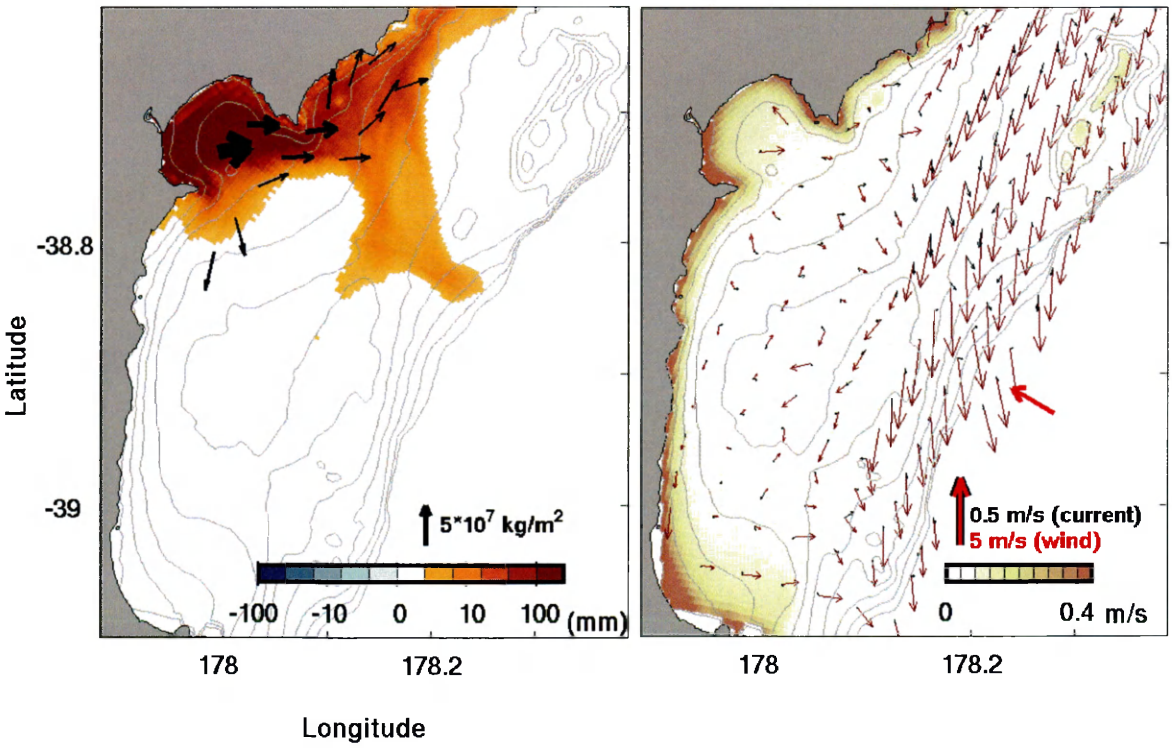

(b) Cumulative sediment fluxes and deposition for March 4 – 13, 2010. Snapshot of hydrodynamic conditions on March 7, 2010.

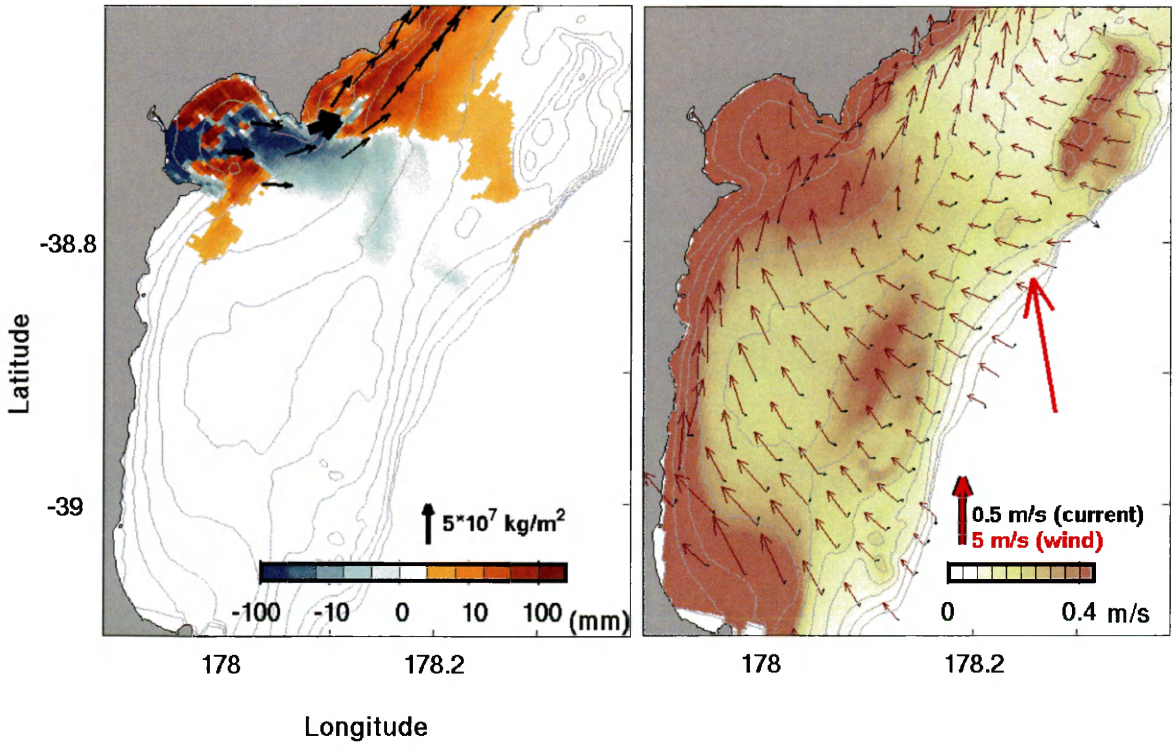

(c) Cumulative sediment fluxes and deposition for February 14 – May 15, 2010. Snapshot of hydrodynamic conditions on April 7, 2010.

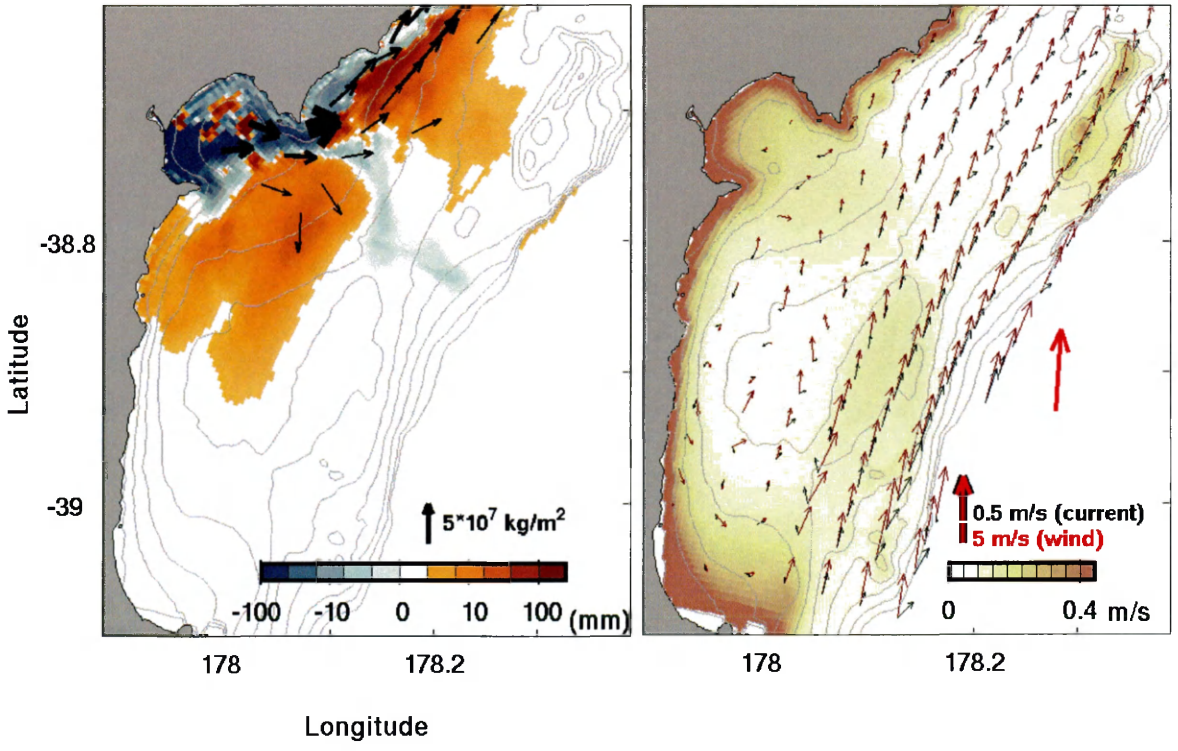

(d) Cumulative sediment fluxes and deposition for July 4 - 22, 2010. *Notice the change in scale from 4a,b,c,e and f*. Snapshot of hydrodynamic conditions on July 9, 2010.

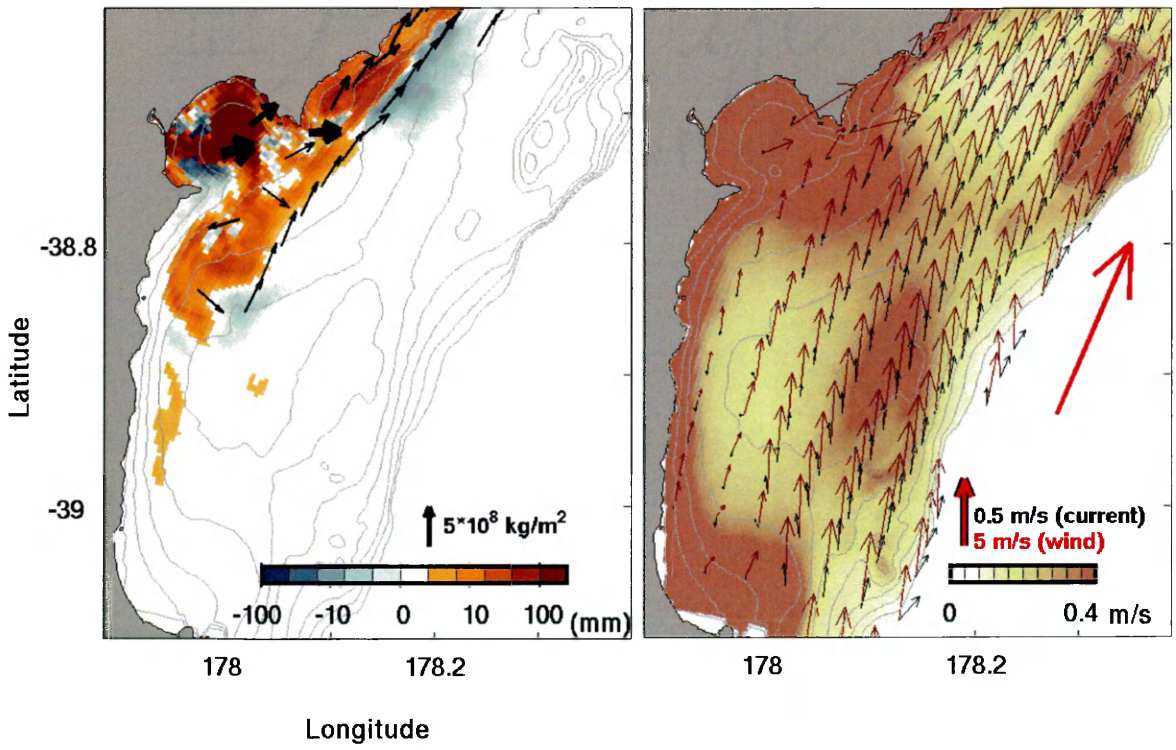

(e) Cumulative sediment fluxes and deposition for August 29 – September 8, 2010. Snapshot of hydrodynamic conditions on September 1, 2010.

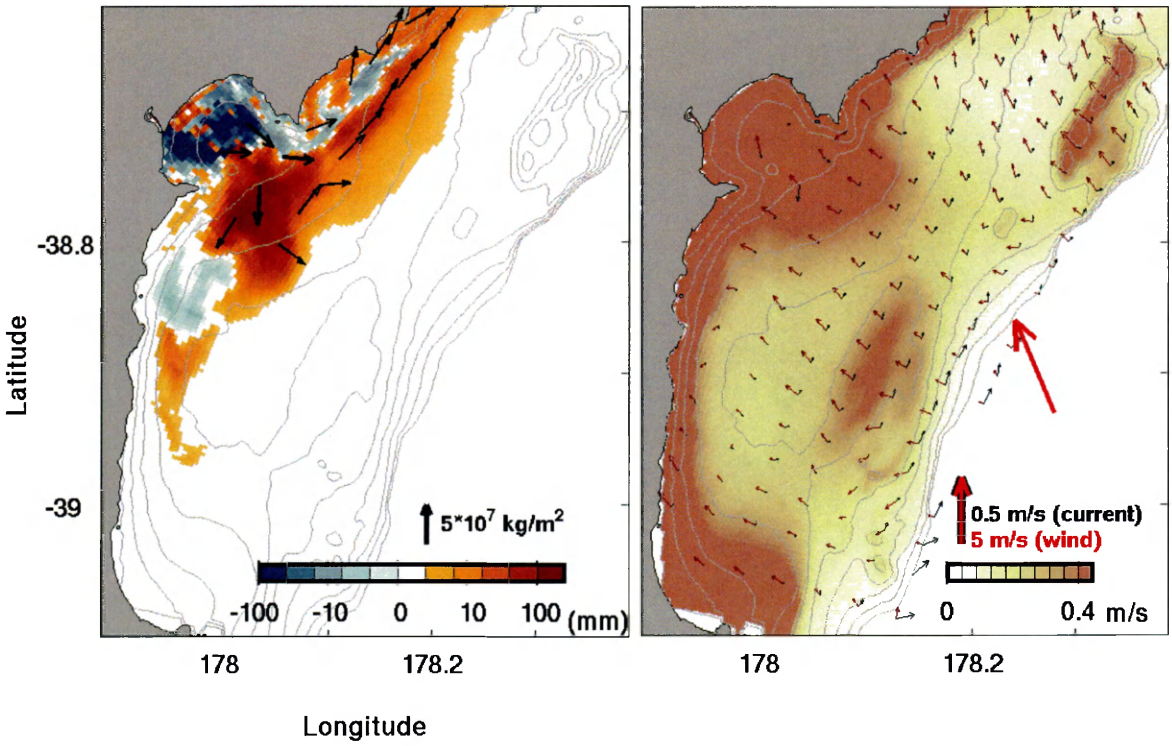

(f) Cumulative sediment fluxes and deposition for July 22 – September 30, 2010. Snapshot of hydrodynamic conditions on August 4, 2010.

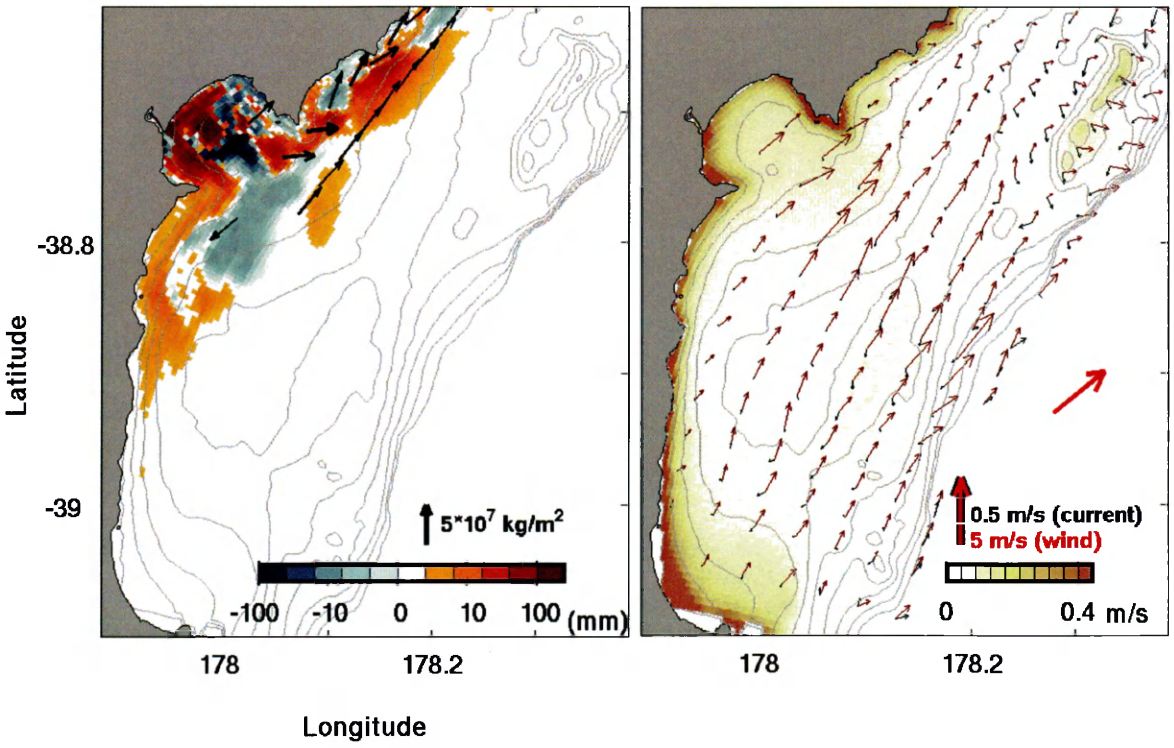

(g) Cumulative sediment fluxes and deposition for January 15, 2010 – February 15, 2011. *Flux arrows are shown for every 10 grid cells, for fluxes greater than 20 ^{x} 10^{6} kg m^{2}. Notice the change in scale from 4a,b,c,e and f.*

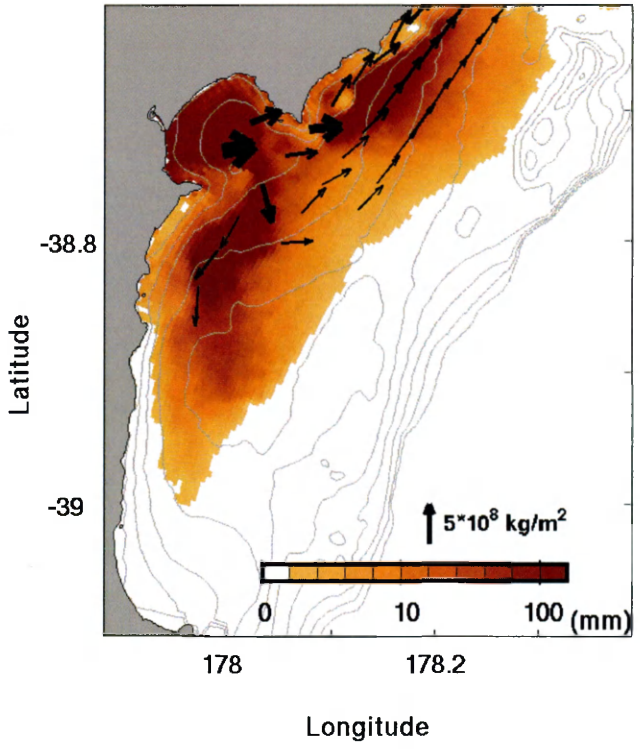

Figure 3-11: Map of flood deposit thickness per percent of riverine load

On (a) February 15, 2010, following the January 31, 2010 flood, and on (b) February 15, 2011, at the end of the field season. Note that slow-settling sediment classes accounted for larger percentages of the riverine load. Settling velocities of 0.15, 0.30, 0.50, and 1.0 mm s^{-1} accounted for 53, 27, 13, and 7 % of the riverine load. To estimate total deposit thickness for each sediment class, multiply the colorbar by 53, 27, 13, and 7, respectively.

(a)

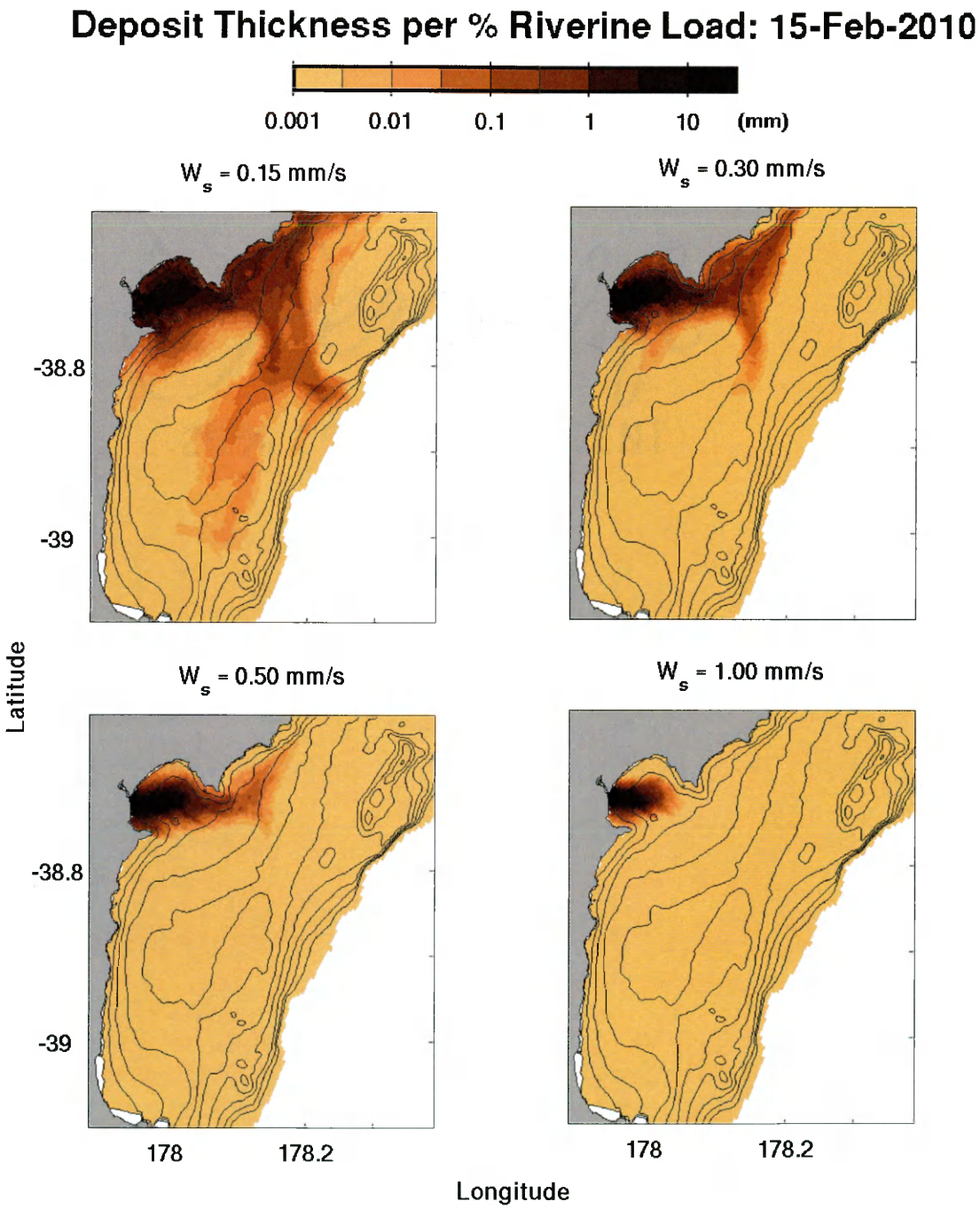
Deposit Thickness per % Riverine Load: 15-Feb-2010
0.001
0.01
0.1
1
10
(mm)
W_s = 0.15 mm/s
W_s = 0.30 mm/s
W_s = 0.50 mm/s
W_s = 1.00 mm/s
-38.8
-39
Latitude
178
178.2
Longitude

(b)

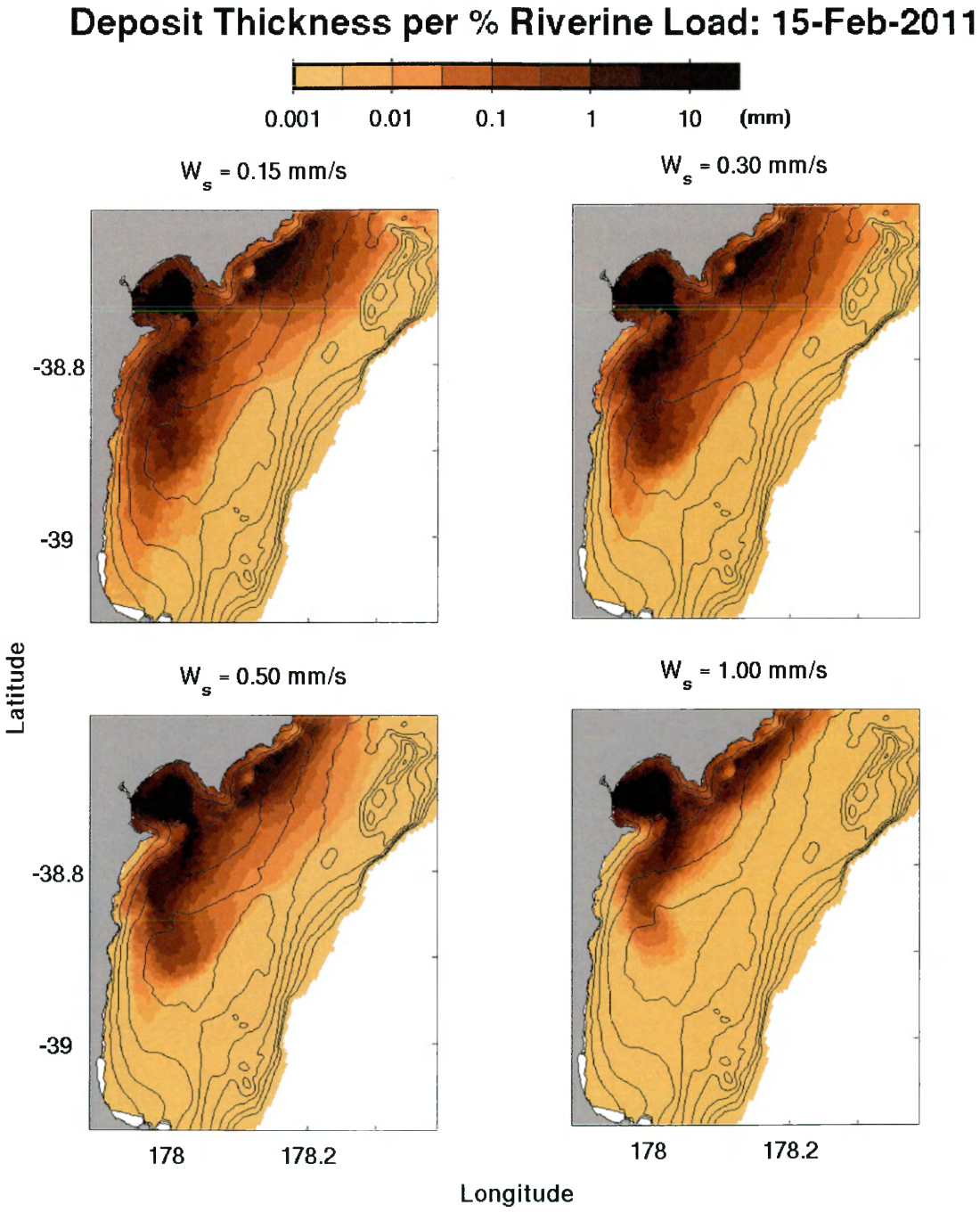
Deposit Thickness per % Riverine Load: 15-Feb-2011
0.001
0.01
0.1
1
10
(mm)
W_s = 0.15 mm/s
W_s = 0.30 mm/s
W_s = 0.50 mm/s
W_s = 1.00 mm/s
-38.8
-39
Latitude
178
178.2
Longitude

Figure 3-12: Wave- and current- induced bed stress

(A) Percent of the time that wave- and current- induced bed shear stresses exceeded 0.1 Pa., (B) average wave-induced bed shear stress, and (C) average current-induced bed shear stress from January 15, 2010 to February 15, 2011.

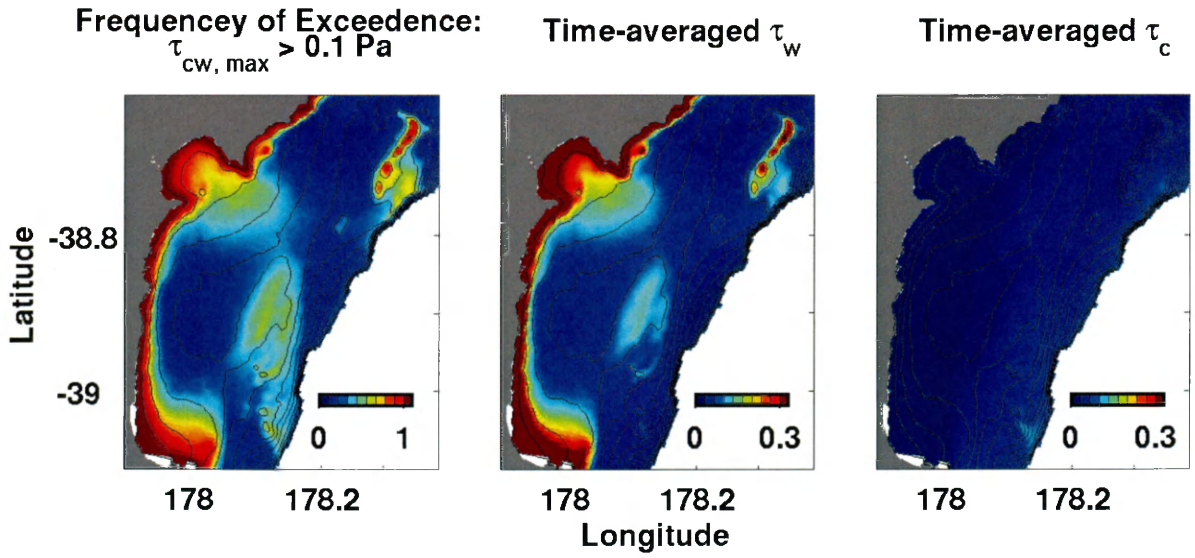

Figure 3-13: Instantaneous Sediment Fluxes

Timeseries of (a) along-shelf and across-shelf instantaneous sediment flux summed over different areas of the shelf. Fluxes were summed over Poverty Bay, the inner shelf (water depths shallower than 30 m), and the mid- and outer- shelf (water depths between 30 and 150 m) as shown in (b). Positive fluxes are northeastward, and offshore. Negative fluxes are southwestward and toward the coast.

(a)

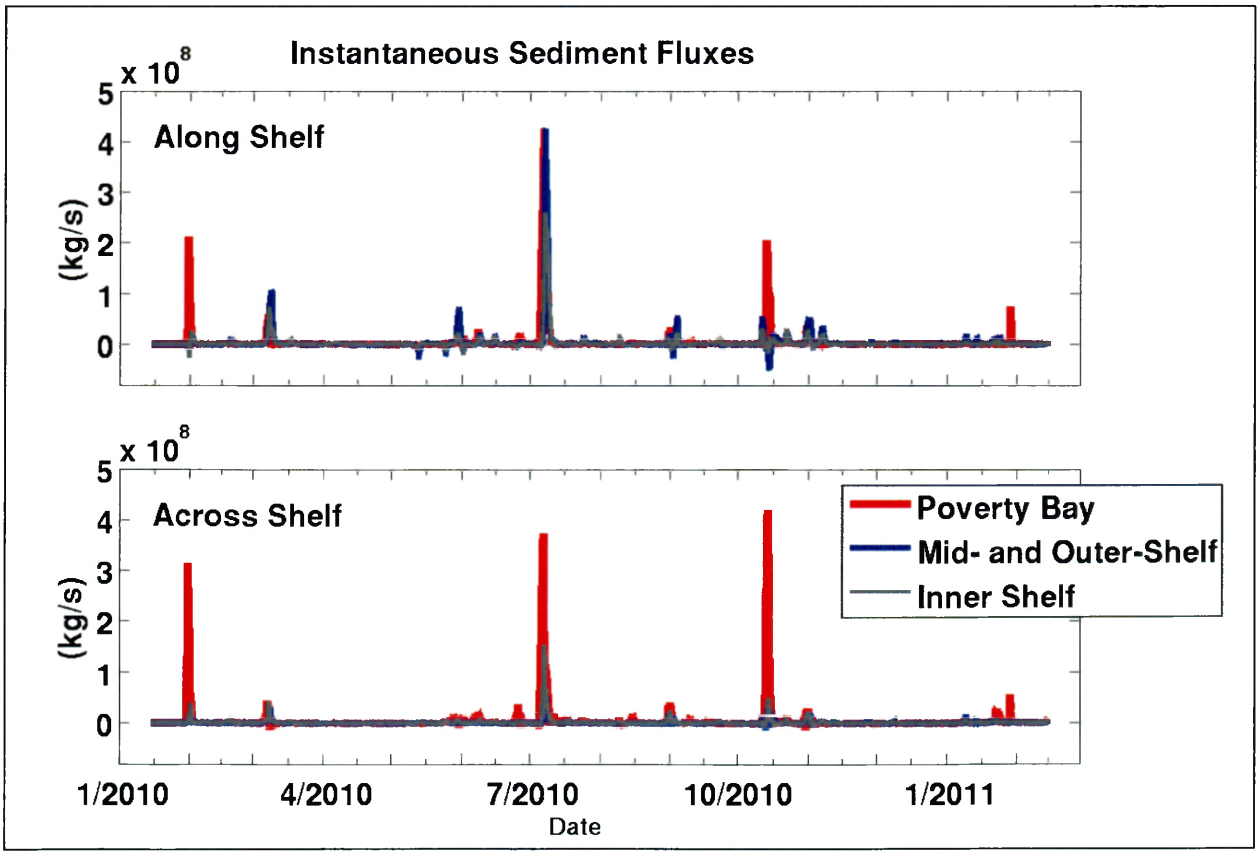

(b)

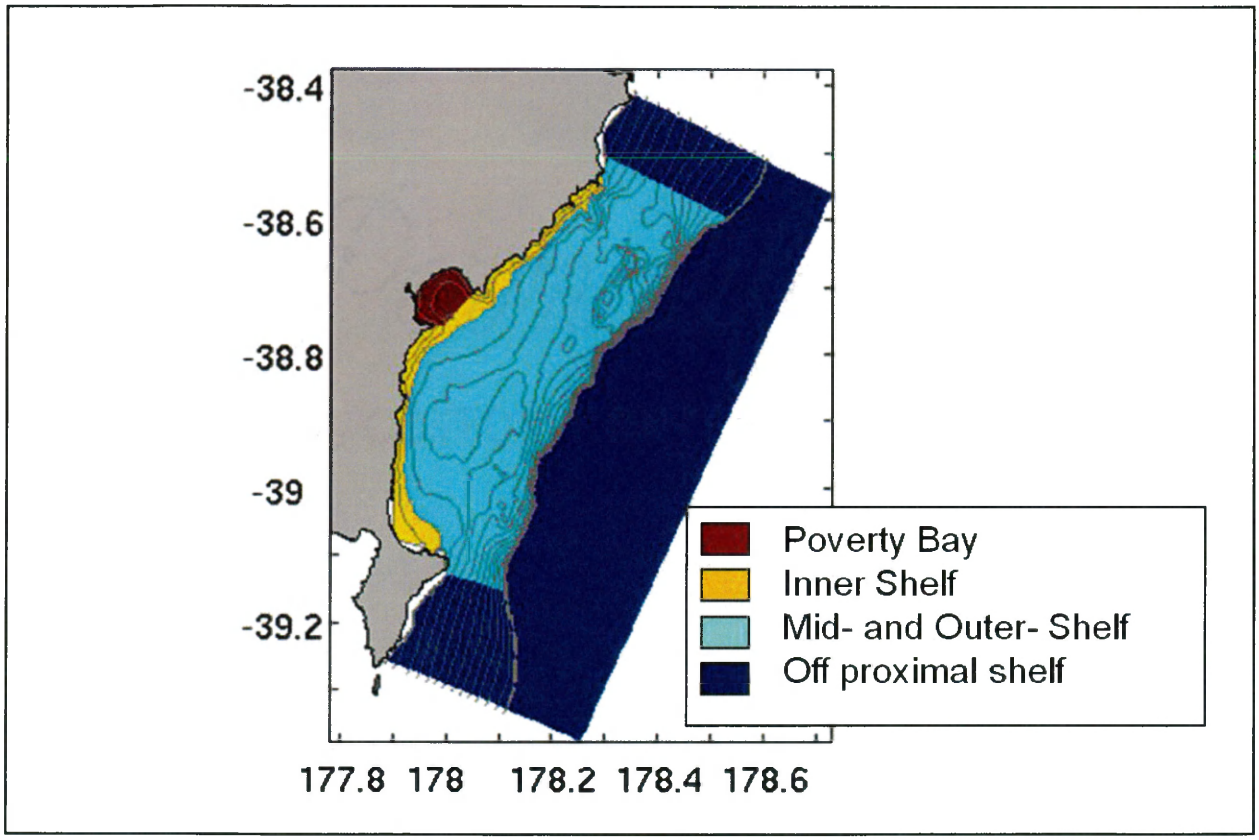
-38.4
-38.6
-38.8
-39
-39.2
177.8
178
178.2
178.4
178.6
Poverty Bay
Inner Shelf
Mid- and Outer- Shelf
Off proximal shelf

Figure 3-14: Timeseries of sediment budget.

Timeseries of cumulative sediment input, mass of sediment in Poverty Bay, and mass of sediment on shelf.

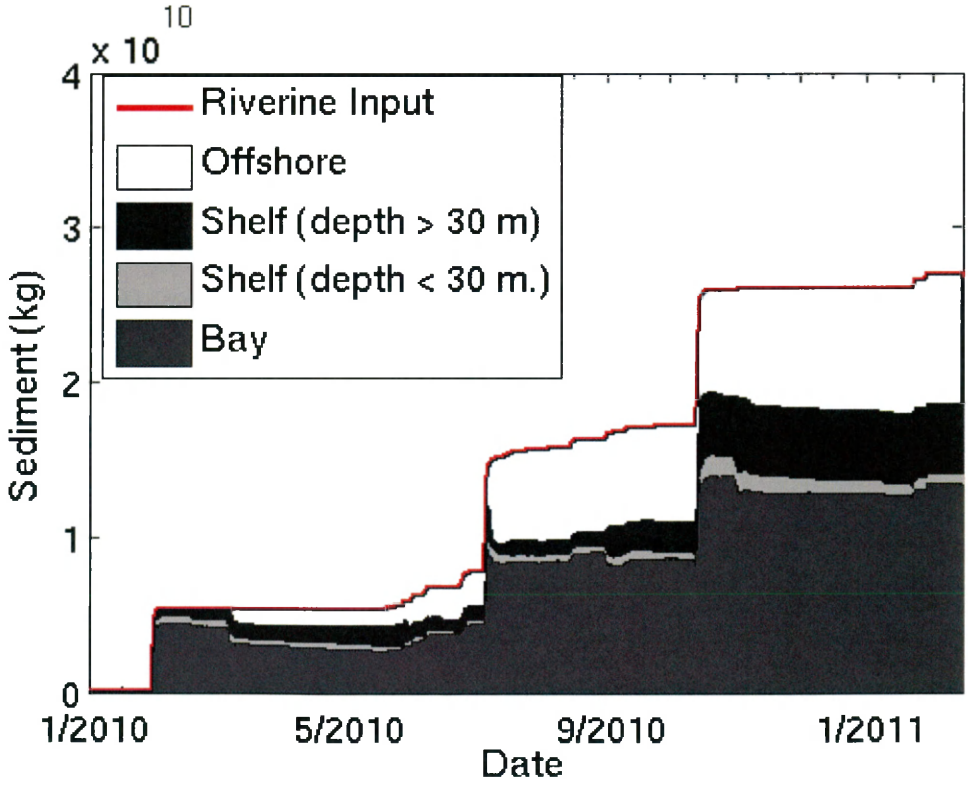

CHAPTER 4: Conclusions

A numerical hydrodynamic and sediment transport model has successfully been implemented for the Waipaoa Shelf, New Zealand. Model nesting, a technique relatively new to sediment transport models, was implemented to account for larger scale ocean currents in the model. This effort was necessary to increase the stability of the model; specifically it reduced reflection of the river plume at the model boundary. In addition to nesting, the coupled hydrodynamic – sediment transport model included wind, wave, river, and tidal processes. A two-layer bottom boundary layer estimated combined wave-current bed stresses. Sediment processes included advection, diffusion, erosion, deposition, and the inclusion of sediment in the equation of state.

This model neglected some processes that may be important for sediment transport and deposition, however. Comparison of model estimates to observations showed that the model underestimated across-shelf transport. Processes neglected in the model, such as seabed consolidation, gravity flows, and flocculation could explain this discrepancy and should be investigated by future efforts. Estimates of sediment fluxes were particularly sensitive to sediment settling characteristics, and so flocculation may be important in river-impacted margins (Hill et al., 2000; Syvitski et al., 1985; Ayukai and Wolanski, 1997). The model assumed that the settling velocity of sediment remained constant. However, if sediment becomes more highly flocculated with distance from the river mouth and water depth, this could help to explain model estimates of sediment deposition in shallow water. Additionally, seabed microcosm experiments indicated that the sediment bed became less erodible with distance from the river mouth and water depth (Corbett et al., 2012; Kiker, 2012). This might imply that sediment in

shallow areas that are frequently subjected to wave agitation might be more erodible, and more easily resuspended than material on the mid- to outer-shelf. Finally, the addition of gravitational forcing by high concentrations of suspended sediment increased export of sediment from Poverty Bay in Bever and Harris (submitted), and ongoing efforts will more fully evaluate the role of gravitational forcing on the Waipaoa Shelf (see, e.g. Moriarty et al., 2012). Even so, buoyant sediment fluxes as included in the model presented in Chapters Two and Three had many consistencies with long-term accumulation. That is, reworking of initial riverine deposits by waves and currents resulted in accumulation landward of shelf depocenters, separated by a zone of low accumulation in Poverty Gap.

Estimated hydrodynamics and sediment fluxes were analyzed for the thirteen month study period and also for individual floods and wave events. Winds strongly influenced the path of the river plume, which in turn controlled the predominantly northward buoyant sediment fluxes during floods. Dispersal of sediment during both floods and wave events depended strongly on the settling characteristics assumed for the material. Faster-settling material remained closer to the river mouth, and formed a more concentrated (less-diffuse) deposit. Sediment having fall velocities in excess of 1 mm/s tended to settle in Poverty Bay and the inner shelf during floods. Energetic waves during and following floods then resuspended this sediment, allowing ocean currents to redistribute riverine deposits along and across the shelf. Shelf depocenters tended to be located in areas of local topographic depressions. The relatively low bed stresses estimated for these sites facilitated sediment accumulation there.

Sedimentary signals were highly modified between arrival on the shelf and accumulation in long-term shelf depocenters. Transport of sediment to shelf depocenters occurred in multiple stages. Therefore, the physical structure of flood deposits from the 2010 field season, which included two approximately

eight-year recurrence interval floods, seems unlikely to be preserved in the geologic record. The destruction of the physical structure of the seabed, however, may not preclude a carbon or radioisotope signature. Overall, sediment delivery to long-term shelf depocenters depended on oceanographic forcing as well as sediment supply.

References

Ayukai, T. and Wolanski, E., 1997. Importance of biologically mediated removal of fine sediments from the Fly River Plume, Papua New Guinea. Estuarine, Coastal and Shelf Science, 44 (6): 629-639.

Bever, A.J. and Harris, C.K., 2012. Storm and fair-weather driven sediment-transport within Poverty Bay, New Zealand, evaluated using coupled numerical models. *Submitted*.

Corbett, D.R., Walsh, J.P., Orpin, A., Ogston, A., Kiker, J., Hale, R., Moriarty, J.M., and Harris, C.K., 2012. Spatial and Temporal Variability of Surface Seabed Properties: Waipaoa River Margin, New Zealand. Proceedings of the AGU Ocean Sciences Conference. Salt Lake City, UT: 20 – 24 February 2012.

Hill, P.S., Milligan, T.G., and Geyer, W.R., 2000. Controls on effective settling velocity of suspended sediment in the Eel River flood plume. Continental Shelf Research, 20: 2095-2111.

Kiker, J.M., 2012. Spatial and temporal variability in surficial seabed character, Waipaoa River Margin, New Zealand. M.S. Thesis, East Carolina University, Greenville, NC.

Moriarty, J.M, Harris, C.K., and Friedrichs, C.T., 2012. Gravity-driven transport on a relatively flat active margin with complicated bathymetry: the Waipaoa River Continental Shelf, NZ. Proceedings of the 16th International Conference on Physics of Estuaries and Coastal Seas, Manhatten, New York.

Syvitski, J.P.M, Asprey, K.W., Clattenburg, D.A., and Hodge, G.D., 1985. The prodelta environment of a fjord: suspended particle dynamics. Sedimentology, 32: 83-107.

APPENDIX: Model Input Files

This appendix contains input files for the ROMS model run described in Chapters Two and Three. The input text files, including waipaoa.h, ocean_waipaoa.in and sediment_waipaoa.in, are included on the pages below. These files, as well as netCDF input files for bathymetry, waves, winds, currents, tracers, tides, and meterological forcing, are contained on the attached CD:

Input text files:

- waipaoa.h
- ocean_waipaoa.in
- sediment_waipaoa.in
- ana_nudgcoef.h
- build.bash

Input netCDF files:

- gridgen_romsformat_redo5.nc
- waipaoa_init_redo7_20100101.nc
- bdry_bclin_*.nc (70 files)
- clim_bclin_*.nc (70 files)
- waipaoa_swradhr_new.nc
- waipaoa_windhr_nzlam_new.nc
- waipaoa_apresshr_new.nc
- waipaoa_clound_new.nc
- waipaoa_rainhr_new.nc
- waipaoa_relhumhr_new.nc
- waipaoa_temphr_new.nc
- waipaoa_waves3_new.nc
- waipaoa_river_newpartitions.nc
- pb_tide_PO_new.nc

waipaoa.h

```
/*
** Options for Waipaoa Shelf Application.
**
** Application flag: WAIPAOA
** Input scripts: ocean_waipaoa.in,
sediment_waipaoa.in
*/

#define UV_ADV
#define UV_COR
#define UV_PSOURCE
#define TS_PSOURCE
#define SSH_TIDES
#define UV_TIDES
#define DJ_GRADPS
#define SPLINES
#define TS_DIF2
#define MIX_GEO_TS
#define NONLIN_EOS
#define SALINITY
#define MASKING
#define SOLVE3D
#define TS_MPDATA
#define GLS_MIXING
#if defined GLS_MIXING || defined MY25_MIXING
# define KANTHA_CLAYSON
# define N2S2_HORAVG
#endif

/*Bottom Boundary Layer and Sediment */
#define SEDIMENT
#ifdef SEDIMENT
# define SUSPLOAD
# define SED_DENS
#endif
#define SSW_BBL
#ifdef SSW_BBL
# define SSW_CALC_ZNOT
#endif

/*Surface Boundary Layer*/
#define BULK_FLUXES
#ifdef BULK_FLUXES
# undef SOLAR_SOURCE
# define ANA_RAIN
# undef COOL_SKIN
#endif
#define CRAIG_BANNER
#define CHARNOK
#define DIURNAL_SRFLUX
#define ANA_SSFLUX
#define ANA_BSFLUX
#define ANA_BPFLUX
#define ANA_BTFLUX
#define ANA_SPFLUX
#define LONGWAVE
```

```
/*Lateral Boundary Conditions and Climatology
Options*/
/*  Grid is rotated so that:
*/
/*  'east' is the coast, 'south' is the
northeast boundary*/


#define EASTERN_WALL

#define SOUTH_FSCHAPMAN
#define SOUTH_M2FLATHER
#define SOUTH_M3RADIATION
#define SOUTH_M3NUDGING
#define SOUTH_TRADIATION
#define SOUTH_TNUDGING

#define NORTH_FSCHAPMAN
#define NORTH_M2FLATHER
#define NORTH_M3RADIATION
#define NORTH_M3NUDGING
#define NORTH_TRADIATION
#define NORTH_TNUDGING

#define WEST_FSCHAPMAN
#define WEST_M2FLATHER
#define WEST_M3RADIATION
#define WEST_M3NUDGING
#define WEST_TRADIATION
#define WEST_TNUDGING

#define M3CLIMATOLOGY
#define TCLIMATOLOGY
#define M3CLM_NUDGING
#define TCLM_NUDGING
#define RADIATION_2D
#define ANA_NUDGCOEF
#define NUDGING_COFF
#define NOSEDIN
```

ocean_waipaoa.in

```
!
!  ROMS/TOMS Standard Input parameters.
!
!svn $Id: ocean_upwelling.in 2249 2012-01-22
22:35:35Z arango $
!=============================================
============ Hernan G. Arango ===
!  Copyright (c) 2002-2012 The ROMS/TOMS Group
!
!    Licensed under a MIT/X style license
!
!    See License_ROMS.txt
!
!=============================================
================================
!
!
! Input parameters can be entered in ANY
order, provided that the parameter   !
! KEYWORD (usually, upper case) is typed
correctly followed by "="  or "=="   !
! symbols. Any comment lines are allowed and
must begin with an exclamation   !
! mark (!) in column one.  Comments may
appear to the right of a parameter   !
! specification to improve documentation.
Comments will be ignored  during   !
! reading.  Blank lines are also allowed and
ignored. Continuation lines in   !
! a parameter specification are allowed and
must be preceded by a backslash   !
! (\).  In some instances, more than one value
is required for a parameter.   !
! If fewer values are provided, the  last
value  is assigned for the entire   !
! parameter array.  The multiplication symbol
(*),  without blank spaces in   !
! between, is allowed for a parameter
specification.  For example, in a two   !
! grids nested application:
!
!
!
!    AKT_BAK == 2*1.0d-6  2*5.0d-6
! m2/s                          !
!
!
! indicates that the first two entries of
array AKT_BAK,  in fortran column-  !
! major order, will have the same value of
"1.0d-6" for grid 1,  whereas the  !
! next two entries will have the same value of
"5.0d-6" for grid 2.           !
!
!
! In multiple levels of nesting and/or
multiple connected domains  step-ups,  !
! "Ngrids" entries are expected for some of
these parameters.  In such case,  !
```

```
! the order of the entries for a parameter is
extremely important.  It  must  !
! follow the same order (1:Ngrids) as in the
state variable declaration. The  !
! USER may follow the above guidelines for
specifying his/her values.  These  !
! parameters are marked by "==" plural symbol
after the KEYWORD.              !
!
!
! Multiple NetCDF files are allowed for input
field(s).  This is useful when  !
! splitting input data (climatology,
boundary,  forcing)  time records into  !
! several files (say monthly, annual, etc). In
this case, each multiple file  !
! entry line needs to be ended by the vertical
bar (|) symbol. For example:   !
!
!
!    NFFILES == 8
number of forcing files
!
!
!    FRCNAME == my_rivers.nc      \
!
!               my_tides.nc       \
!
!               my_lwrad_year1.nc |
!
!               my_lwrad_year2.nc \
!
!               my_swrad_year1.nc |
!
!               my_swrad_year2.nc \
!
!               my_winds_year1.nc |
!
!               my_winds_year2.nc \
!
!               my_Pair_year1.nc  |
!
!               my_Pair_year2.nc  \
!
!               my_Qair_year1.nc  |
!
!               my_Qair_year2.nc  \
!
!               my_Tair_year1.nc  |
!
!               my_Tair_year2.nc
!
!
!
! Notice that NFFILES is 8 and not 14. There
are 8 uniquely different fields  !
! in the file list,  we  DO NOT  count file
entries followed by the vertical  !
! bar symbol.  This is because  multiple file
entries are processed in ROMS  !
! with derived type structures.
!
!
!
```

```
!=============================================
================================
!
! Application title.

       TITLE = Waipaoa River Shelf

! C-preprocessing Flag.

    MyAppCPP = WAIPAOA

! Input variable information file name.  This
file needs to be processed
! first so all information arrays can be
initialized properly.

     VARNAME =
/export/home2/moriarty/ROMS/trunk4/ROMS/Extern
al/varinfo.dat

! Number of nested grids.

      Ngrids =  1

! Grid dimension parameters. See notes below
in the Glossary for how to set
! these parameters correctly.

          Lm == 116           ! Number of I-
direction INTERIOR RHO-points
          Mm == 285           ! Number of J-
direction INTERIOR RHO-points
           N == 20            ! Number of
vertical levels

        Nbed =  8             ! Number of
sediment bed layers

         NAT =  2             ! Number of
active tracers (usually, 2)
         NPT =  0             ! Number of
inactive passive tracers
         NCS =  7             ! Number of
cohesive (mud) sediment tracers
         NNS =  0             ! Number of non-
cohesive (sand) sediment tracers

! Domain decomposition parameters for serial,
distributed-memory or
! shared-memory configurations used to
determine tile horizontal range
! indices (Istr,Iend) and (Jstr,Jend),
[1:Ngrids].

      NtileI == 2
! I-direction partition
      NtileJ == 8
! J-direction partition

! Set lateral boundary conditions keyword.
Notice that a value is expected
! for each boundary segment per nested grid
for each state variable.
!
```

```
! Each tracer variable requires
[1:4,1:NAT+NPT,Ngrids] values. Otherwise,
! [1:4,1:Ngrids] values are expected for other
variables. The boundary
! order is: 1=west, 2=south, 3=east, and
4=north. That is, anticlockwise
! starting at the western boundary.
!
! The keyword is case insensitive and usually
has three characters. However,
! it is possible to have compound keywords, if
applicable. For example, the
! keyword "RadNud" implies radiation boundary
condition with nudging. This
! combination is usually used in
active/passive radiation conditions.
!
!   Keyword    Lateral Boundary Condition Type
!
!   Cha        Chapman
!   Cla        Clamped
!   Clo        Closed
!   Fla        Flather
_____N_____     j=Mm
!   Gra        Gradient
|     4     |
!   Nes        Nested
|           |
!   Nud        Nudging
1 W           E 3
!   Per        Periodic
|           |
!   Rad        Radiation
|_____S_____|
!   Red        Reduced Physics
2          j=1
!
i=1         i=Lm
!                    W       S       E       N
!                    e       o       a       o
!                    s       u       s       r
!                    t       t       t       t
!                            h               h
!
!                    1       2       3       4

   LBC(isFsur) ==   Cha     Cha     Clo
Cha          ! free-surface
   LBC(isUbar) ==   Fla     Fla     Clo
Fla          ! 2D U-momentum
   LBC(isVbar) ==   RadNud  RadNud  Clo
RadNud       ! 2D V-momentum
   LBC(isUvel) ==   RadNud  RadNud  Clo
RadNud       ! 3D U-momentum
   LBC(isVvel) ==   RadNud  RadNud  Clo
RadNud       ! 3D V-momentum
   LBC(isMtke) ==   RadNud  RadNud  Clo
RadNud       ! mixing TKE

   LBC(isTvar) ==   RadNud  RadNud  Clo
RadNud\      ! temperature
                    RadNud  RadNud  Clo
RadNud\      ! salinity
```

```
                    RadNud  RadNud  Clo
RadNud\      ! mud_01
                    RadNud  RadNud  Clo
RadNud\      ! mud_02
                    RadNud  RadNud  Clo
RadNud\      ! mud_03
                    RadNud  RadNud  Clo
RadNud\      ! mud_04
                    RadNud  RadNud  Clo
RadNud\      ! mud_05
                    RadNud  RadNud  Clo
RadNud\      ! mud_06
                    RadNud  RadNud  Clo
RadNud\      ! mud_07

! Adjoint-based algorithms can have different
lateral boundary
! conditions keywords.

ad_LBC(isFsur) ==   Per     Clo     Per
Clo          ! free-surface
ad_LBC(isUbar) ==   Per     Clo     Per
Clo          ! 2D U-momentum
ad_LBC(isVbar) ==   Per     Clo     Per
Clo          ! 2D U-momentum
ad_LBC(isUvel) ==   Per     Clo     Per
Clo          ! 3D U-momentum
ad_LBC(isVvel) ==   Per     Clo     Per
Clo          ! 3D V-momentum
ad_LBC(isMtke) ==   Per     Clo     Per
Clo          ! mixing TKE
ad_LBC(isTvar) ==   Per     Clo     Per
Clo \        ! temperature
                    Per     Clo     Per
Clo          ! salinity

! Set lateral open boundary edge volume
conservation switch for
! nonlinear model and adjoint-based
algorithms. Usually activated
! with radiation boundary conditions to
enforce global mass
! conservation, except if tidal forcing
enabled. [1:Ngrids].

   VolCons(west)  ==  F
! western  boundary
   VolCons(east)  ==  F
! eastern  boundary
   VolCons(south) ==  F
! southern boundary
   VolCons(north) ==  F
! northern boundary

ad_VolCons(west)  ==  F
! western  boundary
ad_VolCons(east)  ==  F
! eastern  boundary
ad_VolCons(south) ==  F
! southern boundary
ad_VolCons(north) ==  F
! northern boundary
```

```
! Time-Stepping parameters.

      NTIMES == 2900000
          DT == 15.0d0
     NDTFAST == 40

! Model iteration loops parameters.

       ERstr =  1
       ERend =  1
      Nouter =  1
      Ninner =  1
  Nintervals =  1

! Number of eigenvalues (NEV) and eigenvectors
(NCV) to compute for the
! Lanczos/Arnoldi problem in the Generalized
Stability Theory (GST)
! analysis. NCV must be greater than NEV (see
documentation below).

         NEV =  2
! Number of eigenvalues
         NCV =  10
! Number of eigenvectors

! Input/Output parameters.

       NRREC == 0
   LcycleRST == T
        NRST == 360
        NSTA == 1
        NFLT == 1
       NINFO == 1

! Output history, average, diagnostic files
parameters.

     LDEFOUT == T
        NHIS == 720
     NDEFHIS == 28800
      NTSAVG == 1
        NAVG == 9999999
     NDEFAVG == 0
      NTSDIA == 1
        NDIA == 999999
     NDEFDIA == 0

! Output tangent linear and adjoint models
parameters.

   LcycleTLM == F
        NTLM == 72
     NDEFTLM == 0
   LcycleADJ == F
        NADJ == 72
     NDEFADJ == 0
        NSFF == 72
        NOBC == 72

! GST output and check pointing restart
parameters.
```

```
   LmultiGST =  F
! one eigenvector per file
     LrstGST =  F
! GST restart switch
  MaxIterGST =  500
! maximum number of iterations
        NGST =  10
! check pointing interval

! Relative accuracy of the Ritz values
computed in the GST analysis.

    Ritz_tol =  1.0d-15

! Harmonic/biharmonic horizontal diffusion of
tracer for nonlinear model
! and adjoint-based algorithms:
[1:NAT+NPT,Ngrids].
!
jmm in old files have: TNU2 = 5, TNU4 = 0

        TNU2 == 0.0d0  0.0d0
! m2/s
        TNU4 == 2*0.0d0
! m4/s

     ad_TNU2 == 0.0d0  0.0d0
! m2/s
     ad_TNU4 == 0.0d0  0.0d0
! m4/s

! Harmonic/biharmonic, horizontal viscosity
coefficient for nonlinear model
! and adjoint-based algorithms: [Ngrids].
!
!jmm in old files have: VISC2= 0, VISC4= 0

       VISC2 == 5.0d0
! m2/s
       VISC4 == 0.0d0
! m4/s

    ad_VISC2 == 0.0d0
! m2/s
    ad_VISC4 == 0.0d0
! m4/s

! Vertical mixing coefficients for tracers in
nonlinear model and
! basic state scale factor in adjoint-based
algorithms: [1:NAT+NPT,Ngrids]
!
!jmm in old files have:5e-06

     AKT_BAK == 1.0d-6 1.0d-6
! m2/s

  ad_AKT_fac == 1.0d0  1.0d0
! nondimensional

! Vertical mixing coefficient for momentum for
nonlinear model and
```

```
! basic state scale factor in adjoint-based
algorithms: [Ngrids].
!
!jmm in old files have:5e-05

     AKV_BAK == 1.0d-5
! m2/s

  ad_AKV_fac == 1.0d0
! nondimensional

! Turbulent closure parameters.

     AKK_BAK == 5.0d-6
! m2/s
     AKP_BAK == 5.0d-6
! m2/s
      TKENU2 == 0.0d0
! m2/s
      TKENU4 == 0.0d0
! m4/s

! Generic length-scale turbulence closure
parameters.

       GLS_P == 3.0d0
! K-epsilon
       GLS_M == 1.5d0
       GLS_N == -1.0d0
    GLS_Kmin == 7.6d-6
    GLS_Pmin == 1.0d-12
    GLS_CMU0 == 0.5477d0
      GLS_C1 == 1.44d0
      GLS_C2 == 1.92d0
     GLS_C3M == -0.4d0
     GLS_C3P == 1.0d0
    GLS_SIGK == 1.0d0
    GLS_SIGP == 1.30d0

! Constants used in surface turbulent kinetic
energy flux computation.

  CHARNOK_ALPHA == 1400.0d0         ! Charnok
surface roughness
 ZOS_HSIG_ALPHA == 0.5d0            !
roughness from wave amplitude
       SZ_ALPHA == 0.25d0           !
roughness from wave dissipation
      CRGBAN_CW == 100.0d0          ! Craig
and Banner wave breaking

! Constants used in momentum stress
computation.
!
!jmm in old files have:Zob = 0.003, Zos = 0.02

        RDRG == 3.0d-04                    !
m/s
       RDRG2 == 3.0d-03                    !
nondimensional
         Zob == 0.02d0                     ! m
         Zos == 0.02d0                     ! m
```

```
! Height (m) of atmospheric measurements for
Bulk fluxes parameterization.

      BLK_ZQ == 10.0d0                      !
air humidity
      BLK_ZT == 10.0d0                      !
air temperature
      BLK_ZW == 10.0d0                      !
winds

! Minimum depth for wetting and drying.

       DCRIT == 0.10d0                      ! m

! Various parameters.

       WTYPE == 1
     LEVSFRC == 15
     LEVBFRC == 1

! Set vertical, terrain-following coordinates
transformation equation and
! stretching function (see below for details),
[1:Ngrids].

  Vtransform == 2                           !
transformation equation
 Vstretching == 3                           !
stretching function

! Vertical S-coordinates parameters (see below
for details), [1:Ngrids].

     THETA_S == 3.0d0                       !
surface stretching parameter
     THETA_B == 0.9d0                       !
bottom  stretching parameter
      TCLINE == 3.0d0                       !
critical depth (m)

! Mean Density and Brunt-Vaisala frequency.

        RHO0 =  1025.0d0                    !
kg/m3
     BVF_BAK =  1.0d-5                      !
1/s2

! Time-stamp assigned for model
initialization, reference time
! origin for tidal forcing, and model
reference time for output
! NetCDF units attribute.

      DSTART =  15198.0d0
days
  TIDE_START =   732678.0d0                 !
days
    TIME_REF =  0.0d0                       !
yyyymmdd.dd

! Nudging/relaxation time scales, inverse
scales will be computed
! internally, [1:Ngrids].
```

```
       TNUDG == 2.5d0                          !
days
       ZNUDG == 2.5d0                          !
days
      M2NUDG == 2.5d0                          !
days
      M3NUDG == 2.5d0                          !
days

! Factor between passive (outflow) and active
(inflow) open boundary
! conditions, [1:Ngrids]. If OBCFAC > 1,
nudging on inflow is stronger
! than on outflow (recommended).

      OBCFAC == 2.5d0
nondimensional

! Linear equation of State parameters:

          R0 == 1027.0d0                      !
kg/m3
          T0 == 16.0d0                        !
Celsius
          S0 == 35.1d0                        !
PSU
       TCOEF == 1.7d-4                        !
1/Celsius
       SCOEF == 7.6d0 !0.0d0                  !
1/PSU

! Slipperiness parameter: 1.0 (free slip) or -
1.0 (no slip)

      GAMMA2 == 1.0d0

! Logical switches (TRUE/FALSE) to specify
which variables to consider on
! tracers point Sources/Sinks (like river
runoff): [1:NAT+NPT,Ngrids].
! See glossary below for details.

  LtracerSrc == T T
temperature, salinity, inert

! Starting (DstrS) and ending (DendS) day for
adjoint sensitivity forcing.
! DstrS must be less or equal to DendS. If
both values are zero, their
! values are reset internally to the full
range of the adjoint integration.

       DstrS == 0.0d0                         !
starting day
       DendS == 0.0d0                         !
ending day

! Starting and ending vertical levels of the
3D adjoint state variables
! whose sensitivity is required.

       KstrS == 1
starting level
```

```
       KendS == 1                                    !
ending level

! Logical switches (TRUE/FALSE) to specify the
adjoint state variables
! whose sensitivity is required.

Lstate(isFsur) == F                                  !
free-surface
Lstate(isUbar) == F                                  !
2D U-momentum
Lstate(isVbar) == F                                  !
2D V-momentum
Lstate(isUvel) == F                                  !
3D U-momentum
Lstate(isVvel) == F                                  !
3D V-momentum

Lstate(isTvar) == F F
NT tracers

! Logical switches (TRUE/FALSE) to specify the
state variables for
! which Forcing Singular Vectors or Stochastic
Optimals is required.

Fstate(isFsur) == F                                  !
free-surface
Fstate(isUbar) == F                                  !
2D U-momentum
Fstate(isVbar) == F                                  !
2D V-momentum
Fstate(isUvel) == F                                  !
3D U-momentum
Fstate(isVvel) == F                                  !
3D V-momentum
Fstate(isTvar) == F F                                !
NT tracers

Fstate(isUstr) == T                                  .
surface U-stress
Fstate(isVstr) == T                                  !
surface V-stress
Fstate(isTsur) == F F                                !
NT surface tracers flux

! Stochastic Optimals time decorrelation scale
(days) assumed for
! red noise processes.

      SO_decay == 2.0d0
days

! Stochastic Optimals surface forcing standard
deviation for
! dimensionalization.

SO_sdev(isFsur) == 1.0d0                             !
free-surface
SO_sdev(isUbar) == 1.0d0                             !
2D U-momentum
SO_sdev(isVbar) == 1.0d0                             !
2D V-momentum
```

```
SO_sdev(isUvel) == 1.0d0                    !
3D U-momentum
SO_sdev(isVvel) == 1.0d0                    !
3D V-momentum
SO_sdev(isTvar) == 1.0d0 1.0d0              !
NT tracers

SO_sdev(isUstr) == 1.0d0                    .
surface U-stress
SO_sdev(isVstr) == 1.0d0                    !
surface V-stress
SO_sdev(isTsur) == 1.0d0 1.0d0              !
NT surface tracers flux

! Logical switches (TRUE/FALSE) to activate
writing of fields into
! HISTORY output file.

Hout(idUvel) == T       ! u
3D U-velocity
Hout(idVvel) == T       ! v
3D V-velocity
Hout(idu3dE) == T       ! u_eastward
3D U-eastward  at RHO-points
Hout(idv3dN) == T       ! v_northward
3D V-northward at RHO-points
Hout(idWvel) == T       ! w
3D W-velocity
Hout(idOvel) == T       ! omega
omega vertical velocity
Hout(idUbar) == T       ! ubar
2D U-velocity
Hout(idVbar) == T       ! vbar
2D V-velocity
Hout(idu2dE) == T       ! ubar_eastward
2D U-eastward  at RHO-points
Hout(idv2dN) == T       ! vbar_northward
2D V-northward at RHO-points
Hout(idFsur) == T       ! zeta
free-surface
Hout(idBath) == T       ! bath
time-dependent bathymetry

Hout(idTvar) == T T     ! temp, salt
temperature and salinity

Hout(idUsms) == T       ! sustr
surface U-stress
Hout(idVsms) == T       ! svstr
surface V-stress
Hout(idUbms) == F       ! bustr
bottom U-stress
Hout(idVbms) == F       ! bvstr
bottom V-stress

Hout(idUbrs) == T       ! bustrc
bottom U-current stress
Hout(idVbrs) == T       ! bvstrc
bottom V-current stress
Hout(idUbws) == T       ! bustrw
bottom U-wave stress
Hout(idVbws) == T       ! bvstrw
bottom V-wave stress
```

```
Hout(idUbcs) == T       ! bustrcwmax
bottom max wave-current U-stress
Hout(idVbcs) == T       ! bvstrcwmax
bottom max wave-current V-stress

Hout(idUbot) == T       ! Ubot
bed wave orbital U-velocity
Hout(idVbot) == T       ! Vbot
bed wave orbital V-velocity
Hout(idUbur) == T       ! Ur
bottom U-velocity above bed
Hout(idVbvr) == T       ! Vr
bottom V-velocity above bed

Hout(idW2xx) == F       ! Sxx_bar
2D radiation stress, Sxx component
Hout(idW2xy) == F       ! Sxy_bar
2D radiation stress, Sxy component
Hout(idW2yy) == F       ! Syy_bar
2D radiation stress, Syy component
Hout(idU2rs) == F       ! Ubar_Rstress
2D radiation U-stress
Hout(idV2rs) == F       ! Vbar_Rstress
2D radiation V-stress
Hout(idU2Sd) == F       ! ubar_stokes
2D U-Stokes velocity
Hout(idV2Sd) == F       ! vbar_stokes
2D V-Stokes velocity

Hout(idW3xx) == F       ! Sxx
3D radiation stress, Sxx component
Hout(idW3xy) == F       ! Sxy
3D radiation stress, Sxy component
Hout(idW3yy) == F       ! Syy
3D radiation stress, Syy component
Hout(idW3zx) == F       ! Szx
3D radiation stress, Szx component
Hout(idW3zy) == F       ! Szy
3D radiation stress, Szy component
Hout(idU3rs) == F       ! u_Rstress
3D U-radiation stress
Hout(idV3rs) == F       ! v_Rstress
3D V-radiation stress
Hout(idU3Sd) == F       ! u_stokes
3D U-Stokes velocity
Hout(idV3Sd) == F       ! v_stokes
3D V-Stokes velocity

Hout(idWamp) == T       ! Hwave
wave height
Hout(idWlen) == T       ! Lwave
wave length
Hout(idWdir) == T       ! Dwave
wave direction
Hout(idWptp) == T       ! Pwave_top
wave surface period
Hout(idWpbt) == T       ! Pwave_bot
wave bottom period
Hout(idWorb) == T       ! Ub_swan
wave bottom orbital velocity
Hout(idWdis) == T       ! Wave_dissip
wave dissipation
```

```
Hout(idPair) == F       ! Pair
surface air pressure
Hout(idUair) == T       ! Uair
surface U-wind component
Hout(idVair) == T       ! Vair
surface V-wind component

Hout(idTsur) == F F     ! shflux, ssflux
surface net heat and salt flux
Hout(idLhea) == F       ! latent
latent heat flux
Hout(idShea) == F       ! sensible
sensible heat flux
Hout(idLrad) == F       ! lwrad
longwave radiation flux
Hout(idSrad) == F       ! swrad
shortwave radiation flux
Hout(idEmPf) == F       ! EminusP
E-P flux
Hout(idevap) == F       ! evaporation
evaporation rate
Hout(idrain) == F       ! rain
precipitation rate

Hout(idDano) == T       ! rho
density anomaly
Hout(idVvis) == F       ! AKv
vertical viscosity
Hout(idTdif) == F       ! AKt
vertical T-diffusion
Hout(idSdif) == F       ! AKs
vertical Salinity diffusion
Hout(idHsbl) == F       ! Hsbl
depth of surface boundary layer
Hout(idHbbl) == F       ! Hbbl
depth of bottom boundary layer
Hout(idMtke) == F       ! tke
turbulent kinetic energy
Hout(idMtls) == F       ! gls
turbulent length scale

! Logical switches (TRUE/FALSE) to activate
writing of extra inert passive
! tracers other than biological and sediment
tracers. An inert passive tracer
! is one that it is only advected and
diffused. Other processes are ignored.
! These tracers include, for example, dyes,
pollutants, oil spills, etc.
! NPT values are expected. However, these
switches can be activated using
! compact parameter specification.

 Hout(inert) == T       ! dye_01, ...
inert passive tracers

! Logical switches (TRUE/FALSE) to activate
writing of exposed sediment
! layer properties into HISTORY output file.
Currently, MBOTP properties
! are expected for the bottom boundary layer
and/or sediment models:
!
```

```
! idBott( 1=isd50)   grain_diameter
mean grain diameter
! idBott( 2=idens)   grain_density
mean grain density
! idBott( 3=iwsed)   settling_vel
mean settling velocity
! idBott( 4=itauc)   erosion_stres
critical erosion stress
! idBott( 5=irlen)   ripple_length
ripple length
! idBott( 6=irhgt)   ripple_height
ripple height
! idBott( 7=ibwav)   bed_wave_amp
wave excursion amplitude
! idBott( 8=izdef)   Zo_def
default bottom roughness
! idBott( 9=izapp)   Zo_app
apparent bottom roughness
! idBott(10=izNik)   Zo_Nik
Nikuradse bottom roughness
! idBott(11=izbio)   Zo_bio
biological bottom roughness
! idBott(12=izbfm)   Zo_bedform
bed form bottom roughness
! idBott(13=izbld)   Zo_bedload
bed load bottom roughness
! idBott(14=izwbl)   Zo_wbl
wave bottom roughness
! idBott(15=iactv)   active_layer_thickness
active layer thickness
! idBott(16=ishgt)   saltation
saltation height
```

```
!
!                                   1 1 1 1 1 1
1
!                1 2 3 4 5 6 7 8 9 0 1 2 3 4 5
6

Hout(idBott) == T T T T T T T T T F F F F F T
F

! Logical switches (TRUE/FALSE) to activate
writing of time-averaged
! fields into AVERAGE output file.

Aout(idUvel) == T       ! u
3D U-velocity
Aout(idVvel) == T       ! v
3D V-velocity
Aout(idu3dE) == F       ! u_eastward
3D U-eastward  at RHO-points
Aout(idv3dN) == F       ! v_northward
3D V-northward at RHO-points
Aout(idWvel) == T       ! w
3D W-velocity
Aout(idOvel) == T       ! omega
omega vertical velocity
Aout(idUbar) == T       ! ubar
2D U-velocity
Aout(idVbar) == T       ! vbar
2D V-velocity
Aout(idu2dE) == F       ! ubar_eastward
2D U-eastward  at RHO-points
```

```
Aout(idv2dN) == F       ! vbar_northward
2D V-northward at RHO-points
Aout(idFsur) == T       ! zeta
free-surface

Aout(idTvar) == T T     ! temp, salt
temperature and salinity

Aout(idUsms) == F       ! sustr
surface U-stress
Aout(idVsms) == F       ! svstr
surface V-stress
Aout(idUbms) == F       ! bustr
bottom U-stress
Aout(idVbms) == F       ! bvstr
bottom V-stress

Aout(idW2xx) == F       ! Sxx_bar
2D radiation stress, Sxx component
Aout(idW2xy) == F       ! Sxy_bar
2D radiation stress, Sxy component
Aout(idW2yy) == F       ! Syy_bar
2D radiation stress, Syy component
Aout(idU2rs) == F       ! Ubar_Rstress
2D radiation U-stress
Aout(idV2rs) == F       ! Vbar_Rstress
2D radiation V-stress
Aout(idU2Sd) == F       ! ubar_stokes
2D U-Stokes velocity
Aout(idV2Sd) == F       ! vbar_stokes
2D V-Stokes velocity

Aout(idW3xx) == F       ! Sxx
3D radiation stress, Sxx component
Aout(idW3xy) == F       ! Sxy
3D radiation stress, Sxy component
Aout(idW3yy) == F       ! Syy
3D radiation stress, Syy component
Aout(idW3zx) == F       ! Szx
3D radiation stress, Szx component
Aout(idW3zy) == F       ! Szy
3D radiation stress, Szy component
Aout(idU3rs) == F       ! u_Rstress
3D U-radiation stress
Aout(idV3rs) == F       ! v_Rstress
3D V-radiation stress
Aout(idU3Sd) == F       ! u_stokes
3D U-Stokes velocity
Aout(idV3Sd) == F       ! v_stokes
3D V-Stokes velocity

Aout(idPair) == F       ! Pair
surface air pressure
Aout(idUair) == F       ! Uair
surface U-wind component
Aout(idVair) == F       ! Vair
surface V-wind component

Aout(idTsur) == F F     ! shflux, ssflux
surface net heat and salt flux
Aout(idLhea) == F       ! latent
latent heat flux
Aout(idShea) == F       ! sensible
sensible heat flux
```

```
Aout(idLrad) == F       ! lwrad
longwave radiation flux
Aout(idSrad) == F       ! swrad
shortwave radiation flux
Aout(idevap) == F       ! evaporation
evaporation rate
Aout(idrain) == F       ! rain
precipitation rate

Aout(idDano) == F       ! rho
density anomaly
Aout(idVvis) == F       ! AKv
vertical viscosity
Aout(idTdif) == F       ! AKt
vertical T-diffusion
Aout(idSdif) == F       ! AKs
vertical Salinity diffusion
Aout(idHsbl) == F       ! Hsbl
depth of surface boundary layer
Aout(idHbbl) == F       ! Hbbl
depth of bottom boundary layer

Aout(id2dRV) == F       ! pvorticity_bar
2D relative vorticity
Aout(id3dRV) == F       ! pvorticity
3D relative vorticity
Aout(id2dPV) == F       ! rvorticity_bar
2D potential vorticity
Aout(id3dPV) == F       ! rvorticity
3D potential vorticity
```

```
Aout(idu3dD) == F       ! u_detided
detided 3D U-velocity
Aout(idv3dD) == F       ! v_detided
detided 3D V-velocity
Aout(idu2dD) == F       ! ubar_detided
detided 2D U-velocity
Aout(idv2dD) == F       ! vbar_detided
detided 2D V-velocity
Aout(idFsuD) == F       ! zeta_detided
detided free-surface

Aout(idTrcD) == F F     ! temp_detided, ...
detided temperature and salinity

Aout(idHUav) == F       ! Huon
u-volume flux, Huon
Aout(idHVav) == F       ! Hvom
v-volume flux, Hvom
Aout(idUUav) == F       ! uu
quadratic <u*u> term
Aout(idUVav) == F       ! uv
quadratic <u*v> term
Aout(idVVav) == F       ! vv
quadratic <v*v> term
Aout(idU2av) == F       ! ubar2
quadratic <ubar*ubar> term
Aout(idV2av) == F       ! vbar2
quadratic <vbar*vbar> term
Aout(idZZav) == F       ! zeta2
quadratic <zeta*zeta> term
```

```
Aout(idTTav) == F F     ! temp2, salt2
quadratic <t*t> T/S terms
Aout(idUTav) == F F     ! utemp, usalt
quadratic <u*t> T/S terms
Aout(idVTav) == F F     ! vtemp, vsalt
quadratic <v*t> T/S terms
Aout(iHUTav) == F F     ! Huontemp, ...
T/S volume flux, <Huon*t>
Aout(iHVTav) == F F     ! Hvomtemp, ...
T/S volume flux, <Hvom*t>

! Logical switches (TRUE/FALSE) to activate
writing of extra inert passive
! tracers other than biological and sediment
tracers into the AVERAGE file.

 Aout(inert) == T       ! dye_01, ...
inert passive tracers

! Logical switches (TRUE/FALSE) to activate
writing of time-averaged,
! 2D momentum (ubar,vbar) diagnostic terms
into DIAGNOSTIC output file.

Dout(M2rate) == T       ! ubar_accel, ...
acceleration
Dout(M2pgrd) == T       ! ubar_prsgrd, ...
pressure gradient
Dout(M2fcor) == T       ! ubar_cor, ...
Coriolis force
Dout(M2hadv) == T       ! ubar_hadv, ...
horizontal total advection
Dout(M2xadv) == T       ! ubar_xadv, ...
horizontal XI-advection
Dout(M2yadv) == T       ! ubar_yadv, ...
horizontal ETA-advection
Dout(M2hrad) == T       ! ubar_hrad, ...
horizontal total radiation stress
Dout(M2hvis) == T       ! ubar_hvisc, ...
horizontal total viscosity
Dout(M2xvis) == T       ! ubar_xvisc, ...
horizontal XI-viscosity
Dout(M2yvis) == T       ! ubar_yvisc, ...
horizontal ETA-viscosity
Dout(M2sstr) == T       ! ubar_sstr, ...
surface stress
Dout(M2bstr) == T       ! ubar_bstr, ...
bottom stress

! Logical switches (TRUE/FALSE) to activate
writing of time-averaged,
! 3D momentum (u,v) diagnostic terms into
DIAGNOSTIC output file.

Dout(M3rate) == T       ! u_accel, ...
acceleration
Dout(M3pgrd) == T       ! u_prsgrd, ...
pressure gradient
Dout(M3fcor) == T       ! u_cor, ...
Coriolis force
Dout(M3hadv) == T       ! u_hadv, ...
horizontal total advection
Dout(M3xadv) == T       ! u_xadv, ...
horizontal XI-advection
```

```
Dout(M3yadv) == T       ! u_yadv, ...
horizontal ETA-advection
Dout(M3vadv) == T       ! u_vadv, ...
vertical advection
Dout(M3hrad) == T       ! u_hrad, ...
horizontal total radiation stress
Dout(M3vrad) == T       ! u_vrad, ...
vertical radiation stress
Dout(M3hvis) == T       ! u_hvisc, ...
horizontal total viscosity
Dout(M3xvis) == T       ! u_xvisc, ...
horizontal XI-viscosity
Dout(M3yvis) == T       ! u_yvisc, ...
horizontal ETA-viscosity
Dout(M3vvis) == T       ! u_vvisc, ...
vertical viscosity

! Logical switches (TRUE/FALSE) to activate
writing of time-averaged,
! active (temperature and salinity) and
passive (inert) tracer diagnostic
! terms into DIAGNOSTIC output file:
[1:NAT+NPT,Ngrids].

Dout(iTrate) == T T     ! temp_rate, ...
time rate of change
Dout(iThadv) == T T     ! temp_hadv, ...
horizontal total advection
Dout(iTxadv) == T T     ! temp_xadv, ...
horizontal XI-advection
Dout(iTyadv) == T T     ! temp_yadv, ...
horizontal ETA-advection
Dout(iTvadv) == T T     ! temp_vadv, ...
vertical advection
Dout(iThdif) == T T     ! temp_hdiff, ...
horizontal total diffusion
Dout(iTxdif) == T T     ! temp_xdiff, ...
horizontal XI-diffusion
Dout(iTydif) == T T     ! temp_ydiff, ...
horizontal ETA-diffusion
Dout(iTsdif) == T T     ! temp_sdiff, ...
horizontal S-diffusion
Dout(iTvdif) == T T     ! temp_vdiff, ...
vertical diffusion

! Generic User parameters, [1:NUSER].

       NUSER =  0
        USER =  0.d0

! NetCDF-4/HDF5 compression parameters for
output files.

  NC_SHUFFLE =  1                ! if non-
zero, turn on shuffle filter
  NC_DEFLATE =  1                ! if non-
zero, turn on deflate filter
   NC_DLEVEL =  1                ! deflate
level [0-9]

! Input NetCDF file names, [1:Ngrids].
```

```
     GRDNAME ==
/export/home2/moriarty/Waipaoa/Modelgrids/Make
Gridgen/gridgen_romsformat_redo5.nc
     ININAME ==
/export/home2/moriarty/Waipaoa/Forcing/Bed/wai
paoa_init_redo7_20100101.nc
     ITLNAME == ocean_itl.nc
     IRPNAME == ocean_irp.nc
     IADNAME == ocean_iad.nc
     FWDNAME == ocean_fwd.nc
     ADSNAME == ocean_ads.nc

! Input lateral boundary conditions and
climatology file names.  The
! USER has the option to split input data time
records into several
! NetCDF files (see prologue instructions
above). If so, use a single
! line per entry with a vertical bar (|)
symbol after each entry,
! except the last one.

     BRYNAME ==
/export/home2/moriarty/Waipaoa/Forcing/NZmark/
NZbaroclinic/bdry_bclin_20090925.nc |
/export/home2/moriarty/Waipaoa/Forcing/NZmark/
NZbaroclinic/bdry_bclin_20091002.nc |
/export/home2/moriarty/Waipaoa/Forcing/NZmark/
NZbaroclinic/bdry_bclin_20091009.nc |
/export/home2/moriarty/Waipaoa/Forcing/NZmark/
NZbaroclinic/bdry_bclin_20091017.nc |
/export/home2/moriarty/Waipaoa/Forcing/NZmark/
NZbaroclinic/bdry_bclin_20091024.nc |
/export/home2/moriarty/Waipaoa/Forcing/NZmark/
NZbaroclinic/bdry_bclin_20091101.nc |
/export/home2/moriarty/Waipaoa/Forcing/NZmark/
NZbaroclinic/bdry_bclin_20091108.nc |
/export/home2/moriarty/Waipaoa/Forcing/NZmark/
NZbaroclinic/bdry_bclin_20091116.nc |
/export/home2/moriarty/Waipaoa/Forcing/NZmark/
NZbaroclinic/bdry_bclin_20091123.nc |
/export/home2/moriarty/Waipaoa/Forcing/NZmark/
NZbaroclinic/bdry_bclin_20091201.nc |
/export/home2/moriarty/Waipaoa/Forcing/NZmark/
NZbaroclinic/bdry_bclin_20091208.nc |
/export/home2/moriarty/Waipaoa/Forcing/NZmark/
NZbaroclinic/bdry_bclin_20091216.nc |
/export/home2/moriarty/Waipaoa/Forcing/NZmark/
NZbaroclinic/bdry_bclin_20091223.nc |
/export/home2/moriarty/Waipaoa/Forcing/NZmark/
NZbaroclinic/bdry_bclin_20091231.nc |
/export/home2/moriarty/Waipaoa/Forcing/NZmark/
NZbaroclinic/bdry_bclin_20100107.nc |
/export/home2/moriarty/Waipaoa/Forcing/NZmark/
NZbaroclinic/bdry_bclin_20100115.nc |
/export/home2/moriarty/Waipaoa/Forcing/NZmark/
NZbaroclinic/bdry_bclin_20100122.nc |
/export/home2/moriarty/Waipaoa/Forcing/NZmark/
NZbaroclinic/bdry_bclin_20100130.nc |
/export/home2/moriarty/Waipaoa/Forcing/NZmark/
NZbaroclinic/bdry_bclin_20100206.nc |
/export/home2/moriarty/Waipaoa/Forcing/NZmark/
NZbaroclinic/bdry_bclin_20100214.nc |
```

```
/export/home2/moriarty/Waipaoa/Forcing/NZmark/
NZbaroclinic/bdry_bclin_20100221.nc |
/export/home2/moriarty/Waipaoa/Forcing/NZmark/
NZbaroclinic/bdry_bclin_20100301.nc |
/export/home2/moriarty/Waipaoa/Forcing/NZmark/
NZbaroclinic/bdry_bclin_20100308.nc |
/export/home2/moriarty/Waipaoa/Forcing/NZmark/
NZbaroclinic/bdry_bclin_20100316.nc |
/export/home2/moriarty/Waipaoa/Forcing/NZmark/
NZbaroclinic/bdry_bclin_20100323.nc |
/export/home2/moriarty/Waipaoa/Forcing/NZmark/
NZbaroclinic/bdry_bclin_20100330.nc |
/export/home2/moriarty/Waipaoa/Forcing/NZmark/
NZbaroclinic/bdry_bclin_20100407.nc |
/export/home2/moriarty/Waipaoa/Forcing/NZmark/
NZbaroclinic/bdry_bclin_20100414.nc |
/export/home2/moriarty/Waipaoa/Forcing/NZmark/
NZbaroclinic/bdry_bclin_20100422.nc |
/export/home2/moriarty/Waipaoa/Forcing/NZmark/
NZbaroclinic/bdry_bclin_20100429.nc |
/export/home2/moriarty/Waipaoa/Forcing/NZmark/
NZbaroclinic/bdry_bclin_20100507.nc |
/export/home2/moriarty/Waipaoa/Forcing/NZmark/
NZbaroclinic/bdry_bclin_20100514.nc |
/export/home2/moriarty/Waipaoa/Forcing/NZmark/
NZbaroclinic/bdry_bclin_20100522.nc |
/export/home2/moriarty/Waipaoa/Forcing/NZmark/
NZbaroclinic/bdry_bclin_20100529.nc |
/export/home2/moriarty/Waipaoa/Forcing/NZmark/
NZbaroclinic/bdry_bclin_20100606.nc |
/export/home2/moriarty/Waipaoa/Forcing/NZmark/
NZbaroclinic/bdry_bclin_20100613.nc |
/export/home2/moriarty/Waipaoa/Forcing/NZmark/
NZbaroclinic/bdry_bclin_20100621.nc |
/export/home2/moriarty/Waipaoa/Forcing/NZmark/
NZbaroclinic/bdry_bclin_20100628.nc |
/export/home2/moriarty/Waipaoa/Forcing/NZmark/
NZbaroclinic/bdry_bclin_20100706.nc |
/export/home2/moriarty/Waipaoa/Forcing/NZmark/
NZbaroclinic/bdry_bclin_20100713.nc |
/export/home2/moriarty/Waipaoa/Forcing/NZmark/
NZbaroclinic/bdry_bclin_20100721.nc |
/export/home2/moriarty/Waipaoa/Forcing/NZmark/
NZbaroclinic/bdry_bclin_20100728.nc |
/export/home2/moriarty/Waipaoa/Forcing/NZmark/
NZbaroclinic/bdry_bclin_20100805.nc |
/export/home2/moriarty/Waipaoa/Forcing/NZmark/
NZbaroclinic/bdry_bclin_20100812.nc |
/export/home2/moriarty/Waipaoa/Forcing/NZmark/
NZbaroclinic/bdry_bclin_20100820.nc |
/export/home2/moriarty/Waipaoa/Forcing/NZmark/
NZbaroclinic/bdry_bclin_20100827.nc |
/export/home2/moriarty/Waipaoa/Forcing/NZmark/
NZbaroclinic/bdry_bclin_20100904.nc |
/export/home2/moriarty/Waipaoa/Forcing/NZmark/
NZbaroclinic/bdry_bclin_20100911.nc |
/export/home2/moriarty/Waipaoa/Forcing/NZmark/
NZbaroclinic/bdry_bclin_20100919.nc |
/export/home2/moriarty/Waipaoa/Forcing/NZmark/
NZbaroclinic/bdry_bclin_20100926.nc |
/export/home2/moriarty/Waipaoa/Forcing/NZmark/
NZbaroclinic/bdry_bclin_20101004.nc |
/export/home2/moriarty/Waipaoa/Forcing/NZmark/
NZbaroclinic/bdry_bclin_20101011.nc |
```

```
/export/home2/moriarty/Waipaoa/Forcing/NZmark/
NZbaroclinic/bdry_bclin_20101019.nc |
/export/home2/moriarty/Waipaoa/Forcing/NZmark/
NZbaroclinic/bdry_bclin_20101026.nc |
/export/home2/moriarty/Waipaoa/Forcing/NZmark/
NZbaroclinic/bdry_bclin_20101103.nc |
/export/home2/moriarty/Waipaoa/Forcing/NZmark/
NZbaroclinic/bdry_bclin_20101110.nc |
/export/home2/moriarty/Waipaoa/Forcing/NZmark/
NZbaroclinic/bdry_bclin_20101118.nc |
/export/home2/moriarty/Waipaoa/Forcing/NZmark/
NZbaroclinic/bdry_bclin_20101125.nc |
/export/home2/moriarty/Waipaoa/Forcing/NZmark/
NZbaroclinic/bdry_bclin_20101203.nc |
/export/home2/moriarty/Waipaoa/Forcing/NZmark/
NZbaroclinic/bdry_bclin_20101210.nc |
/export/home2/moriarty/Waipaoa/Forcing/NZmark/
NZbaroclinic/bdry_bclin_20101218.nc |
/export/home2/moriarty/Waipaoa/Forcing/NZmark/
NZbaroclinic/bdry_bclin_20101225.nc |
/export/home2/moriarty/Waipaoa/Forcing/NZmark/
NZbaroclinic/bdry_bclin_20110102.nc |
/export/home2/moriarty/Waipaoa/Forcing/NZmark/
NZbaroclinic/bdry_bclin_20110109.nc |
/export/home2/moriarty/Waipaoa/Forcing/NZmark/
NZbaroclinic/bdry_bclin_20110117.nc |
/export/home2/moriarty/Waipaoa/Forcing/NZmark/
NZbaroclinic/bdry_bclin_20110124.nc |
/export/home2/moriarty/Waipaoa/Forcing/NZmark/
NZbaroclinic/bdry_bclin_20110201.nc |
/export/home2/moriarty/Waipaoa/Forcing/NZmark/
NZbaroclinic/bdry_bclin_20110208.nc |
/export/home2/moriarty/Waipaoa/Forcing/NZmark/
NZbaroclinic/bdry_bclin_20110216.nc |
/export/home2/moriarty/Waipaoa/Forcing/NZmark/
NZbaroclinic/bdry_bclin_20110223.nc
     CLMNAME ==
/export/home2/moriarty/Waipaoa/Forcing/NZmark/
NZbaroclinic/clim_bclin_20090925.nc |
/export/home2/moriarty/Waipaoa/Forcing/NZmark/
NZbaroclinic/clim_bclin_20091002.nc |
/export/home2/moriarty/Waipaoa/Forcing/NZmark/
NZbaroclinic/clim_bclin_20091009.nc |
/export/home2/moriarty/Waipaoa/Forcing/NZmark/
NZbaroclinic/clim_bclin_20091017.nc |
/export/home2/moriarty/Waipaoa/Forcing/NZmark/
NZbaroclinic/clim_bclin_20091024.nc |
/export/home2/moriarty/Waipaoa/Forcing/NZmark/
NZbaroclinic/clim_bclin_20091101.nc |
/export/home2/moriarty/Waipaoa/Forcing/NZmark/
NZbaroclinic/clim_bclin_20091108.nc |
/export/home2/moriarty/Waipaoa/Forcing/NZmark/
NZbaroclinic/clim_bclin_20091116.nc |
/export/home2/moriarty/Waipaoa/Forcing/NZmark/
NZbaroclinic/clim_bclin_20091123.nc |
/export/home2/moriarty/Waipaoa/Forcing/NZmark/
NZbaroclinic/clim_bclin_20091201.nc |
/export/home2/moriarty/Waipaoa/Forcing/NZmark/
NZbaroclinic/clim_bclin_20091208.nc |
/export/home2/moriarty/Waipaoa/Forcing/NZmark/
NZbaroclinic/clim_bclin_20091216.nc |
/export/home2/moriarty/Waipaoa/Forcing/NZmark/
NZbaroclinic/clim_bclin_20091223.nc |
```

```
/export/home2/moriarty/Waipaoa/Forcing/NZmark/
NZbaroclinic/clim_bclin_20091231.nc |
/export/home2/moriarty/Waipaoa/Forcing/NZmark/
NZbaroclinic/clim_bclin_20100107.nc |
/export/home2/moriarty/Waipaoa/Forcing/NZmark/
NZbaroclinic/clim_bclin_20100115.nc |
/export/home2/moriarty/Waipaoa/Forcing/NZmark/
NZbaroclinic/clim_bclin_20100122.nc |
/export/home2/moriarty/Waipaoa/Forcing/NZmark/
NZbaroclinic/clim_bclin_20100130.nc |
/export/home2/moriarty/Waipaoa/Forcing/NZmark/
NZbaroclinic/clim_bclin_20100206.nc |
/export/home2/moriarty/Waipaoa/Forcing/NZmark/
NZbaroclinic/clim_bclin_20100214.nc |
/export/home2/moriarty/Waipaoa/Forcing/NZmark/
NZbaroclinic/clim_bclin_20100221.nc |
/export/home2/moriarty/Waipaoa/Forcing/NZmark/
NZbaroclinic/clim_bclin_20100301.nc |
/export/home2/moriarty/Waipaoa/Forcing/NZmark/
NZbaroclinic/clim_bclin_20100308.nc |
/export/home2/moriarty/Waipaoa/Forcing/NZmark/
NZbaroclinic/clim_bclin_20100316.nc |
/export/home2/moriarty/Waipaoa/Forcing/NZmark/
NZbaroclinic/clim_bclin_20100323.nc |
/export/home2/moriarty/Waipaoa/Forcing/NZmark/
NZbaroclinic/clim_bclin_20100330.nc |
/export/home2/moriarty/Waipaoa/Forcing/NZmark/
NZbaroclinic/clim_bclin_20100407.nc |
/export/home2/moriarty/Waipaoa/Forcing/NZmark/
NZbaroclinic/clim_bclin_20100414.nc |
/export/home2/moriarty/Waipaoa/Forcing/NZmark/
NZbaroclinic/clim_bclin_20100422.nc |
/export/home2/moriarty/Waipaoa/Forcing/NZmark/
NZbaroclinic/clim_bclin_20100429.nc |
/export/home2/moriarty/Waipaoa/Forcing/NZmark/
NZbaroclinic/clim_bclin_20100507.nc |
/export/home2/moriarty/Waipaoa/Forcing/NZmark/
NZbaroclinic/clim_bclin_20100514.nc |
/export/home2/moriarty/Waipaoa/Forcing/NZmark/
NZbaroclinic/clim_bclin_20100522.nc |
/export/home2/moriarty/Waipaoa/Forcing/NZmark/
NZbaroclinic/clim_bclin_20100529.nc |
/export/home2/moriarty/Waipaoa/Forcing/NZmark/
NZbaroclinic/clim_bclin_20100606.nc |
/export/home2/moriarty/Waipaoa/Forcing/NZmark/
NZbaroclinic/clim_bclin_20100613.nc |
/export/home2/moriarty/Waipaoa/Forcing/NZmark/
NZbaroclinic/clim_bclin_20100621.nc |
/export/home2/moriarty/Waipaoa/Forcing/NZmark/
NZbaroclinic/clim_bclin_20100628.nc |
/export/home2/moriarty/Waipaoa/Forcing/NZmark/
NZbaroclinic/clim_bclin_20100706.nc |
/export/home2/moriarty/Waipaoa/Forcing/NZmark/
NZbaroclinic/clim_bclin_20100713.nc |
/export/home2/moriarty/Waipaoa/Forcing/NZmark/
NZbaroclinic/clim_bclin_20100721.nc |
/export/home2/moriarty/Waipaoa/Forcing/NZmark/
NZbaroclinic/clim_bclin_20100728.nc |
/export/home2/moriarty/Waipaoa/Forcing/NZmark/
NZbaroclinic/clim_bclin_20100805.nc |
/export/home2/moriarty/Waipaoa/Forcing/NZmark/
NZbaroclinic/clim_bclin_20100812.nc |
/export/home2/moriarty/Waipaoa/Forcing/NZmark/
NZbaroclinic/clim_bclin_20100820.nc |
```

```
/export/home2/moriarty/Waipaoa/Forcing/NZmark/
NZbaroclinic/clim_bclin_20100827.nc |
/export/home2/moriarty/Waipaoa/Forcing/NZmark/
NZbaroclinic/clim_bclin_20100904.nc |
/export/home2/moriarty/Waipaoa/Forcing/NZmark/
NZbaroclinic/clim_bclin_20100911.nc |
/export/home2/moriarty/Waipaoa/Forcing/NZmark/
NZbaroclinic/clim_bclin_20100919.nc |
/export/home2/moriarty/Waipaoa/Forcing/NZmark/
NZbaroclinic/clim_bclin_20100926.nc |
/export/home2/moriarty/Waipaoa/Forcing/NZmark/
NZbaroclinic/clim_bclin_20101004.nc |
/export/home2/moriarty/Waipaoa/Forcing/NZmark/
NZbaroclinic/clim_bclin_20101011.nc |
/export/home2/moriarty/Waipaoa/Forcing/NZmark/
NZbaroclinic/clim_bclin_20101019.nc |
/export/home2/moriarty/Waipaoa/Forcing/NZmark/
NZbaroclinic/clim_bclin_20101026.nc |
/export/home2/moriarty/Waipaoa/Forcing/NZmark/
NZbaroclinic/clim_bclin_20101103.nc |
/export/home2/moriarty/Waipaoa/Forcing/NZmark/
NZbaroclinic/clim_bclin_20101110.nc |
/export/home2/moriarty/Waipaoa/Forcing/NZmark/
NZbaroclinic/clim_bclin_20101118.nc |
/export/home2/moriarty/Waipaoa/Forcing/NZmark/
NZbaroclinic/clim_bclin_20101125.nc |
/export/home2/moriarty/Waipaoa/Forcing/NZmark/
NZbaroclinic/clim_bclin_20101203.nc |
/export/home2/moriarty/Waipaoa/Forcing/NZmark/
NZbaroclinic/clim_bclin_20101210.nc |
/export/home2/moriarty/Waipaoa/Forcing/NZmark/
NZbaroclinic/clim_bclin_20101218.nc |
/export/home2/moriarty/Waipaoa/Forcing/NZmark/
NZbaroclinic/clim_bclin_20101225.nc |
/export/home2/moriarty/Waipaoa/Forcing/NZmark/
NZbaroclinic/clim_bclin_20110102.nc |
/export/home2/moriarty/Waipaoa/Forcing/NZmark/
NZbaroclinic/clim_bclin_20110109.nc |
/export/home2/moriarty/Waipaoa/Forcing/NZmark/
NZbaroclinic/clim_bclin_20110117.nc |
/export/home2/moriarty/Waipaoa/Forcing/NZmark/
NZbaroclinic/clim_bclin_20110124.nc |
/export/home2/moriarty/Waipaoa/Forcing/NZmark/
NZbaroclinic/clim_bclin_20110201.nc |
/export/home2/moriarty/Waipaoa/Forcing/NZmark/
NZbaroclinic/clim_bclin_20110208.nc |
/export/home2/moriarty/Waipaoa/Forcing/NZmark/
NZbaroclinic/clim_bclin_20110216.nc |
/export/home2/moriarty/Waipaoa/Forcing/NZmark/
NZbaroclinic/clim_bclin_20110223.nc

! Input forcing NetCDF file name(s).  The USER
has the option to enter
! several file names for each nested grid.
For example, the USER may
! have different files for wind products, heat
fluxes, rivers, tides,
! etc.  The model will scan the file list and
will read the needed data
! from the first file in the list containing
the forcing field. Therefore,
! the order of the file names is very
important. If using multiple forcing
```

```
! files per grid, first enter all the file
names for grid 1, then grid 2,
! and so on.  It is also possible to split
input data time records into
! several NetCDF files (see prologue
instructions above). Use a single line
! per entry with a continuation (\) or
vertical bar (|) symbol after each
! entry, except the last one.

     NFFILES == 10
number of unique forcing files

     FRCNAME ==
/export/home2/moriarty/Waipaoa/Forcing/Winds/C
liflo/New/waipaoa_swradhr_new.nc \
/export/home2/moriarty/Waipaoa/Forcing/Winds/C
liflo/New/waipaoa_windhr_nzlam_new.nc \
/export/home2/moriarty/Waipaoa/Forcing/Winds/C
liflo/New/waipaoa_apresshr_new.nc \
/export/home2/moriarty/Waipaoa/Forcing/Winds/C
liflo/New/waipaoa_cloud_new.nc \
/export/home2/moriarty/Waipaoa/Forcing/Winds/C
liflo/New/waipaoa_rainhr_new.nc \
/export/home2/moriarty/Waipaoa/Forcing/Winds/C
liflo/New/waipaoa_relhumhr_new.nc \
/export/home2/moriarty/Waipaoa/Forcing/Winds/C
liflo/New/waipaoa_temphr_new.nc \
/export/home2/moriarty/Waipaoa/Forcing/NZwave/
waipaoa_waves3_new.nc \
/export/home2/moriarty/Waipaoa/Forcing/RIVER/w
aipaoa_river_newpartitions.nc \
/export/home2/moriarty/Waipaoa/Forcing/TIDES/O
SUtides/OTPS/pb_tide_PO_new.nc

! Output NetCDF file names, [1:Ngrids].

     GSTNAME == ocean_gst.nc
     RSTNAME == Results/ocean_rst2.nc
     HISNAME == Results/ocean_his2.nc
     TLMNAME == ocean_tlm.nc
     TLFNAME == ocean_tlf.nc
     ADJNAME == ocean_adj.nc
     AVGNAME == ocean_avg.nc
     DIANAME == ocean_dia.nc
     STANAME == ocean_sta.nc
     FLTNAME == ocean_flt.nc

! Input ASCII parameter filenames.

     APARNAM =  s4dvar.in
     SPOSNAM =  stations.in
     FPOSNAM =  floats.in
     BPARNAM =  bio_Fennel.in
     SPARNAM =  External/sediment_waipaoa2.in
     USRNAME =  MyFile.dat

!
!  GLOSSARY:
!  =========
!
!-----------------------------------------
--------------------------------
```

```
! Application title (string with a maximum of
eighty characters) and
! C-preprocessing flag.
!-----------------------------------------
---------------------------------
!
!  TITLE       Application title.
!
!  MyAppCPP    Application C-preprocessing
option.
!
!-----------------------------------------
---------------------------------
! Variable information file name (string with
a maximum of 256 characters).
!-----------------------------------------
---------------------------------
!
!  VARNAME     Input/Output variable
information file name.  This file needs to
!              be processed first so all
information arrays and indices can be
!              initialized properly in
"mod_ncparam.F".
!
!-----------------------------------------
---------------------------------
! Nested grid parameters.
!-----------------------------------------
---------------------------------
!
!  Ngrids      Number of nested grids. It
needs to be read at the top of all
!              other parameters in order to
allocate all model variables.
!
!-----------------------------------------
---------------------------------
! Grid dimension parameters.
!-----------------------------------------
---------------------------------
!
! These parameters are very important since
they determine the grid of the
! application to solve. They need to be read
first in order to dynamically
! allocate all model variables.
!
! WARNING: It is trivial and possible to
change these dimension parameters in
! -------  idealized applications via
analytical expressions.  However, in
! realistic applications any change to these
parameters requires redoing all
! input NetCDF files.
!
!  Lm          Number of INTERIOR grid RHO-
points in the XI-direction for
!                each nested grid, [1:Ngrids].
If using NetCDF files as
!                input, Lm=xi_rho-2 where
"xi_rho" is the NetCDF file
```

```
!                dimension of RHO-points.
Recall that all RHO-point
!                variables have a
computational I-range of [0:Lm+1].
!
!  Mm          Number of INTERIOR grid RHO-
points in the ETA-direction for
!                each nested grid, [1:Ngrids].
If using NetCDF files as
!                input, Mm=eta_rho-2 where
"eta_rho" is the NetCDF file
!                dimension of RHO-points.
Recall that all RHO-point
!                variables have a
computational J-range of [0:Mm+1].
!
!  N           Number of vertical terrain-
following levels at RHO-points,
!                [1:Ngrids].
!
!  Nbed        Number of sediment bed layers,
[1:Ngrids]. This parameter
!                is only relevant if CPP
option SEDIMENT is activated.
!
!                Mm+1  ____________________
_______  Kw = N
!                   |                    |
|       |
!                 Mm |   _____________    |
|       | Kr = N
```

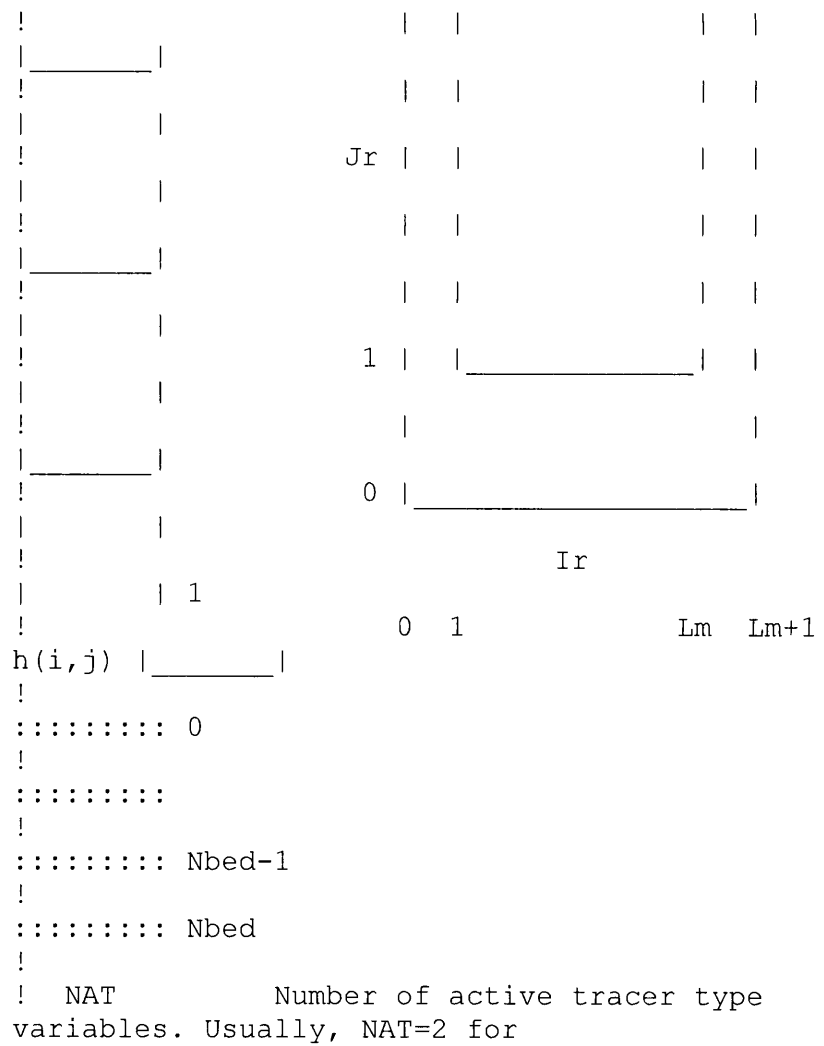


```
!  NAT         Number of active tracer type
variables. Usually, NAT=2 for
```

```
!                potential temperature and
salinity.
!
!  NPT          Number of inert (dyes, age,
etc) passive tracer type variables
!                to advect and diffuse only.
This parameter is only relevant
!                if CPP option T_PASSIVE is
activated.
!
!  NCS          Number of cohesive (mud)
sediment tracer type variables. This
!                parameter is only relevant if
CPP option SEDIMENT is
!                activated.
!
!  NNS          Number of non-cohesive (sand)
sediment tracer type variables.
!                This parameter is only
relevant if CPP option SEDIMENT is
!                activated.
!
!              The total number of sediment
tracers is NST=NCS+NNS.  Notice
!              that NST must be greater than
zero (NST>0).
!
!-----------------------------------------
--------------------------------
! Domain tile partition parameters.
!-----------------------------------------
--------------------------------
!
! Model tile decomposition parameters for
serial and parallel configurations
! which are used to determine tile horizontal
range indices (Istr,Iend) and
! (Jstr,Jend). In some computers, it is
advantageous to have tile partitions
! in serial applications.
!
!  NtileI       Number of domain partitions in
the I-direction (XI-coordinate).
!               It must be equal to or greater
than one.
!
!  NtileJ       Number of domain partitions in
the J-direction (ETA-coordinate).
!               It must be equal to or greater
than one.
!
!  WARNING:     In shared-memory (OpenMP), the
product of NtileI and NtileJ must
!               be a MULTIPLE of the number of
parallel threads specified with
!               the OpenMP environmental
variable OMP_NUM_THREADS.
!
!               In distributed-memory (MPI),
the product of NtileI and NtileJ
!               must be EQUAL to the number of
parallel nodes specified during
!               execution with the "mprun" or
"mpirun" command.
```

```
!
!-------------------------------------------
--------------------------------
! Lateral boundary conditions parameters.
!-------------------------------------------
--------------------------------
!
! The lateral boundary conditions are now
specified with logical switches
! instead of CPP flags to allow nested grid
configurations. Their values are
! loaded into structured array:
!
!    LBC(1:4, nLBCvar, Ngrids)
!
! where 1:4 are the number of boundary edges,
nLBCvar are the number LBC state
! variables, and Ngrids is the number of
nested grids. For Example, to apply
! gradient boundary conditions we use:
!
!    LBC(iwest,  isFsur, ng) % gradient
!    LBC(ieast,  ...   , ng) % gradient
!    LBC(isouth, ...   , ng) % gradient
!    LBC(inorth, ...   , ng) % gradient
!
! The lateral boundary conditions are entered
with a keyword. This keyword
! is case insensitive and usually has three
characters. However, it is
! possible to have compound keywords, if
applicable. For example, the
! keyword "RadNud" implies radiation boundary
condition with nudging. This
! combination is usually used in
active/passive radiation conditions.
!
!   Keyword    Lateral Boundary Condition Type
!
!   Cha        Chapman
!   Cla        Clamped
!   Clo        Closed
!   Fla        Flather
_____N_____     j=Mm
!   Gra        Gradient
|     4     |
!   Nes        Nested
|           |
!   Nud        Nudging
1 W           E 3
!   Per        Periodic
|           |
!   Rad        Radiation
|_____S_____|
!   Red        Reduced Physics
2          j=1
!
i=1         i=Lm
!
!  LBC(isFsur) Free-surface,  [1:4, Ngrids]
values are expected.
!  LBC(isUbar) 2D U-momentum, [1:4, Ngrids]
values are expected.
```

```
!  LBC(isVbar) 2D V-momentum, [1:4, Ngrids]
values are expected.
!  LBC(isUvel) 3D U-momentum, [1:4, Ngrids]
values are expected.
!  LBC(isVvel) 3D V-momentum, [1:4, Ngrids]
values are expected.
!  LBC(isMtke) Mixing TKE,    [1:4, Ngrids]
values are expected.
!  LBC(isTvar) Tracers,       [1:4, 1:NAT+NPT,
Ngrids] values are expected.
!
! Similarly, the adjoint-based algorithms
(ADM, TLM, RPM) can have different
! lateral boundary conditions keywords:
!
!  ad_LBC(isFsur) Free-surface,  [1:4, Ngrids]
values are expected.
!  ad_LBC(isUbar) 2D U-momentum, [1:4, Ngrids]
values are expected.
!  ad_LBC(isVbar) 2D V-momentum, [1:4, Ngrids]
values are expected.
!  ad_LBC(isUvel) 3D U-momentum, [1:4, Ngrids]
values are expected.
!  ad_LBC(isVvel) 3D V-momentum, [1:4, Ngrids]
values are expected.
!  ad_LBC(isMtke) Mixing TKE,    [1:4, Ngrids]
values are expected.
!  ad_LBC(isTvar) Tracers,       [1:4,
1:NAT+NPT, Ngrids] values are expected.
!
! Lateral open boundary edge volume
conservation switch for nonlinear model
! and adjoint-based algorithm. Usually
activated with radiation boundary
! conditions to enforce global mass
conservation. Notice that these switches
! should not be activated if tidal forcing
enabled, [1:Ngrids] values are
! expected.
!
!  VolCons(west)       Western  boundary
volume conservation switch.
!  VolCons(east)       Eastern  boundary
volume conservation switch.
!  VolCons(south)      Southern boundary
volume conservation switch.
!  VolCons(north)      Northern boundary
volume conservation switch.
!
!  ad_VolCons(west)    Western  boundary
volume conservation switch.
!  ad_VolCons(east)    Eastern  boundary
volume conservation switch.
!  ad_VolCons(south)   Southern boundary
volume conservation switch.
!  ad_VolCons(north)   Northern boundary
volume conservation switch.
!
!-----------------------------------------
--------------------------------
! Time-Stepping parameters.
!-----------------------------------------
--------------------------------
!
```

```
!  NTIMES      Total number time-steps in
current run.  If 3D configuration,
!              NTIMES is the total of
baroclinic time-steps.  If only 2D
!              configuration, NTIMES is the
total of barotropic time-steps.
!
!  DT          Time-Step size in seconds.  If
3D configuration, DT is the
!              size of the baroclinic time-
step.  If only 2D configuration,
!              DT is the size of the
barotropic time-step.
!
!  NDTFAST     Number of barotropic time-steps
between each baroclinic time
!              step. If only 2D configuration,
NDTFAST should be unity since
!              there is no need to split time-
stepping.
!
!-----------------------------------------
--------------------------------
! Model iteration loops parameters.
!-----------------------------------------
--------------------------------
!
!  ERstr       Starting ensemble run
(perturbation or iteration) number.
!
!  ERend       Ending   ensemble run
(perturbation or iteration) number.
!
!  Nouter      Maximum number of 4DVAR outer
loop iterations.
!
!  Ninner      Maximum number of 4DVAR inner
loop iterations.
!
!  Nintervals  Number of time interval
divisions for Stochastic Optimals
!              computations. It must be a
multiple of NTIMES. The tangent
!              linear model (TLM) and the
adjoint model (ADM) are integrated
!              forward and backward at
different intervals.  For example,
!              if Nintervals=3,
!
!              1               NTIMES/3
2*NTIMES/3           NTIMES
!
+..................+..................+.....
.....+
!
<==========================================
==========> (1)
!
<====================================> (2)
!
<==================> (3)
!
!              In the first iteration (1), the
TLM is integrated forward from
```

```
!               1 to NTIMES and the ADM is
integrated backward from NTIMES to 1.
!               In the second iteration (2),
the TLM is integrated forward from
!               NTIMES/3 to NTIMES and the ADM
is integrated backward from
!               NTIMES to NTIMES/3. And so on.
!
!-----------------------------------------
---------------------------------
!  Eigenproblem parameters.
!-----------------------------------------
---------------------------------
!
!  NEV          Number of eigenvalues to
compute for the Lanczos/Arnoldi
!               problem.  Notice that the model
memory requirement increases
!               substantially as NEV increases.
The GST requires NEV+1
!               copies of the model state
vector.  The memory requirements
!               are decreased in distributed-
memory applications.
!
!  NCV          Number of eigenvectors to
compute for the Lanczos/Arnoldi
!               problem. NCV must be greater
than NEV.
!
!  At present, there is no a-priori analysis
to guide the selection of NCV
!  relative to NEV.  The only formal
requirement is that NCV > NEV. However
!  in optimal perturbations, it is recommended
to have NCV greater than or
!  equal to 2*NEV. In Finite Time Eigenmodes
(FTE) and Adjoint Finite Time
!  Eigenmodes (AFTE) the requirement is to
have NCV greater than or equal to
!  2*NEV+1.
!
!  The efficiency of calculations depends
critically on the combination of
!  NEV and NCV.  If NEV is large (greater than
10 say), you can use NCV=2*NEV+1
!  but for NEV small (less than 6) it will be
inefficient to use NCV=2*NEV+1.
!  In complicated applications, you can start
with NEV=2 and NCV=10. Otherwise,
!  it will iterate for a very long time.
!
!-----------------------------------------
---------------------------------
! Input/Output parameters.
!-----------------------------------------
---------------------------------
!
!  NRREC        Switch to indicate re-start
from a previous solution.  Use
!               NRREC=0 for new solutions. In a
re-start solution, NRREC
!               is the time index of the re-
start NetCDF file assigned for
```

```
!               initialization.  If NRREC is
negative (say NRREC=-1), the
!               model will re-start from the
most recent time record. That
!               is, the initialization record
is assigned internally.
!               Notice that it is also possible
to re-start from a history
!               or time-averaged NetCDF file.
If a history file is used
!               for re-start, it must contains
all the necessary primitive
!               variables at all levels.
!
!  LcycleRST    Logical switch (T/F) used to
recycle time records in output
!               re-start file.  If TRUE,  only
the latest two re-start time
!               records are maintained.  If
FALSE, all re-start fields are
!               saved every NRST time-steps
without recycling.  The re-start
!               fields are written at all
levels in double precision.
!
!  NRST         Number of time-steps between
writing of re-start fields.
!
!  NSTA         Number of time-steps between
writing data into stations file.
!               Station data is written at all
levels.
!
!  NFLT         Number of time-steps between
writing data into floats file.
!
!  NINFO        Number of time-steps between
print of single line information
!               to standard output.  It also
determines the interval between
!               computation of global energy
diagnostics.
!
!-------------------------------------------
--------------------------------
!  Output history and average files
parameters.
!-------------------------------------------
--------------------------------
!
!  LDEFOUT      Logical switch (T/F) used to
create new output files when
!               initializing from a re-start
file, abs(NRREC) > 0.  If TRUE
!               and applicable, a new history,
average, diagnostic and
!               station files are created
during the initialization stage.
!               If FALSE and applicable, data
is appended to existing
!               history, average, diagnostic
and station files.  See also
!               parameters NDEFHIS, NDEFAVG and
NDEFDIA below.
```

```
!
!  NHIS        Number of time-steps between
writing fields into history file.
!
!  NDEFHIS     Number of time-steps between
the creation of new history file.
!              If NDEFHIS=0, the model will
only process one history file.
!              This feature is useful for long
simulations when history files
!              get too large; it creates a new
file every NDEFHIS time-steps.
!
!  NTSAVG      Starting time-step for the
accumulation of output time-averaged
!              data.
!
!  NAVG        Number of time-steps between
writing time-averaged data
!              into averages file.  Averaged
date is written for all fields.
!
!  NDEFAVG     Number of time-steps between
the creation of new average
!              file.  If NDEFAVG=0, the model
will only process one average
!              file.  This feature is useful
for long simulations when
!              average files get too large; it
creates a new file every
!              NDEFAVG time-steps.
!
!  NTSDIA      Starting time-step for the
accumulation of output time-averaged
!              diagnostics data.
!
!  NDIA        Number of time-steps between
writing time-averaged diagnostics
!              data into diagnostics file.
Averaged date is written for all
!              fields.
!
!  NDEFDIA     Number of time-steps between
the creation of new time-averaged
!              diagnostics file.  If
NDEFDIA=0, the model will only process one
!              diagnostics file.  This feature
is useful for long simulations
!              when diagnostics files get too
large; it creates a new file
!              every NDEFDIA time-steps.
!
!-----------------------------------------
---------------------------------
!  Output tangent linear and adjoint model
parameters.
!-----------------------------------------
---------------------------------
!
!  LcycleTLM   Logical switch (T/F) used to
recycle time records in output
!              tangent linear file.  If TRUE,
only the latest two time
```

```
!               records are maintained.  If
FALSE, all tangent linear fields
!               are saved every NTLM time-steps
without recycling.
!
!  NTLM         Number of time-steps between
writing fields into tangent linear
!               model file.
!
!  NDEFTLM      Number of time-steps between
the creation of new tangent linear
!               file. If NDEFTLM=0, the model
will only process one tangent
!               linear file. This feature is
useful for long simulations when
!               output NetCDF files get too
large; it creates a new file every
!               NDEFTLM time-steps.
!
!  LcycleADJ    Logical switch (T/F) used to
recycle time records in output
!               adjoint file.  If TRUE, only
the latest two time records are
!               maintained.  If FALSE, all
tangent linear fields re saved
!               every NADJ time-steps without
recycling.
!
!  NADJ         Number of time-steps between
writing fields into adjoint model
!               file.
!
!  NDEFADJ      Number of time-steps between
the creation of new adjoint file.
!               If NDEFADJ=0, the model will
only process one adjoint file.
!               This feature is useful for long
simulations when output NetCDF
!               files get too large; it creates
a new file every NDEFADJ
!               time-steps.
!
!  NSFF         Number of time-steps between
4DVAR adjustment of surface forcing
!               fluxes. In strong constraint
4DVAR, it is possible to adjust
!               surface forcing at other time
intervals in addition to initial
!               time.  This parameter is used
to store the appropriate number
!               of surface forcing records in
the output history NetCDF files:
!               1+NTIMES/NSFF records. NSFF
must be a factor of NTIMES or
!               greater than NTIMES. If NSFF >
NTIMES, only one record is
!               stored in the NetCDF files and
the adjustment is for constant
!               forcing with constant
correction. This parameter is only
!               relevant in 4DVAR when
activating either ADJUST_STFLUX or
!               ADJUST_WSTRESS.
!
```

```
!  NOBC        Number of time-steps between
4DVAR adjustment of open boundary
!              fields. In strong constraint
4DVAR, it is possible to adjust
!              open boundaries at other time
intervals in addition to initial
!              time.  This parameter is used
to store the appropriate number
!              of open boundary records in the
output history NetCDF files:
!              1+NTIMES/NOBC records. NOBC
must be a factor of NTIMES or
!              greater than NTIMES. If NOBC >
NTIMES, only one record is
!              stored in the NetCDF files and
the adjustment is for constant
!              forcing with constant
correction. This parameter is only
!              relevant in 4DVAR when
activating ADJUST_BOUNDARY.
!
!-----------------------------------------
--------------------------------
!  Generalized Stability Theory (GST) analysis
parameters.
!-----------------------------------------
--------------------------------
!
!  LmultiGST   Logical switch (TRUE/FALSE) to
write out one GST analysis
!              eigenvector per history file.
!
!  LrstGST     Logical switch (TRUE/FALSE) to
restart GST analysis. If TRUE,
!              the check pointing data is read
in from the GST restart NetCDF
!              file.  If FALSE and applicable,
the check pointing GST data is
!              saved and overwritten every
NGST iterations of the algorithm.
!
!  MaxIterGST  Maximum number of GST algorithm
iterations.
!
!  NGST        Number of GST iterations
between storing of check pointing
!              data into NetCDF file. The
restart data is always saved if
!              MaxIterGST is reached without
convergence. It is also saved
!              when convergence is achieved.
It is always a good idea to
!              save the check pointing data at
regular intervals so there
!              is a mechanism to recover from
an unexpected interruption
!              in this very expensive
computation. The check pointing data
!              can be used also to recompute
the Ritz vectors by changing
!              some of the parameters, like
convergence criteria (Ritz_tol)
!              and number of Arnoldi
iterations (iparam(3)).
```

```
!
!  Ritz_tol    Relative accuracy of the Ritz
values computed in the GST
!              analysis.
!
!-----------------------------------------
---------------------------------
! Harmonic/Biharmonic horizontal diffusion for
active tracers.
!-----------------------------------------
---------------------------------
!
!  TNU2        Nonlinear model lateral,
harmonic, constant, mixing
!              coefficient (m2/s) for active
(NAT) and inert (NPT) tracer
!              variables. If variable
horizontal diffusion is activated,
!              TNU2 is the mixing coefficient
for the largest grid-cell
!              in the domain.
!
!  TNU4        Nonlinear model lateral,
biharmonic, constant, mixing
!              coefficient (m4/s) for active
(NAT) and inert (NPT) tracer
!              variables. If variable
horizontal diffusion is activated,
!              TNU4 is the mixing coefficient
for the largest grid-cell
!              in the domain.
!
!  ad_TNU2     Adjoint-based algorithms
lateral, harmonic, constant, mixing
!              coefficient (m2/s) for active
(NAT) and inert (NPT) tracer
!              variables. If variable
horizontal diffusion is activated,
!              ad_TNU2 is the mixing
coefficient for the largest grid-cell
!              in the domain. In some
applications, a larger value than
!              that used in the nonlinear
model (basic state) is necessary
!              for stability.
!
!  ad_TNU4     Adjoint-based algorithms
lateral, biharmonic, constant, mixing
!              coefficient (m4/s) for active
(NAT) and inert (NPT) tracer
!              variables. If variable
horizontal diffusion is activated,
!              ad_TNU4 is the mixing
coefficient for the largest grid-cell
!              in the domain. In some
applications, a larger value than
!              that used in the nonlinear
model (basic state) is necessary
!              for stability.
!
!-----------------------------------------
---------------------------------
! Harmonic/biharmonic horizontal viscosity
coefficients.
```

```
!-------------------------------------------
---------------------------------
!
!  VISC2       Nonlinear model lateral,
harmonic, constant, mixing
!              coefficient (m2/s) for
momentum. If variable horizontal
!              viscosity is activated, UVNU2
is the mixing coefficient
!              for the largest grid-cell in
the domain.
!
!  VISC4       Nonlinear model lateral,
biharmonic, constant mixing
!              coefficient (m4/s) for
momentum. If variable horizontal
!              viscosity is activated, UVNU4
is the mixing coefficient
!              for the largest grid-cell in
the domain.
!
!  ad_VISC2    Adjoint-based algorithms
lateral, harmonic, constant, mixing
!              coefficient (m2/s) for
momentum. If variable horizontal
!              viscosity is activated,
ad_UVNU2 is the mixing coefficient
!              for the largest grid-cell in
the domain. In some applications,
!              a larger value than that used
in the nonlinear model (basic
!              state) is necessary for
stability.
!
!  ad_VISC4    Adjoint-based algorithms
lateral, biharmonic, constant mixing
!              coefficient (m4/s) for
momentum. If variable horizontal
!              viscosity is activated,
ad_UVNU4 is the mixing coefficient
!              for the largest grid-cell in
the domain. In some applications,
!              a larger value than that used
in the nonlinear model (basic
!              state) is necessary for
stability.
!
!-------------------------------------------
---------------------------------
! Vertical mixing coefficients for active
tracers.
!-------------------------------------------
---------------------------------
!
!  AKT_BAK     Background vertical mixing
coefficient (m2/s) for active
!              (NAT) and inert (NPT) tracer
variables.
!
!  ad_AKT_fac  Adjoint-based algorithms
vertical mixing, basic state, scale
!              factor (nondimensional) for
active (NAT) and inert (NPT)
```

```
!              tracer variables. In some
applications, a smaller/larger
!              values of vertical mixing are
necessary for stability. It
!              is only used when
FORWARD_MIXING is activated.
!
!-----------------------------------------
---------------------------------
! Vertical mixing coefficient for momentum.
!-----------------------------------------
---------------------------------
!
!  AKV_BAK     Background vertical mixing
coefficient (m2/s) for momentum.
!
!  ad_AKV_fac  Adjoint-based algorithms
vertical mixing, basic state, scale
!              factor (nondimensional) for
momentum. In some applications,
!              a smaller/larger values of
vertical mixing are necessary for
!              stability. It is only used when
FORWARD_MIXING is activated.
!
!-----------------------------------------
---------------------------------
! Turbulent closure parameters.
!-----------------------------------------
---------------------------------
!
!  AKK_BAK     Background vertical mixing
coefficient (m2/s) for turbulent
!              kinetic energy.
!
!  AKP_BAK     Background vertical mixing
coefficient (m2/s) for turbulent
!              generic statistical field,
"psi".
!
!  TKENU2      Lateral, harmonic, constant,
mixing coefficient (m2/s) for
!              turbulent closure variables.
!
!  TKENU4      Lateral, biharmonic, constant
mixing coefficient (m4/s) for
!              turbulent closure variables.
!
!-----------------------------------------
---------------------------------
! Generic length-scale turbulence closure
parameters.
!-----------------------------------------
---------------------------------
!
!  GLS_P       Stability exponent (non-
dimensional).
!
!  GLS_M       Turbulent kinetic energy
exponent (non-dimensional).
!
!  GLS_N       Turbulent length scale exponent
(non-dimensional).
```

```
!
!  GLS_Kmin    Minimum value of specific
turbulent kinetic energy
!
!  GLS_Pmin    Minimum Value of dissipation.
!
! Closure independent constraint parameters
(non-dimensional):
!
!  GLS_CMU0    Stability coefficient.
!
!  GLS_C1      Shear production coefficient.
!
!  GLS_C2      Dissipation coefficient.
!
!  GLS_C3M     Buoyancy production coefficient
(minus).
!
!  GLS_C3P     Buoyancy production coefficient
(plus).
!
!  GLS_SIGK    Constant Schmidt number (non-
dimensional) for turbulent
!              kinetic energy diffusivity.
!
!  GLS_SIGP    Constant Schmidt number (non-
dimensional) for turbulent
!              generic statistical field,
"psi".
!
! Suggested values for various
parameterizations:
!
!               k-kl          k-epsilon    k-
omega      gen
!
!      GLS_P = 0.d0           3.0d0
1.0d0         2.0d0
!      GLS_M = 1.d0           1.5d0
0.5d0         1.0d0
!      GLS_N = 1.d0          -1.0d0
1.0d0        -0.67d0
!   GLS_Kmin = 5.0d-6         7.6d-6
7.6d-6        1.0d-8
!   GLS_Pmin = 5.0d-6         1.0d-12
1.0d-12       1.0d-8
!
!   GLS_CMU0 = 0.5544d0       0.5477d0
0.5477d0      0.5544d0
!     GLS_C1 = 0.9d0          1.44d0
0.555d0       1.00d0
!     GLS_C2 = 0.52d0         1.92d0
0.833d0       1.22d0
!    GLS_C3M = 2.5d0         -0.4d0
0.6d0         0.1d0
!    GLS_C3P = 1.0d0          1.0d0
1.0d0         1.0d0
!   GLS_SIGK = 1.96d0         1.0d0
2.0d0         0.8d0
!   GLS_SIGP = 1.96d0         1.30d0
2.0d0         1.07d0
!
!-----------------------------------------
--------------------------------
```

```
! Constants used in the various formulations
of surface turbulent kinetic
! energy flux in the GLS.
!-----------------------------------------
---------------------------------
!
!  CHARNOK_ALPHA   Charnok surface roughness,
!                    Zos:   (charnok_alpha *
u_star**2) / g
!
!  ZOS_HSIG_ALPHA  Roughness from wave
amplitude,
!                    Zos:   zos_hsig_alpha *
Hsig
!
!  SZ_ALPHA        Surface flux from wave
dissipation,
!                    flux:  dt * sz_alpha *
Wave_dissip
!
!  CRGBAN_CW       Surface flux due to Craig
and Banner wave breaking,
!                    flux:  dt * crgban_cw *
u_star**3
!
!-----------------------------------------
---------------------------------
! Constants used in the computation of
momentum stress.
!-----------------------------------------
---------------------------------
!
!  RDRG        Linear bottom drag coefficient
(m/s).
!
!  RDRG2       Quadratic bottom drag
coefficient.
!
!  Zob         Bottom roughness (m).
!
!  Zos         Surface roughness (m).
!
!-----------------------------------------
---------------------------------
! Height of atmospheric measurements for bulk
fluxes parameterization.
!-----------------------------------------
---------------------------------
!
!  BLK_ZQ      Height (m) of surface air
humidity measurement. Usually,
!                recorded at 10 m.
!
!  BLK_ZT      Height (m) of surface air
temperature measurement. Usually,
!                recorded at 2 or 10 m.
!
!  BLK_ZW      Height (m) of surface winds
measurement. Usually, recorded
!                at 10 m.
!
!-----------------------------------------
---------------------------------
! Wetting and drying parameters.
```

```
!-----------------------------------------
--------------------------------
!
!  DCRIT       Minimum depth (m) for wetting
and drying.
!
!-----------------------------------------
--------------------------------
! Jerlow Water type.
!-----------------------------------------
--------------------------------
!
!  WTYPE       Jerlov water type: an integer
value from 1 to 5.
!
!-----------------------------------------
--------------------------------
! Body-force parameters. Used when CPP option
BODYFORCE is activated.
!-----------------------------------------
--------------------------------
!
!  LEVSFRC     Deepest level to apply surface
momentum stress as a body-force.
!
!  LEVBFRC     Shallowest level to apply
bottom momentum stress as a body-force.
!
!-----------------------------------------
--------------------------------
! Vertical S-coordinates parameters.
!-----------------------------------------
--------------------------------
!
! The parameters below must be consistent in
all input fields associated with
! the vertical grid.  The same vertical grid
transformation (depths) needs to
! be used when preparing initial conditions,
boundary conditions, climatology,
! observations, and so on. Please check:
!
!
https://www.myroms.org/wiki/index.php/Vertical
_S-coordinate
!
! for details, rules and examples.
!
!
!  Vtransform  Vertical transformation
equation:
!
!                (1) Original formulation
(Shchepetkin and McWilliams, 2005),
!                    Vtransform=1 (In ROMS
since 1999)
!
!
z(x,y,s,t)=Zo(x,y,s)+zeta(x,y,t)*[1+Zo(x,y,s)/
h(x,y)]
!
!                    where
!
```

```
!                       Zo(x,y,s)=hc*s+[h(x,y)-
hc]*C(s)
!
!                  (2) Improved formulation (A.
Shchepetkin, 2005),
!                      Vtransform=2
!
!
z(x,y,s,t)=zeta(x,y,t)*[zeta(x,y,t)+h(x,y)]*Zo
(x,y,s)
!
!                      where
!
!
Zo(x,y,s)=[hc*s(k)+h(x,y)*C(k)]/[hc+h(x,y)]
!
!                      The true sigma-coordinate
system is recovered as hc goes
!                      to INFINITY. This is
useful when configuring applications
!                      with flat bathymetry and
uniform level thickness.
!                      Practically, you can
achieve this by setting:
!
!                        THETA_S = 0.0d0
!                        THETA_B = 0.0d0
!                        TCLINE  = 1.0d+17
(a large number)
!
!
```

```
!  Vstretching Vertical stretching function,
C(s):
!
!                  (1) Original function (Song
and Haidvogel, 1994),
!                      Vstretching=1
!
!                      C(s)=(1-
theta_b)*[SINH(s*theta_s)/SINH(theta_s)]+
!                           theta_b*[-
0.5+0.5*TANH(theta_s*(s+0.5))/
!
TANH(0.5*theta_s)]
!
!                  (2) A. Shchepetkin (2005)
function,
!                      Vstretching=2
!
!
C(s)=Cweight*Csur(s)+(1-Cweight)*Cbot(s)
!
!                      where
!
!                        Csur(s)=[1-
COSH(theta_s*s)]/[COSH(theta_s)-1]
!
!                        Cbot(s)=-1+[1-
SINH(theta_b*(s+1))]/SINH(theta_b)
!
!                        Cweight=(s+1)**alpha*
!
(1+(alpha/beta)*(1-(s+1)**beta))
```

```
!
!                 (3) R. Geyer function for
shallow sediment applications,
!                     Vstretching=3
!
!
C(s)=Cweight*Cbot(s)+(1-Cweight)*Csur(s)
!
!                     where
!
!                       Csur(s)=-
LOG(COSH(Hscale*ABS(s)** alpha))/
!
LOG(COSH(Hscale))
!
!                       Cbot(s)=
LOG(COSH(Hscale*(s+1)** beta))/
!
LOG(COSH(Hscale))-1
!
!                       Cweight=0.5*(1-
TANH(Hscale*(s+0.5))
!
!                 (4) A. Shchepetkin (2010)
improved double stretching function,
!                     Vstretching=4
!
!                       C(s)=[1-
COSH(theta_s*s)]/[COSH(theta_s)-1]
!
!                     with bottom refinement
!
!
C(s)=[EXP(theta_b*C(s))-1]/[1-EXP(-theta_b)]
!
!                     The resulting double
transformation is continuous with
!                     respect control
parameters theta_s and theta_b with a
!                     meaningful range of:
!
!                       0 <  theta_s <= 10.0
!                       0 <= theta_b <=  4.0
!
!               Many other stretching functions
(Vstretching>4) are possible
!               provided that:
!
!                 * C(s) is a dimensionless,
nonlinear, monotonic function.
!                 * C(s) is a continuous
differentiable function, or
!                   a differentiable piecewise
function with smooth transition.
!                 * The stretching vertical
coordinate ,s, is constrained
!                   between -1 <= s <= 0, with
s=0 corresponding to the
!                   free-surface and s=-1
corresponding to the bathymetry.
!                 * Similarly, the stretching
function, C(s), is constrained
!                   between -1 <= C(s) <= 0,
with C(0)=0 corresponding to the
```

```
!                  free-surface and C(-1)=-1
corresponding to the bathymetry.
!
!               These functions are coded in
routine "Utility/set_scoord.F".
!
! Due to its functionality and properties, the
default and recommended vertical
! coordinates transformation is:
!
!               Vtransform  = 2
!               Vstretching = 4
!
!
!  THETA_S      S-coordinate surface control
parameter. The range of optimal
!               values depends on the vertical
stretching function, C(s).
!
!  THETA_B      S-coordinate bottom  control
parameter. The range of optimal
!               values depends on the vertical
stretching function, C(s).
!
!  TCLINE       Critical depth (hc) in meters
(positive) controlling the
!               stretching. It can be
interpreted as the width of surface or
!               bottom boundary layer in which
higher vertical resolution
!               (levels) is required during
stretching.
!
!-----------------------------------------------
--------------------------------
! Mean Density and background Brunt-Vaisala
frequency.
!-----------------------------------------------
--------------------------------
!
!  RHO0         Mean density (Kg/m3) used when
the Boussinesq approximation
!               is inferred.
!
!  BVF_BAK      Background Brunt-Vaisala
frequency squared (1/s2). Typical
!               values for the ocean range (as
a function of depth) from
!               1.0E-4 to 1.0E-6.
!
!-----------------------------------------------
--------------------------------
! Time Stamps.
!-----------------------------------------------
--------------------------------
!
!  DSTART       Time stamp assigned to model
initialization (days).  Usually
!               a Calendar linear coordinate,
like modified Julian Day.  For
!               Example:
!
!                       Julian Day = 1  for
Nov 25, 0:0:0 4713 BCE
```

```
!               modified Julian Day = 1  for
May 24, 0:0:0 1968  CE GMT
!
!               It is called truncated or
modified Julian day because an offset
!               of 2440000 needs to be added.
!
!  TIDE_START   Reference time origin for tidal
forcing (days). This is the
!               time used when processing input
tidal model data. It is needed
!               in routine "set_tides" to
compute the correct phase lag with
!               respect ROMS/TOMS
initialization time.
!
!  TIME_REF     Reference time (yyyymmdd.f)
used to compute relative time:
!               elapsed time interval since
reference-time.  The "units"
!               attribute takes the form "time-
unit since reference-time".
!               This parameter also provides
information about the calendar
!               used:
!
!               If TIME_REF = -2, model time
and DSTART are in modified Julian
!               days units.  The "units"
attribute is:
!
!                       'time-units since 1968-
05-23 00:00:00 GMT'
!
!               If TIME_REF = -1, model time
and DSTART are in a calendar
!               with 360 days in every year (30
days each month).  The "units"
!               attribute is:
!
!                       'time-units since 0001-
01-01 00:00:00'
!
!               If TIME_REF = 0, model time and
DSTART are in a common year
!               calendar with 365.25 days.  The
"units" attribute is:
!
!                       'time-units since 0001-
01-01 00:00:00'
!
!               If TIME_REF > 0, model time and
DSTART are the elapsed time
!               units since specified reference
time.  For example,
!               TIME_REF=20020115.5 will yield
the following attribute:
!
!                       'time-units since 2002-
01-15 12:00:00'
!
!-----------------------------------------
--------------------------------
```

```
! Nudging/relaxation time scales, inverse
scales will be computed internally.
!-------------------------------------------
--------------------------------
!
! When passive/active open boundary conditions
are activated, these nudging
! values correspond to the passive (outflow)
nudging time scales.
!
!  TNUDG       Nudging time scale (days) for
active tracer variables.
!              (1:NAT+NPT,1:Ngrids) values are
expected.
!
!  ZNUDG       Nudging time scale (days) for
free-surface.
!
!  M2NUDG      Nudging time scale (days) for
2D momentum.
!
!  M3NUDG      Nudging time scale (days) for
3D momentum.
!
!  OBCFAC      Factor between passive
(outflow) and active (inflow) open
!              boundary conditions.  The
nudging time scales for the
!              active (inflow) conditions are
obtained by multiplying
!              the passive values by OBCFAC.
If OBCFAC > 1, nudging on
!              inflow is stronger than on
outflow (recommended).
!
!-------------------------------------------
--------------------------------
! Linear equation of State parameters.
!-------------------------------------------
--------------------------------
!
! Ignoring pressure, the linear equation of
state is:
!
!              rho(:,:,:) = R0 - R0 * TCOEF *
(t(:,:,:,:,itemp) - T0)
!                                   + R0 * SCOEF *
(t(:,:,:,:,isalt) - S0)
!
!              Typical values:     R0 = 1027.0
kg/m3
!                                  T0 = 10.0
Celsius
!                                  S0 = 35.0
PSU
!                                TCOEF = 1.7d-4
1/Celsius
!                                SCOEF = 7.6d-4
1/PSU
!
!  R0          Background density value
(Kg/m3) used in Linear Equation of
!              State.
!
```

```
!  T0          Background potential
temperature (Celsius) constant.
!
!  S0          Background salinity (PSU)
constant.
!
!  TCOEF       Thermal expansion coefficient
in Linear Equation of State.
!
!  SCOEF       Saline contraction coefficient
in Linear Equation of State.
!
!-----------------------------------------
--------------------------------
! Slipperiness parameter.
!-----------------------------------------
--------------------------------
!
!  GAMMA2      Slipperiness variable, either
1.0 (free slip) or -1.0 (no slip).
!
!-----------------------------------------
--------------------------------
!  Tracer point Sources/Sink sources switches.
!-----------------------------------------
--------------------------------
!
!  LtracerSrc  Logical switches (T/F) to
specify which tracer variables
!              to consider when the option
TS_PSOURCE is activated. Only
!              NAT active tracers
(temperature, salinity) and NPT inert
!              tracers need to be specified
here:
!
!                LtracerSrc(itemp,ng)     for
temperature (itemp=1)
!                LtracerSrc(isalt,ng)     for
salinity    (isalt=2)
!                LtracerSrc(NAT+1,ng)     for
inert tracer 1
!                ...                      ...
!                LtracerSrc(NAT+NPT,ng)   for
inert tracer NPT
!
!              Other biological and sediment
tracers switches are specified in
!              their respective input scripts.
!
!              Recall that TS_PSOURCE is
usually activated to add river runoff
!              as a point source. At minimum,
it is necessary to specify both
!              temperature and salinity for
all rivers.  The other tracers are
!              optional.
!
!              This logical switch REPLACES
and ELIMINATES the need to have
!              or read the variable
"river_flag(river)" in the input rivers
!              forcing NetCDF file:
```

```
!
!                 double river_flag(river)
!                        river_flag:long_name
= "river runoff tracer flag"
!                        river_flag:option_0 =
"all tracers are off"
!                        river_flag:option_1 =
"only temperature"
!                        river_flag:option_2 =
"only salinity"
!                        river_flag:option_3 =
"both temperature and salinity"
!                        river_flag:units =
"nondimensional"
!
!              This logic was too cumbersome
and complicated when additional
!              tracers are considered.
However, this change is backward
!              compatible.
!
!              The LtracerSrc switch will be
used to activate the reading of
!              respective tracer variable from
input river forcing NetCDF
!              file. If you want to add other
tracer variables (other than
!              temperature and salinity) as a
source for a particular river(s),
!              you just need to specify such
values on those river(s). Then,
!              set the values to ZERO on the
other river(s) that do NOT
!              require such river forcing for
that tracer. Recall that you
!              need to specify the tracer
values for all rivers, even if
!              their values are zero.
!
!-----------------------------------------
--------------------------------
!  Adjoint sensitivity parameters.
!-----------------------------------------
--------------------------------
!
!  DstrS       Starting day for adjoint
sensitivity forcing.
!
!  DendS       Ending   day for adjoint
sensitivity forcing.
!
!              The adjoint forcing is applied
at every time step according to
!              desired state functional stored
in the adjoint sensitivity
!              NetCDF file. DstrS must be less
than or equal to DendS. If both
!              values are zero, their values
are reset internally to the full
!              range of the adjoint
integration.
!
```

```
!  KstrS       Starting vertical level of the
3D adjoint state variables whose
!                sensitivity is required.
!  KendS       Ending   vertical level of the
3D adjoint state variables whose
!                sensitivity is required.
!
!  Lstate      Logical switches (TRUE/FALSE)
to specify the adjoint state
!                variables whose sensitivity
is required.
!
!                Lstate(isFsur):   Free-
surface
!                Lstate(isUbar):   2D U-
momentum
!                Lstate(isVbar):   2D V-
momentum
!                Lstate(isUvel):   3D U-
momentum
!                Lstate(isVvel):   3D V-
momentum
!                Lstate(isTvar):   Traces (NT
values expected)
!
!-----------------------------------------
--------------------------------
!  Forcing Singular Vectors or Stochastic
Optimals parameters.
!-----------------------------------------
--------------------------------
!
!  Fstate      Logical switches (TRUE/FALSE)
to specify state variables for
!                which Forcing Singular
Vectors or Stochastic Optimals is
!                required.
!
!                Fstate(isFsur):   Free-
surface
!                Fstate(isUbar):   2D U-
momentum
!                Fstate(isVbar):   2D V-
momentum
!                Fstate(isUvel):   3D U-
momentum
!                Fstate(isVvel):   3D V-
momentum
!                Fstate(isTvar):   Traces (NT
values expected)
!
!                Fstate(isUstr):   surface U-
stress
!                Fstate(isVstr):   surface V-
stress
!                Fstate(isTsur):   surface
tracers flux (NT values expected)
!
!  SO_decay    Stochastic Optimals time
decorrelation scale (days) assumed
!                for red noise processes.
!
!  SO_sdev     Stochastic Optimals surface
forcing standard deviation for
```

```
!                dimensionalization.
!
!                SO_sdev(isFsur):  Free-
surface
!                SO_sdev(isUbar):  2D U-
momentum
!                SO_sdev(isVbar):  2D V-
momentum
!                SO_sdev(isUvel):  3D U-
momentum
!                SO_sdev(isVvel):  3D V-
momentum
!                SO_sdev(isTvar):  Traces (NT
values expected)
!
!                SO_sdev(isUstr):  surface U-
stress
!                SO_sdev(isVstr):  surface V-
stress
!                SO_sdev(isTsur):  surface
tracer flux (NT values expected)
!
!-----------------------------------------
--------------------------------
! Logical switches (T/F) to activate writing
of instantaneous fields into
! HISTORY file.
!-----------------------------------------
--------------------------------
!
!  Hout(idUvel)  Write out 3D U-velocity
component.
!  Hout(idVvel)  Write out 3D V-velocity
component.
!  Hout(idu3dE)  Write out 3D Eastward
velocity component at RHO-points.
!  Hout(idv3dN)  Write out 3D Northward
velocity component at RHO-points.
!  Hout(idWvel)  Write out 3D W-velocity
component.
!  Hout(idOvel)  Write out 3D omega vertical
velocity.
!  Hout(idUbar)  Write out 2D U-velocity
component.
!  Hout(idVbar)  Write out 2D V-velocity
component.
!  Hout(idu2dE)  Write out 2D Eastward
velocity component at RHO-points.
!  Hout(idv2dN)  Write out 2D Northward
velocity component at RHO-points.
!  Hout(idFsur)  Write out free-surface.
!  Hout(idBath)  Write out time-dependent
bathymetry.
!
!  Hout(idTvar)  Write out active (NAT)
tracers: temperature and salinity.
!
!  Hout(idUsms)  Write out surface U-momentum
stress.
!  Hout(idVsms)  Write out surface V-momentum
stress.
!  Hout(idUbms)  Write out bottom  U-momentum
stress.
```

```
!  Hout(idVbms)  Write out bottom  V-momentum
stress.
!
!  Hout(idUbrs)  Write out current-induced, U-
momentum stress.
!  Hout(idVbrs)  Write out current-induced, V-
momentum stress.
!  Hout(idUbws)  Write out wind-induced,
bottom U-wave stress.
!  Hout(idVbws)  Write out wind-induced,
bottom V-wave stress.
!  Hout(idUbcs)  Write out bottom maximum wave
and current U-stress.
!  Hout(idVbcs)  Write out bottom maximum wave
and current V-stress.
!
!  Hout(idUbot)  Write out wind-induced, bed
wave orbital U-velocity.
!  Hout(idVbot)  Write out wind-induced, bed
wave orbital V-velocity.
!  Hout(idUbur)  Write out bottom U-velocity
above bed.
!  Hout(idVbvr)  Write out bottom V-velocity
above bed.
!
!  Hout(idW2xx)  Write out 2D radiation
stress, Sxx component.
!  Hout(idW2xy)  Write out 2D radiation
stress, Sxy component.
!  Hout(idW2yy)  Write out 2D radiation
stress, Syy component.
!  Hout(idU2rs)  Write out 2D U-radiation
stress.
!  Hout(idV2rs)  Write out 2D V-radiation
stress.
!  Hout(idU2Sd)  Write out 2D U-Stokes
velocity.
!  Hout(idV2Sd)  Write out 2D V-Stokes
velocity.
!
!  Hout(idW3xx)  Write out 3D radiation
stress, Sxx component.
!  Hout(idW3xy)  Write out 3D radiation
stress, Sxy component.
!  Hout(idW3yy)  Write out 3D radiation
stress, Syy component.
!  Hout(idW3zx)  Write out 3D radiation
stress, Szx component.
!  Hout(idW3zy)  Write out 3D radiation
stress, Szy component.
!  Hout(idU3rs)  Write out 3D U-radiation
stress.
!  Hout(idV3rs)  Write out 3D V-radiation
stress.
!  Hout(idU3Sd)  Write out 3D U-Stokes
velocity.
!  Hout(idV3Sd)  Write out 3D V-Stokes
velocity.
!
!  Hout(idWamp)  Write out wave height.
!  Hout(idWlen)  Write out wave length.
!  Hout(idWdir)  Write out wave direction.
```

```
!  Hout(idWptp)  Write out wave surface
period.
!  Hout(idWpbt)  Write out wave bottom period.
!  Hout(idWorb)  Write out wave bottom orbital
velocity.
!  Hout(idWdis)  Write out wave dissipation.
!
!  Hout(idPair)  Write out surface air
pressure.
!  Hout(idUair)  Write out surface U-wind
component.
!  Hout(idVair)  Write out surface V-wind
component.
!
!  Hout(idTsur)  Write out surface net heat
and salt flux
!  Hout(idLhea)  Write out latent heat flux.
!  Hout(idShea)  Write out sensible heat flux.
!  Hout(idLrad)  Write out long-wave radiation
flux.
!  Hout(idSrad)  Write out short-wave
radiation flux.
!  Hout(idEmPf)  Write out E-P flux.
!  Hout(idevap)  Write out evaporation rate.
!  Hout(idrain)  Write out precipitation rate.
!
!  Hout(idDano)  Write out density anomaly.
!  Hout(idVvis)  Write out vertical viscosity
coefficient.
!  Hout(idTdif)  Write out vertical diffusion
coefficient of temperature.
!  Hout(idSdif)  Write out vertical diffusion
coefficient of salinity.
!  Hout(idHsbl)  Write out depth of oceanic
surface boundary layer.
!  Hout(idHbbl)  Write out depth of oceanic
bottom boundary layer.
!  Hout(idMtke)  Write out turbulent kinetic
energy.
!  Hout(idMtls)  Write out turbulent kinetic
energy times length scale.
!
!  Hout(inert)   Write out extra inert passive
tracers.
!
!  Hout(idBott)  Write out exposed sediment
layer properties, 1:MBOTP.
!
!-------------------------------------------
--------------------------------
! Logical switches (T/F) to activate writing
of time-averaged fields into
! AVERAGE file.
!-------------------------------------------
--------------------------------
!
!  Aout(idUvel)  Write out 3D U-velocity
component.
!  Aout(idVvel)  Write out 3D V-velocity
component.
!  Aout(idu3dE)  Write out 3D Eastward
velocity component at RHO-points.
```

```
!  Aout(idv3dN)  Write out 3D Northward
velocity component at RHO-points.
!  Aout(idWvel)  Write out 3D W-velocity
component.
!  Aout(idOvel)  Write out 3D omega vertical
velocity.
!  Aout(idUbar)  Write out 2D U-velocity
component.
!  Aout(idVbar)  Write out 2D V-velocity
component.
!  Aout(idu2dE)  Write out 2D Eastward
velocity component at RHO-points.
!  Aout(idv2dN)  Write out 2D Northward
velocity component at RHO-points.
!  Aout(idFsur)  Write out free-surface.
!
!  Aout(idTvar)  Write out active (NAT)
tracers: temperature and salinity.
!
!  Aout(idUsms)  Write out surface U-momentum
stress.
!  Aout(idVsms)  Write out surface V-momentum
stress.
!  Aout(idUbms)  Write out bottom  U-momentum
stress.
!  Aout(idVbms)  Write out bottom  V-momentum
stress.
!
!  Aout(idW2xx)  Write out 2D radiation
stress, Sxx component.
!  Aout(idW2xy)  Write out 2D radiation
stress, Sxy component.
!  Aout(idW2yy)  Write out 2D radiation
stress, Syy component.
!  Aout(idU2rs)  Write out 2D U-radiation
stress.
!  Aout(idV2rs)  Write out 2D V-radiation
stress.
!  Aout(idU2Sd)  Write out 2D U-Stokes
velocity.
!  Aout(idV2Sd)  Write out 2D V-Stokes
velocity.
!
!  Aout(idW3xx)  Write out 3D radiation
stress, Sxx component.
!  Aout(idW3xy)  Write out 3D radiation
stress, Sxy component.
!  Aout(idW3yy)  Write out 3D radiation
stress, Syy component.
!  Aout(idW3zx)  Write out 3D radiation
stress, Szx component.
!  Aout(idW3zy)  Write out 3D radiation
stress, Szy component.
!  Aout(idU3rs)  Write out 3D U-radiation
stress.
!  Aout(idV3rs)  Write out 3D V-radiation
stress.
!  Aout(idU3Sd)  Write out 3D U-Stokes
velocity.
!  Aout(idV3Sd)  Write out 3D V-Stokes
velocity.
!
!  Aout(idPair)  Write out surface air
pressure.
```

```
!  Aout(idUair)  Write out surface U-wind
component.
!  Aout(idVair)  Write out surface V-wind
component.
!
!  Aout(idTsur)  Write out surface net heat
and salt flux
!  Aout(idLhea)  Write out latent heat flux.
!  Aout(idShea)  Write out sensible heat flux.
!  Aout(idLrad)  Write out long-wave radiation
flux.
!  Aout(idSrad)  Write out short-wave
radiation flux.
!  Aout(idevap)  Write out evaporation rate.
!  Aout(idrain)  Write out precipitation rate.
!
!  Aout(idDano)  Write out density anomaly.
!  Aout(idVvis)  Write out vertical viscosity
coefficient.
!  Aout(idTdif)  Write out vertical diffusion
coefficient of temperature.
!  Aout(idSdif)  Write out vertical diffusion
coefficient of salinity.
!  Aout(idHsbl)  Write out depth of oceanic
surface boundary layer.
!  Aout(idHbbl)  Write out depth of oceanic
bottom boundary layer.
!
!  Aout(id2dRV)  Write out 2D relative
vorticity (vertically integrated).
!  Aout(id3dRV)  Write out 3D relative
vorticity.
!  Aout(id2dPV)  Write out 2D potential
vorticity (shallow water).
!  Aout(id3dPV)  Write out 3D potential
vorticity.
!
!  Aout(idu3dD)  Write out detided 3D U-
velocity.
!  Aout(idv3dD)  Write out detided 3D V-
velocity.
!  Aout(idu2dD)  Write out detided 2D U-
velocity.
!  Aout(idv2dD)  Write out detided 2D V-
velocity.
!  Aout(idFsuD)  Write out detided free-
surface
!
!  Aout(idTrcD)  Write out detided temperature
and salinity.
!
!  Aout(idHUav)  Write out u-volume flux,
Huon.
!  Aout(idHVav)  Write out v-volume flux,
Hvom.
!  Aout(idUUav)  Write out quadratic <u*u>
term.
!  Aout(idUVav)  Write out quadratic <u*v>
term.
!  Aout(idVVav)  Write out quadratic <v*v>
term.
!  Aout(idU2av)  Write out quadratic
<ubar*ubar> term.
```

```
!  Aout(idV2av)  Write out quadratic
<vbar*vbar> term.
!  Aout(idZZav)  Write out quadratic
<zeta*zeta> term.
!
!  Aout(idTTav)  Write out quadratic <t*t>
temperature and salinity terms.
!  Aout(idUTav)  Write out quadratic <u*t>
temperature and salinity terms.
!  Aout(idVTav)  Write out quadratic <v*t>
temperature and salinity terms.
!  Aout(iHUTav)  Write out temperature and
salinity volume flux, <Huon*t>.
!  Aout(iHVTav)  Write out temperature and
salinity volume flux, <Hvom*t>.
!
!  Aout(inert)   Write out extra inert passive
tracers.
!
!-------------------------------------------
--------------------------------
! Logical switches (T/F) to activate writing
of time-averaged fields into
! DIAGNOSTIC file.
!-------------------------------------------
--------------------------------
!
! Time-averaged, 2D momentum (ubar,vbar)
diagnostic terms:
! (if DIAGNOSTICS_UV)
!
! Dout(M2rate)   Write out acceleration.
! Dout(M2pgrd)   Write out pressure gradient.
! Dout(M2fcor)   Write out Coriolis force, if
UV_COR.
! Dout(M2hadv)   Write out horizontal total
advection, if UV_ADV.
! Dout(M2xadv)   Write out horizontal  XI-
advection, if UV_ADV.
! Dout(M2yadv)   Write out horizontal ETA-
advection, if UV_ADV.
! Dout(M2hrad)   Write out horizontal total
radiation stress, NEARSHORE_MELLOR.
! Dout(M2hvis)   Write out horizontal total
viscosity, if UV_VIS2 or UV_VIS4.
! Dout(M2xvis)   Write out horizontal  XI-
viscosity, if UV_VIS2 or UV_VIS4.
! Dout(M2yvis)   Write out horizontal ETA-
viscosity, if UV_VIS2 or UV_VIS4.
! Dout(M2sstr)   Write out surface stress.
! Dout(M2bstr)   Write out bottom stress
!
! Time-averaged, 3D momentum (u,v) diagnostic
terms:
! (if SOLVE3D and DIAGNOSTICS_UV)
!
! Dout(M3rate)   Write out acceleration.
! Dout(M3pgrd)   Write out pressure gradient.
! Dout(M3fcor)   Write out Coriolis force, if
UV_COR.
! Dout(M3hadv)   Write out horizontal total
advection, if UV_ADV.
! Dout(M3xadv)   Write out horizontal  XI-
advection, if UV_ADV.
```

```
! Dout(M3yadv)   Write out horizontal ETA-
advection, if UV_ADV.
! Dout(M3hrad)   Write out horizontal total
radiation stress, NEARSHORE_MELLOR.
! Dout(M3vrad)   Write out vertical radiation
stress, if NEARSHORE_MELLOR.
! Dout(M3hvis)   Write out horizontal total
viscosity, if UV_VIS2 or UV_VIS4.
! Dout(M3xvis)   Write out horizontal  XI-
viscosity, if UV_VIS2 or UV_VIS4.
! Dout(M3yvis)   Write out horizontal ETA-
viscosity, if UV_VIS2 or UV_VIS4.
! Dout(M3yvis)   Write out horizontal ETA-
viscosity, if UV_VIS2 or UV_VIS4.
! Dout(M3vvis)   Write out vertical viscosity.
!
! Time-averaged, active (temperature and
salinity) and passive (inert) tracer
! diagnostic terms, [1:NAT+NPT,Ngrids] values
expected:
! (if SOLVE3D and DIAGNOSTICS_TS)
!
! Dout(iTrate)   Write out time rate of
change.
! Dout(iThadv)   Write out horizontal total
advection.
! Dout(iTxadv)   Write out horizontal  XI-
advection.
! Dout(iTyadv)   Write out horizontal ETA-
advection.
! Dout(iTvadv)   Write out vertical advection.
! Dout(iThdif)   Write out horizontal total
diffusion, if TS_DIF2 or TS_DIF4.
! Dout(iTxdif)   Write out horizontal  XI-
diffusion, if TS_DIF2 or TS_DIF4.
! Dout(iTydif)   Write out horizontal ETA-
diffusion, if TS_DIF2 or TS_DIF4.
! Dout(iTsdif)   Write out horizontal   S-
diffusion, if TS_DIF2 or TS_DIF4 and
!                  rotated tensor (MIX_GEO_TS
or MIX_ISO_TS).
! Dout(iTvdif)   Write out vertical diffusion.
!
!-----------------------------------------
--------------------------------
! Generic User parameters.
!-----------------------------------------
--------------------------------
!
!  NUSER       Number of User parameters to
consider (integer).
!  USER        Vector containing user
parameters (real array). This array
!                is used with the SANITY_CHECK
to test the correctness of
!                the tangent linear adjoint
models.  It contains information
!                of the model variable and
grid point to perturb:
!
!                INT(user(1)):  tangent state
variable to perturb
```

```
!                INT(user(2)):  adjoint state
variable to perturb
!                               [isFsur=1]
free-surface
!                               [isUbar=2] 2D
U-momentum
!                               [isVbar=3] 2D
V-momentum
!                               [isUvel=4] 3D
U-momentum
!                               [isVvel=5] 3D
V-momentum
!                               [isTvar=6]
First tracer (temperature)
!                               [   ...  ]
!                               [isTvar=?]
Last tracer
!
!                INT(user(3)):  I-index of
tangent variable to perturb
!                INT(user(4)):  I-index of
adjoint variable to perturb
!                INT(user(5)):  J-index of
tangent variable to perturb
!                INT(user(6)):  J-index of
adjoint variable to perturb
!                INT(user(7)):  K-index of
tangent variable to perturb, if 3D
!                INT(user(8)):  K-index of
adjoint variable to perturb, if 3D
!
```

```
!                Set tangent and adjoint
parameters to the same values
!                if perturbing and reporting
the same variable.
!
!-----------------------------------------
---------------------------------
! I/O NetCDF files parameters.
!-----------------------------------------
---------------------------------
!
! NetCDF-4/HDF5 compression parameters for
output files. This capability
! is used when both HDF5 and DEFLATE C-
preprocessing options are
! activated. The user needs to compile with
the NetCDF-4/HDF5 and MPI
! libraries. File deflation cannot be used in
parallel I/O for writing
! because the compression makes it impossible
for the HDF5 library
! to exactly map the data to the disk
location.  For more information,
! check NetCDF official website:
www.unidata.ucar.edu/software/netcdf.
!
! NC_SHUFFLE    Shuffle filter integer flag.
If non-zero, turn on shuffle
!                 filter.
!
! NC_DEFLATE    Deflate filter integer flag,
If non-zero, turn on deflate
```

```
!                 filter at the level
specified by the NC_DLEVEL parameter.
!
! NC_DLEVEL     Deflate filter level parameter
(integer). If NC_DEFLATE is
!                 non-zero, set the deflate
level to this value. Must be
!                 between 0 and 9.
!
!-----------------------------------------
--------------------------------
! Input/output NetCDF file names (string with
a maximum of 256 characters).
!-----------------------------------------
--------------------------------
!
! Input file names:
!
!  GRDNAME     Input grid file name.
!
!  ININAME     Input nonlinear initial
conditions file name. It can be a
!               re-start file.
!  ITLNAME     Input tangent linear model
initial conditions file name.
!  IRPNAME     Input representer model initial
conditions file name.
!  IADNAME     Input adjoint model initial
conditions file name.
!
!  FWDNAME     Input forward solution fields
file name.
!  ADSNAME     Input adjoint sensitivity
functional file name.
!
! Input lateral boundary conditions and
climatology file names:
!
!  BRYNAME     Input open boundary data file
name(s) per nested grid.
!  CLMNAME     Input climatology fields file
name(s) per nested grid
!
!  The USER has the option to split input data
time records into several
!  NetCDF files, as many as required. If so,
use a single line per entry
!  with a vertical bar (|) symbol after each
entry, except the last one:
!
!    BRYNAME == my_bry_year1.nc |
!               my_bry_year2.nc
!
!    CLMNAME == my_clm_year1.nc |
!               my_clm_year2.nc
!
! Input forcing file(s) name:
!
!  NFFILES     Number of unique forcing files
per nested grid.
!  FRCNAME     Input forcing fields file name
per nested grid.
!
```

```
!  The USER has the option to enter several
file names for forcing fields
!  and/or split input data time records for
each nested grid. For example,
!  the USER may have different files for wind
products, heat fluxes, rivers,
!  tides, etc.  The model will scan the file
list and will read the needed
!  data from the first file in the list
containing the forcing field.
!  Therefore, the order of the file names is
very important. It is also
!  possible to split input data time records
into several NetCDF files.
!
!  Use a single line per entry with a
continuation (\) or vertical bar (|)
!  symbol after each entry, except the last
one:
!
!    NFFILES == 8
number of unique forcing files
!
!    FRCNAME == my_rivers.nc      \        !
river forcing
!               my_tides.nc       \        !
tidal forcing
!               my_lwrad_year1.nc |        !
net longwave radiation flux
!               my_lwrad_year2.nc \
!               my_swrad_year1.nc |
solar shortwave radiation flux
!               my_swrad_year2.nc \
!               my_winds_year1.nc |
surface winds
!               my_winds_year2.nc \
!               my_Pair_year1.nc  |
surface air pressure
!               my_Pair_year2.nc  \
!               my_Qair_year1.nc  |
surface air relative humidity
!               my_Qair_year2.nc  \
!               my_Tair_year1.nc  |
surface air temperature
!               my_Tair_year2.nc
!
! Output file names:
!
!  GSTNAME     Output GST analysis re-start
file name.
!  RSTNAME     Output re-start file name.
!  HISNAME     Output history file name.
!  TLFNAME     Output impulse forcing for
tangent linear (TLM and RPM) models.
!  TLMNAME     Output tangent linear file
name.
!  ADJNAME     Output adjoint file name.
!  AVGNAME     Output averages file name.
!  DIANAME     Output diagnostics file name.
!  STANAME     Output stations file name.
!  FLTNAME     Output floats file name.
!
!-----------------------------------------
--------------------------------
```

```
! Input ASCII parameters file names.
!-----------------------------------------
---------------------------------
!
!  APARNAM     Input assimilation parameters
file name.
!  SPOSNAM     Input stations positions file
name.
!  FPOSNAM     Input initial drifters
positions file name.
!  BPARNAM     Input biological parameters
file name.
!  SPARNAM     Input sediment transport
parameters file name.
!  USRNAME     USER's input generic file name.
!
```

sediment_waipaoa.in

```
!
!  ROMS/TOMS Cohesive and Non-cohesive
Sediment Model Parameters.
!
!svn $Id: sediment_sed_toy.in 2232 2012-01-03
18:55:20Z arango $
!=============================================
============ Hernan G. Arango ===
!  Copyright (c) 2002-2012 The ROMS/TOMS Group
!
!    Licensed under a MIT/X style license
!
!    See License_ROMS.txt
!
!=============================================
================================
!
!
! Input parameters can be entered in ANY
order, provided that the parameter   !
! KEYWORD (usually, upper case) is typed
correctly followed by "="  or "=="   !
! symbols. Any comment lines are allowed and
must begin with an exclamation   !
! mark (!) in column one.  Comments may
appear to the right of a parameter   !
! specification to improve documentation.
Comments will be ignored  during   !
! reading.  Blank lines are also allowed and
ignored. Continuation lines in   !
! a parameter specification are allowed and
must be preceded by a backslash   !
! (\).  In some instances, more than one value
is required for a parameter.   !
! If fewer values are provided, the  last
value  is assigned for the entire   !
! parameter array.  The multiplication symbol
(*),  without blank spaces in   !
! between, is allowed for a parameter
specification.  For example, in a two   !
! grids nested application:
!
!
!
!    AKT_BAK == 2*1.0d-6  2*5.0d-6
! m2/s                          !
!
!
! indicates that the first two entries of
array AKT_BAK,  in fortran column-  !
! major order, will have the same value of
"1.0d-6" for grid 1,  whereas the  !
! next two entries will have the same value of
"5.0d-6" for grid 2.           !
!
!
! In multiple levels of nesting and/or
multiple connected domains  step-ups,  !
! "Ngrids" entries are expected for some of
these parameters.  In such case,  !
```

```
! the order of the entries for a parameter is
extremely important.  It  must  !
! follow the same order (1:Ngrids) as in the
state variable declaration. The  !
! USER may follow the above guidelines for
specifying his/her values.  These  !
! parameters are marked by "==" plural symbol
after the KEYWORD.              !
!
!
!=============================================
================================
!
!-------------------------------------------
--------------------------------
!  Sediment model control switch.
!-------------------------------------------
--------------------------------

! Switch is used to control sediment model
computation within nested and/or
! multiple connected grids, [1:Ngrids].

   Lsediment == T

!-------------------------------------------
--------------------------------
!  General sediment bed model parameters.
!-------------------------------------------
--------------------------------

! Depositional bed layer thickness criteria to
create a new layer (m). If
! deposition exceeds this value, then a new
layer is created, [1:Ngrids].

    NEWLAYER_THICK == 0.1d0

! Bed load transport rate coefficient.
[1:Ngrids].

    BEDLOAD_COEFF == 0.05d0

!-------------------------------------------
--------------------------------
!  Lateral boundary condition flags for all
sediment tracers.
!-------------------------------------------
--------------------------------
!
! Set lateral boundary conditions keyword.
Notice that a value is expected
! for each boundary segment per nested grid
for each state variable.
!
! The sediment tracer variables (cohesive and
noncohesive) require
! [1:4,1:NCS+NNS,Ngrids] values. If specifying
every tracer, enter first
! 1:NCS cohesive sediment entries followed by
1:NNS noncohesive sediment
! entries. The boundary order is: 1=west,
2=south, 3=east, and 4=north.
```

```
! That is, anticlockwise starting at the
western boundary.
!
! The keyword is case insensitive and usually
has three characters. However,
! it is possible to have compound keywords, if
applicable. For example, the
! keyword "RadNud" implies radiation boundary
condition with nudging. This
! combination is usually used in
active/passive radiation conditions.
!
! NOTICE: It is possible to specify the
lateral boundary conditions for
! ======  all sediment tracers (cohesive and
noncohesive) in a compact
! form with a single entry. If so, all the
sediment tracers are assumed to
! have the same boundary  as in the single
entry.
!
!   Keyword    Lateral Boundary Condition Type
!
!   Cla        Clamped
_____N_____     j=Mm
!   Clo        Closed
|     4     |
!   Gra        Gradient
|           |
!   Nes        Nested
1 W           E 3
!   Nud        Nudging
|           |
!   Per        Periodic
|_____S_____|
!   Rad        Radiation
2          j=1
!
i=1         i=Lm
!                    W       S       E       N
!                    e       o       a       o
!                    s       u       s       r
!                    t       t       t       t
!                            h               h
!
!                    1       2       3       4

   LBC(isTvar) ==   RadNud  RadNud  RadNud
RadNud   ! idsed(:), compact

! Adjoint-based algorithmsn have different
lateral boundary
! conditions keywords.

ad_LBC(isTvar) ==   RadNud  RadNud  RadNud
RadNud   ! idsed(:), compact

!-----------------------------------------
--------------------------------
! Suspended Cohesive Sediment Parameters,
[1:NCS,1:Ngrids] values expected.
!-----------------------------------------
--------------------------------
```

```
! Median sediment grain diameter (mm).

    MUD_SD50 == 0.063d0 0.5d0 1.0d0 0.016d0
0.022d0 0.03d0 0.04d0

! Sediment concentration (kg/m3).

    MUD_CSED == 0.0d0  10.0d0

! Sediment grain density (kg/m3).

    MUD_SRHO == 2650.0d0 2650.0d0 2650.0d0
2650.0d0 2650.0d0 2650.0d0 2650.0d0

! Particle settling velocity (mm/s).

    MUD_WSED == 2.4d0 65.0d0 125.0d0 0.15d0
0.3d0 0.5d0 1.0d0

! Surface erosion rate (kg/m2/s).

   MUD_ERATE ==  2.0d-4 2.0d-4 2.0d-4 2.0d-4
2.0d-4 2.0d-4 2.0d-4

! Critical shear for erosion and deposition
(N/m2).

  MUD_TAU_CE ==  0.094d0 0.28d0 0.53d0 0.1d0
0.1d0 0.1d0 0.1d0
  MUD_TAU_CD ==  0.094d0 0.28d0 0.53d0 0.1d0
0.1d0 0.1d0 0.1d0

! Porosity (nondimensional: 0.0-1.0):
Vwater/(Vwater+Vsed).

   MUD_POROS == 0.9d0  0.9d0  0.9d0  0.9d0
0.9d0  0.9d0  0.9d0

! Harmonic/biharmonic horizontal diffusion of
tracer for nonlinear model
! and adjoint-based algorithms.

    MUD_TNU2 == 0.0d0  0.0d0  0.0d0 0.0d0
0.0d0  0.0d0 0.0d0  ! m2/s
    MUD_TNU4 == 0.0d0  0.0d0  0.0d0 0.0d0
0.0d0  0.0d0 0.0d0  ! m4/s

 ad_MUD_TNU2 == 0.0d0  0.0d0
! m2/s
 ad_MUD_TNU4 == 0.0d0  0.0d0
! m4/s

! Vertical mixing coefficients for tracers in
nonlinear model and
! basic state scale factor in adjoint-based
algorithms.

 MUD_AKT_BAK == 5.0d-6  5.0d-6
! m2/s

 MUD_AKT_fac == 2*1.0d0
! nondimensional
```

```
! Nudging/relaxation time scales, inverse
scales will be computed
! internally.

   MUD_TNUDG == 2.5d0  2.5d0  2.5d0  2.5d0
2.5d0  2.5d0  2.5d0  2.5d0 ! days

! Morphological time scale factor (greater
than or equal to 1.0). A
! value of 1.0 has no scale effect.

MUD_MORPH_FAC == 1.0d0 1.0d0 1.0d0 1.0d0 1.0d0
1.0d0 1.0d0  ! nondimensional

! Logical switches (TRUE/FALSE) to specify
which variables to consider on
! tracers point Sources/Sinks (like river
runoff). See glossary below for
! details.

 MUD_Ltracer == T T T T T T T

! Logical switches (TRUE/FALSE) to activate
writing of cohesive sediment
! fields into HISTORY output file.

Hout(idmud)   == T       ! mud_01, ...
suspended concentration
Hout(iMfrac) == T       ! mudfrac_01, ...
bed layer fraction
Hout(iMmass) == T       ! mudmass_01, ...
bed layer mass
Hout(iMUbld) == T       ! bedload_Umud_01, ...
bed load at U-points
Hout(iMVbld) == T       ! bedload_Vmud_01, ...
bed load at V-points

! Logical switches (TRUE/FALSE) to activate
writing of time-averaged
! cohesive sediment fields into AVERAGE output
file.

Aout(idmud)   == T       ! mud_01, ...
suspended concentration
Aout(iMUbld) == T       ! bedload_Umud_01, ...
bed load at U-points
Aout(iMVbld) == T       ! bedload_Vmud_01, ...
bed load at V-points

! Logical switches (TRUE/FALSE) to activate
writing of time-averaged,
! cohesive sediment diagnostic terms into
DIAGNOSTIC output file.

Dout(MTrate) == T       ! mud_01_rate, ...
time rate of change
Dout(MThadv) == T       ! mud_01_hadv, ...
horizontal total advection
Dout(MTxadv) == T       ! mud_01_xadv, ...
horizontal XI-advection
Dout(MTyadv) == T       ! mud_01_yadv, ...
horizontal ETA-advection
Dout(MTvadv) == T       ! mud_01_vadv, ...
vertical advection
```

```
Dout(MThdif) == T       ! mud_01_hdiff, ...
horizontal total diffusion
Dout(MTxdif) == T       ! mud_01_xdiff, ...
horizontal XI-diffusion
Dout(MTydif) == T       ! mud_01_ydiff, ...
horizontal ETA-diffusion
Dout(MTsdif) == T       ! mud_01_sdiff, ...
horizontal S-diffusion
Dout(MTvdif) == T       ! mud_01_vdiff, ...
vertical diffusion

!-----------------------------------------
--------------------------------
! Non-cohesive Sediment Parameters,
[1:NNS,1:Ngrids] values expected.
!-----------------------------------------
--------------------------------

! Median sediment grain diameter (mm).

   SAND_SD50 == 1.0d0

! Sediment concentration (kg/m3).

   SAND_CSED == 0.0d0

! Sediment grain density (kg/m3).

   SAND_SRHO == 2650.0d0

! Particle settling velocity (mm/s).

   SAND_WSED == 1.0d0

! Surface erosion rate (kg/m2/s).

  SAND_ERATE == 5.0d-4

! Critical shear for erosion and deposition
(N/m2).

 SAND_TAU_CE == 0.1d0
 SAND_TAU_CD == 0.1d0

! Porosity (nondimensional: 0.0-1.0):
Vwater/(Vwater+Vsed).

  SAND_POROS == 0.5d0

! Harmonic/biharmonic horizontal diffusion of
tracer for nonlinear model
! and adjoint-based algorithms.

   SAND_TNU2 == 0.0d0
! m2/s
   SAND_TNU4 == 0.0d0
! m4/s

ad_SAND_TNU2 == 0.0d0
! m2/s
ad_SAND_TNU4 == 0.0d0
! m4/s
```

```
! Vertical mixing coefficients for tracers in
nonlinear model and
! basic state scale factor in adjoint-based
algorithms.

SAND_AKT_BAK == 5.0d-6
! m2/s

SAND_AKT_fac == 1.0d0
! nondimensional

! Nudging/relaxation time scales, inverse
scales will be computed
! internally.

  SAND_TNUDG == 0.0d0
! days

! Morphological time scale factor (greater
than or equal to 1.0). A
! value of 1.0 has no scale effect.

SAND_MORPH_FAC == 1.0d0
! nondimensional

! Logical switches (TRUE/FALSE) to specify
which variables to consider on
! tracers point Sources/Sinks (like river
runoff). See glossary below for
! details.

SAND_Ltracer == F

! Logical switches (TRUE/FALSE) to activate
writing of non-cohesive
! sediment fields into HISTORY output file.

Hout(idsand) == T       ! sand_01, ...
suspended concentration
Hout(iSfrac) == T       ! sandfrac_01, ...
bed layer fraction
Hout(iSmass) == T       ! sandmass_01, ...
bed layer mass
Hout(iSUbld) == T       ! bedload_Usand_01,
...   bed load at U-points
Hout(iSVbld) == T       ! bedload_Vsand_01,
...   bed load at V-points

! Logical switches (TRUE/FALSE) to activate
writing of time-averaged
! non-cohesive sediment fields into AVERAGE
output file.

Aout(idsand) == T       ! sand_01, ...
suspended concentration
Aout(iSUbld) == T       ! bedload_Usand_01,
...   bed load at U-points
Aout(iSVbld) == T       ! bedload_Vsand_01,
...   bed load at V-points

! Logical switches (TRUE/FALSE) to activate
writing of time-averaged,
! non-cohesive sediment diagnostic terms into
DIAGNOSTIC output file.
```

```
Dout(STrate) == T       ! sand_01_rate, ...
time rate of change
Dout(SThadv) == T       ! sand_01_hadv, ...
horizontal total advection
Dout(STxadv) == T       ! sand_01_xadv, ...
horizontal XI-advection
Dout(STyadv) == T       ! sand_01_yadv, ...
horizontal ETA-advection
Dout(STvadv) == T       ! sand_01_vadv, ...
vertical advection
Dout(SThdif) == T       ! sand_01_hdiff, ...
horizontal total diffusion
Dout(STxdif) == T       ! sand_01_xdiff, ...
horizontal XI-diffusion
Dout(STydif) == T       ! sand_01_ydiff, ...
horizontal ETA-diffusion
Dout(STsdif) == T       ! sand_01_sdiff, ...
horizontal S-diffusion
Dout(STvdif) == T       ! sand_01_vdiff, ...
vertical diffusion

!-------------------------------------------
--------------------------------
! Bed layer and bottom sediment parameters,
[1:Ngrids] values expected.
!-------------------------------------------
--------------------------------

 Hout(ithck) == T       ! bed_thickness
sediment layer thickness
 Hout(iaged) == T       ! bed_age
sediment layer age
 Hout(iporo) == T       ! bed_porosity
sediment layer porosity
 Hout(idiff) == F       ! bed_biodiff
biodiffusivity

!
!  GLOSSARY:
!  =========
!
!-------------------------------------------
--------------------------------
!  Sediment model control switch, [1:Ngrids].
!-------------------------------------------
--------------------------------
!
!  Lsediment       Switch to control sediment
model computation within nested
!                    and/or multiple connected
grids. By default this switch
!                    is set to TRUE in
"mod_scalars" for all grids. The USER
!                    has the option, for
example, to compute sediment in just
!                    one of the nested grids.
If so, this switch needs to be
!                    consistent with the
dimension parameter NST in input
!                    script (ocean.in).  In
order to make the model more
```

```
!                     efficient in  memory
usage, NST(:) should be zero in
!                     such grids.
!
!-------------------------------------------
-------------------------------
!  General sediment bed model controls,
[1:Ngrids] values are expected.
!-------------------------------------------
-------------------------------
!
!  NEWLAYER_THICK  Depositional bed layer
thickness criteria to create a new
!                     layer (m). If deposition
exceeds this value, then a new
!                     layer is created.
!
!  BEDLOAD_COEFF   Bed load transport rate
coefficient.
!
!-------------------------------------------
-------------------------------
! Lateral boundary conditions parameters for
all sediment tracers.
!-------------------------------------------
-------------------------------
!
! The lateral boundary conditions are now
specified with logical switches
! instead of CPP flags to allow nested grid
configurations. Their values are
! load into structured array:
!
!    LBC(1:4, nLBCvar, Ngrids)
!
! where 1:4 are the number of boundary edges,
nLBCvar are the number LBC state
! variables, and Ngrids is the number of
nested grids. For Example, to apply
! gradient boundary conditions to any tracer
we use:
!
!    LBC(iwest,  isTvar(itrc), ng) % gradient
!    LBC(ieast,  isTvar(itrc), ng) % gradient
!    LBC(isouth, isTvar(itrc), ng) % gradient
!    LBC(inorth, isTvar(itrc), ng) % gradient
!
! The lateral boundary conditions for all
sediment tracers (cohesive plus
! noncohesive) are entered with a keyword.
This keyword is case insensitive
! and usually has three characters. However,
it is possible to have compound
! keywords, if applicable. For example, the
keyword "RadNud" implies radiation
! boundary condition with nudging. This
combination is usually used in
! active/passive radiation conditions.
!
! It is possible to specify the lateral
boundary conditions for all sediment
! tracers in a compact form with a single
entry.  for example, in a East-West
! periodic application we can just have:
```

```
!                                                                      !   Rad        Radiation
!                    W       S       E       N                      2          j=1
!                    e       o       a       o                      !
!                    s       u       s       r                      i=1         i=Lm
!                    t       t       t       t                      !
!                            h               h                      !  LBC(isTvar)    Sediment Tracers, [1:4,
!                                                                   1:NST, Ngrids] values are expected.
!                    1       2       3       4                      !
!                                                                   ! Similarly, the adjoint-based algorithms
!  LBC(isTvar) ==    Per     Clo     Per                            (ADM, TLM, RPM) can have different
Clo                                                                ! lateral boundary conditions keywords:
!                                                                    !
! Then, the standard input processing routine                       !  ad_LBC(isTvar) Sediment Tracers, [1:4,
will assume that all the                                           1:NBT, Ngrids] values are expected.
! sediment tracers have the same lateral                            !
boundary condition specified by                                    !-----------------------------------------
! the single entry.                                                 ---------------------------------
!                                                                  ! Suspended Cohesive Sediment KEYWORDS,
!   Keyword    Lateral Boundary Condition Type                     [1:NCS,1:Ngrids] values expected.
!                                                                  !-----------------------------------------
!   Cla        Clamped                                             ---------------------------------
_____N_____     j=Mm                                               !
!   Clo        Closed                                             !  MUD_SD50        Median sediment grain
|     4     |                                                      diameter (mm).
!   Gra        Gradient                                           !
|           |                                                      !  MUD_CSED        Sediment concentration
!   Nes        Nested                                             (kg/m3). It may be used to initialize
1 W           E 3                                                  !                  sediment fields using
!   Nud        Nudging                                            analytical expressions.
|           |                                                      !
!   Per        Periodic                                           !  MUD_SRHO        Sediment grain density
|_____S_____|                                                     (kg/m3).
```

```
!
!  MUD_WSED        Particle settling velocity
(mm/s).
!
!  MUD_ERATE       Surface erosion rate
(kg/m2/s).
!
!  MUD_TAU_CE      Critical shear for erosion
(N/m2).
!
!  MUD_TAU_CD      Critical shear for
deposition (N/m2).
!
!  MUD_POROS       Porosity (nondimensional:
0.0-1.0):  Vwater/(Vwater+Vsed).
!
!  MUD_TNU2        Nonlinar model lateral,
harmonic, constant, mixing
!                    coefficient (m2/s) for
suspended cohesive sediment;
!                    [1:NCS,1:Ngrids]. If
variable horizontal diffusion is
!                    activated, MUD_TNU2 is
the mixing coefficient for
!                    the largest grid-cell in
the domain.
!
!  MUD_TNU4        Nonlinar model lateral,
biharmonic, constant, mixing
!                    coefficient (m4/s) for
suspended cohesive sediment;
!                    [1:NCS,1:Ngrids]. If
variable horizontal diffusion is
!                    activated, MUD_TNU4 is
the mixing coefficient for
!                    the largest grid-cell in
the domain.
!
!  ad_MUD_TNU2     Adjoint-based algorithms
lateral, harmonic, constant,
!                    mixing coefficient (m2/s)
for suspended cohesive
!                    sediment;
[1:NCS,1:Ngrids]. If variable horizontal
!                    diffusion is activated,
ad_MUD_TNU2 is the mixing
!                    coefficient for the
largest grid-cell in the domain.
!
!  ad_MUD_TNU4     Adjoint-based algorithms
lateral, harmonic, constant,
!                    mixing coefficient (m4/s)
for suspended cohesive
!                    sediment;
[1:NCS,1:Ngrids]. If variable horizontal
!                    diffusion is activated,
ad_MUD_TNU4 is the mixing
!                    coefficient for the
largest grid-cell in the domain.
!
!  MUD_AKT_BAK     Background vertical mixing
coefficient (m2/s),
```

```
!                    AKT_BAK(idsed(i)) with
i=1:NCS.
!
!  MUD_AKT_fac     Adjoint-based algorithms
vertical mixing, basic state,
!                    scale factor
(nondimensional) for biological tracer
!                    variables;
[1:NCS,1:Ngrids] values are expected. In
!                    some applications, a
smaller/larger values of vertical
!                    mixing are necessary for
stability. It is only used
!                    when FORWARD_MIXING is
activated.
!
!  MUD_TNUDG       Nudging time scale (days),
TNUDG(idsed(i)) with i=1:NCS.
!                    Inverse scale will be
computed internally.
!
!  MUD_MORPH_FAC   Morphological time scale
factor (nondimensional; greater
!                    than or equal to 1.0). A
value of 1.0 has no scale
!                    effect.
!
!  MUD_Ltracer     Logical switches (T/F) to
specify which tracer variables
!                    to consider when the
option TS_PSOURCE is activated;
!                    [1:NCS,1:Ngrids] values
are expected.
!
!                      MUD_Ltracer(  1,ng)
sand_01
!                      ...
...
!                      MUD_Ltracer(NCS,ng)
...
!
!                    Recall that TS_PSOURCE is
usually activated to add river
!                    runoff as a point source.
At minimum, it is necessary to
!                    specify both temperature
and salinity for all rivers. The
!                    other tracers are
optional. The user needs to know the
!                    correspondence between
biological variables and indices
!                    idbio(1:NBT) when
activating one or more of these switches.
!
!                    This logical switch
REPLACES and ELIMINATES the need to
!                    have or read the variable
"river_flag(river)" in the input
!                    rivers forcing NetCDF
file:
!
!                      double
river_flag(river)
```

```
!                       river_flag:long_name
= "river runoff tracer flag"
!                       river_flag:option_0 =
"all tracers are off"
!                       river_flag:option_1 =
"only temperature"
!                       river_flag:option_2 =
"only salinity"
!                       river_flag:option_3 =
"both temperature and salinity"
!                       river_flag:units =
"nondimensional"
!
!                     This logic was too
cumbersome and complicated when
!                     additional tracers are
considered. However, this change
!                     is backward compatible.
!
!                     This logical switch will
be used to activate the reading
!                     of respective tracer
variable from input river forcing
!                     NetCDF file. If you want
to add other tracer variables
!                      (other than temperature
and salinity) as a source for a
!                     particular river(s), you
just need to specify such values
!                     on those river(s). Then,
set the values to ZERO on the
!                     other river(s) that do
NOT require such river forcing for
!                     that tracer. Recall that
you need to specify the tracer
!                     values for all rivers,
even if their values are zero.
!
!  Hout(idmud)     Logical switches to
activate writing of cohesive sediment
!                     concentration into
HISTORY NetCDF file,
!                     HOUT(idTvar(idsed(i)))
with i=1:NCS.
!
!  Hout(iMfrac)    Logical switches to
activate writing of cohesive sediment
!                     class fraction
composition of each bed layer into HISTORY
!                     NetCDF file,
HOUT(idfrac(i)) with i=1,NCS.
!
!  Hout(iMmass)    Logical switches to
activate writing of cohesive sediment
!                     mass of each bed layer
into HISTORY NetCDF file,
!                     HOUT(idsed(i)) with
i=1,NCS.
!
!  Hout(iMUbld)    Logical switches to
activate writing of cohesive sediment
!                     bed load at U-points into
HISTORY NetCDF file,
```

```
!                     HOUT(idsed(i)) with
i=1,NCS.
!
!  Hout(iMVbld)     Logical switches to
activate writing of cohesive sediment
!                     bed load at V-points into
HISTORY NetCDF file,
!                     HOUT(idsed(i)) with
i=1,NCS.
!
!  Aout(idmud)      Logical switches to
activate writing of time-averaged
!                     cohesive sediment
concentration into AVERAGE NetCDF
!                     file,
AOUT(idTvar(idsed(i))) with i=1:NCS.
!
!  Aout(iMUbld)     Logical switches to
activate writing of time-averaged
!                     cohesive sediment bed
load at U-points into AVERAGE
!                     NetCDF file,
AOUT(idsed(i)) with i=1,NCS.
!
!  Aout(iMVbld)     Logical switches to
activate writing of time-averaged
!                     cohesive sediment bed
load at V-points into AVERAGE
!                     NetCDF file,
AOUT(idsed(i)) with i=1,NCS.
!
!  Dout(MT....)     Logical switches to
activate writing of time-averaged
!                     cohesive tracers
diagnostic terms into DIAGNOSTIC
!                     NetCDF file,
DOUT(idsed(i),MT....) with i=1,NCS.
!
!                     Dout(MTrate)    Time rate
of change
!                     Dout(MThadv)    Horizontal
total advection
!                     Dout(MTxadv)    Horizontal
XI-advection
!                     Dout(MTyadv)    Horizontal
ETA-advection
!                     Dout(MTvadv)    Vertical
advection
!                     Dout(MThdif)    Horizontal
total diffusion
!                     Dout(MTxdif)    Horizontal
XI-diffusion
!                     Dout(MTydif)    Horizontal
ETA-diffusion
!                     Dout(MTsdif)    Horizontal
S-diffusion
!                     Dout(MTvdif)    Vertical
diffusion
!
!-----------------------------------------
--------------------------------
! Suspended Non-cohesive Sediment KEYWORDS,
[1:NNS,1:Ngrids] values expected.
```

```
!-------------------------------------------
---------------------------------
!
!  SAND_SD50       Median sediment grain
diameter (mm).
!
!  SAND_CSED       Sediment concentration
(kg/m3). It may be used to initialize
!                    sediment fields using
analytical expressions.
!
!  SAND_SRHO       Sediment grain density
(kg/m3).
!
!  SAND_WSED       Particle settling velocity
(mm/s).
!
!  SAND_Erate      Surface erosion rate
(kg/m2/s).
!
!  SAND_TAU_CE     Critical shear for erosion
(N/m2).
!
!  SAND_TAU_CD     Critical shear for
deposition (N/m2).
!
!  SAND_POROS      Porosity (nondimensional:
0.0-1.0):  Vwater/(Vwater+Vsed).
!
!  SAND_TNU2       Nonlinar model lateral,
harmonic, constant, mixing
!                    coefficient (m2/s) for
suspended non-cohesive sediment;
!                    [1:NNS,1:Ngrids]. If
variable horizontal diffusion
!                    is activated, SAND_TNU2
is the mixing coefficient for
!                    the largest grid-cell in
the domain.
!
!  SAND_TNU4       Nonlinar model lateral,
harmonic, constant, mixing
!                    coefficient (m4/s) for
suspended non-cohesive sediment;
!                    [1:NNS,1:Ngrids]. If
variable horizontal diffusion
!                    is activated, SAND_TNU4
is the mixing coefficient for
!                    the largest grid-cell in
the domain.
!
!  ad_SAND_TNU2    Adjoint-based algorithms
lateral, harmonic, constant,
!                    mixing coefficient (m2/s)
for suspended non-cohesive
!                    sediment;
[1:NNS,1:Ngrids]. If variable horizontal
!                    diffusion is activated,
SAND_TNU2 is the mixing
!                    coefficient for the
largest grid-cell in the domain.
!
```

```
!  ad_SAND_TNU4    Adjoint-based algorithms
lateral, harmonic, constant,
!                    mixing coefficient (m4/s)
for suspended non-cohesive
!                    sediment;
[1:NNS,1:Ngrids]. If variable horizontal
!                    diffusion is activated,
SAND_TNU4 is the mixing
!                    coefficient for the
largest grid-cell in the domain.
!
!  SAND_AKT_BAK    Background vertical mixing
coefficient (m2/s),
!                    AKT_BAK(idsed(i)) with
i=NCS+1:NST.
!
!  SAND_AKT_fac    Adjoint-based algorithms
vertical mixing, basic state,
!                    scale factor
(nondimensional) for biological tracer
!                    variables;
[1:NNS,1:Ngrids] values are expected.
!                    In some applications, a
smaller/larger values of
!                    vertical mixing are
necessary for stability. It is
!                    only used when
FORWARD_MIXING is activated.
!
!  SAND_TNUDG      Nudging time scale (days),
TNUDG(idsed(i)) with i=NCS+1:NST.
!                    Inverse scale will be
computed internally,
!
!  SAND_MORPH_FAC  Morphological time scale
factor (nondimensional; greater
!                    than or equal to 1.0). A
value of 1.0 has no scale effect.
!
!  SAND_Ltracer     Logical switches (T/F) to
specify which tracer variables
!                    to consider when the
option TS_PSOURCE is activated;
!                    [1:NNS,1:Ngrids] values
are expected.
!
!                      SAND_Ltracer(  1,ng)
sand_01
!                      ...
...
!                      SAND_Ltracer(NNS,ng)
...
!
!                    Recall that TS_PSOURCE is
usually activated to add river
!                    runoff as a point source.
At minimum, it is necessary to
!                    specify both temperature
and salinity for all rivers. The
!                    other tracers are
optional. The user needs to know the
!                    correspondence between
biological variables and indices
```

```
!                     idbio(1:NBT) when
activating one or more of these switches.
!
!                     This logical switch
REPLACES and ELIMINATES the need to
!                     have or read the variable
"river_flag(river)" in the input
!                     rivers forcing NetCDF
file:
!
!                       double
river_flag(river)
!                         river_flag:long_name
= "river runoff tracer flag"
!                         river_flag:option_0 =
"all tracers are off"
!                         river_flag:option_1 =
"only temperature"
!                         river_flag:option_2 =
"only salinity"
!                         river_flag:option_3 =
"both temperature and salinity"
!                         river_flag:units =
"nondimensional"
!
!                     This logic was too
cumbersome and complicated when
!                     additional tracers are
considered. However, this change
!                     is backward compatible.
!                     This logical switch will
be used to activate the reading
!                     of respective tracer
variable from input river forcing
!                     NetCDF file. If you want
to add other tracer variables
!                     (other than temperature
and salinity) as a source for a
!                     particular river(s), you
just need to specify such values
!                     on those river(s). Then,
set the values to ZERO on the
!                     other river(s) that do
NOT require such river forcing for
!                     that tracer. Recall that
you need to specify the tracer
!                     values for all rivers,
even if their values are zero.
!
!  Hout(idsand)    Logical switches to
activate writing of non-cohesive
!                     sediment concentration
into HISTORY NetCDF file,
!                     HOUT(idTvar(idsed(i)))
with i=1:NCS+1,NST.
!
!  Hout(iSfrac)    Logical switches to
activate writing of non-cohesive
!                     sediment class fraction
composition of each bed layer
!                     into HISTORY NetCDF file,
HOUT(idfrac(i)) with
```

```
!                     i=NCS+1,NST.
!
!  Hout(iSmass)     Logical switches to
activate writing of non-cohesive
!                     sediment mass of each bed
layer into HISTORY NetCDF file,
!                     HOUT(idsed(i)) with
i=NCS+1,NST.
!
!  Hout(iSUbld)     Logical switches to
activate writing of non-cohesive
!                     sediment bed load at U-
points into HISTORY NetCDF file,
!                     HOUT(idsed(i)) with
i=NCS+1,NST.
!
!  Hout(iSVbld)     Logical switches to
activate writing of non-cohesive
!                     sediment bed load at V-
points into HISTORY NetCDF file,
!                     HOUT(idsed(i)) with
i=NCS+1,NST.
!
!  Aout(idsand)     Logical switches to
activate writing of time-averaged
!                     non-cohesive sediment
concentration into AVERAGE
!                     NetCDF file,
AOUT(idTvar(idsed(i))) with i=1:NCS+1,NST.
!
!  Aout(iSUbld)     Logical switches to
activate writing of time-averaged
!                     non-cohesive sediment bed
load at U-points into AVERAGE
!                     NetCDF file,
AOUT(idsed(i)) with i=NCS+1,NST.
!
!  Aout(iSVbld)     Logical switches to
activate writing of time-averaged
!                     non-cohesive sediment bed
load at V-points into AVERAGE
!                     NetCDF file,
AOUT(idsed(i)) with i=NCS+1,NST.
!
!  Dout(ST....)     Logical switches to
activate writing of time-averaged
!                     non-cohesive tracers
diagnostic terms into DIAGNOSTIC
!                     NetCDF file,
DOUT(idsed(i),ST....) with i=NCS+1,NST.
!
!                     Dout(STrate)    Time rate
of change
!                     Dout(SThadv)    Horizontal
total advection
!                     Dout(STxadv)    Horizontal
XI-advection
!                     Dout(STyadv)    Horizontal
ETA-advection
!                     Dout(STvadv)    Vertical
advection
!                     Dout(SThdif)    Horizontal
total diffusion
```

```
!                     Dout(STxdif)   Horizonta1
XI-diffusion
!                     Dout(STydif)   Horizontal
ETA-diffusion
!                     Dout(STsdif)   Horizontal
S-diffusion
!                     Dout(STvdif)   Vertical
diffusion
!
!-------------------------------------------
--------------------------------
! Bed layer and bottom sediment KEYWORDS,
[1:Ngrids] values expected.
!-------------------------------------------
--------------------------------
!
!  Hout(ithck)     Sediment layer thickness.
!
!  Hout(iaged)     Sediment layer age.
!
!  Hout(iporo)     Sediment layer porosity.
!
!  Hout(idiff)     Biodiffusivity at the
bottom of each layer.
!
```

VITA

Julia M. Moriarty

Born in Washington, D.C. on 10 December 1987. Graduated from Walter Johnson High School, Bethesda, MD in June 2005. Earned B.S. with Honors in the Geophysical Sciences and a B.A. with Honors in Physics from University of Chicago, Chicago, IL in June 2009. Entered M.S. program in the College of William & Mary, School of Marine Science, Gloucester Point, VA in August 2009.